UNIVERSITY OF CALGARY

Role of Titin and Collagen in the Diastolic Dysfunction of Cirrhotic Cardiomyopathy

by

Tamara Glenn

A THESIS

SUBMITTED TO THE FACULTY OF GRADUATE STUDIES

IN PARTIAL FULFILMENT OF THE REQUIREMENTS FOR THE

DEGREE OF MASTER OF SCIENCE

DEPARTMENT OF GASTROINTESTINAL SCIENCES

CALGARY, ALBERTA

AUGUST, 2008

ISBN: 978-0-494-44591-4

ABSTRACT

Significance of diastolic dysfunction in cirrhotic cardiomyopathy has been brought to the forefront with several reports of unexpected heart failure following liver transplantation and transjugular intrahepatic portosystemic stent-shunt, but the etiology remains unclear. The present study investigated the role of passive tension regulators - titin and collagen - in the pathogenesis of this condition. Cirrhosis was induced by bile duct ligation (BDL) in rats, while controls underwent bile duct inspection with no ligation. In BDL animals, diastolic return velocity was significantly decreased, relaxation time increased and passive tension increased. However, no significant difference in mRNA and protein levels of titin was observed. Protein kinase A (PKA) mRNA and protein levels were significantly decreased in BDL animals. Collagen levels were also significantly altered in the BDL group. Therefore, diastolic dysfunction exists in cirrhosis with alterations in titin modulation, PKA levels and collagen configuration contributing to the pathogenesis of this condition.

ACKNOWLEDGEMENTS

I would like to thank my supervisor, Dr. Samuel S. Lee, for his support, guidance and encouragement throughout my study. I am also very grateful to Dr. Henk E.D.J. ter Keurs for his advice, use of his lab facilities and technical assistance. I would also like to thank Dr. Donna-Marie McCafferty for her guidance and assistance throughout the years. Special thanks to Dr. Hongqun Liu and Dr. Hooman Hoonar for their help with experimental procedures.

I would also like to thank my mother for all her love, support and inspiration throughout my life, for teaching me the importance of learning and for guiding me on the path to success. Thank you to my sister, who helped to raise, guide and support me throughout my life. The sacrifices that you both have made will never be forgotten. To my boyfriend, thank you for all your support, understanding and encouragement as well as for your brighter outlook at times when I really needed it the most. Finally, thank you to all my friends that have supported me through my studies.

TABLE OF CONTENTS

LIST OF TABLES

LIST OF FIGURES AND ILLUSTRATIONS

LIST OF ABBREVIATIONS

ATP	adenosine triphosphate
BDL	bile duct ligated cirrhotic rats
cAMP	cyclic adenosine monophosphate
CCD	charge-coupled device
cGMP	cyclic guanosine monophosphate
CO	carbon monoxide
COL I(α1)	collagen type I, alpha chain 1
COL I(α2)	collagen type I, alpha chain 2
COL III	collagen type III
E/A	ratio of early (E) to late (A) phase of ventricular filling
GAPDH	glyceraldehyde 3-phosphate dehydrogenase
HO	heme oxygenase
MHC	myosin heavy chain
MMP	matrix metalloproteinases
mRNA	messenger ribonucleic acid
N2B, N2BA	titin isoforms
NCX	sodium-calcium exchanger
NO	nitric oxide
PKA	protein kinase A
RT-PCR	reverse transcriptase - polymerase chain reaction

RyR2	ryanodine receptor 2
SD	standard deviation
SERCA2	sarcoplasmic/ endoplasmic reticulum calcium ATPase
SR	sarcoplasmic reticulum
TIMP	tissue inhibitor of metalloproteinases
TNF-α	tumor necrosis factor - alpha

CHAPTER ONE: INTRODUCTION

1.1 The Liver

The liver is the largest visceral organ in the human body, weighing between 1.4-1.6 kg (Desmet, 2001). The structural organization of the liver reflects its multifaceted role in the body. It possesses two main lobes (right and left) and two accessory lobes (quadrate and caudate). The liver is provided with a dual blood supply from the portal vein and the hepatic artery. The portal vein delivers venous blood from the intestine, stomach, spleen and pancreas, while the hepatic artery provides the liver with oxygenated blood. A major function of the liver involves the uptake of amino acids, carbohydrates, lipids, vitamins and iron, and their subsequent storage, metabolic conversion and release into the blood (Kutchai, 2000; Desmet, 2001). It is a major site of glycogen storage in the body, and is also responsible for the synthesis of bile. In addition, the liver provides defense against foreign macromolecules and particles such as bacteria. The liver is also involved in drug metabolism, the breakdown of haemoglobin and the conversion of ammonia to urea. It possesses the remarkable ability to regenerate and return to a normal size and functional state in response to parenchymal cell loss (Wallace et al., 2008). Due to its countless metabolic functions and secretions into the blood, the liver qualifies as a metabolic and endocrine gland. At the same time, its bile production and secretion impose on it the organizational principles of an exocrine organ (Desmet, 2001).

1.2 Liver Cirrhosis

Cirrhosis of the liver is defined as a chronic disease characterized by an advanced stage of fibrosis and the conversion of normal parenchymal cells into structurally abnormal regenerative nodules (Harrison and Burt, 1993). Three major mechanisms are involved in the generation of cirrhosis: cell death, aberrant extracellular matrix deposition (fibrosis) and vascular reorganization (Guyot et al., 2006). Many pathogenic factors have been shown to cause cirrhosis, including alcohol, viral hepatitis B and C, non-alcoholic fatty liver disease, autoimmune disorders of the bile duct such as primary biliary cirrhosis and hereditary conditions such as Wilson's disease. Patients with cirrhosis often have an apparently normal (compensated) liver function for long periods of time with the appearance of symptoms such as abdominal swelling and pain, indigestion, fatigue, itching, edema and jaundice (Wallace et al., 2008). In more advanced stages of cirrhosis, ascites, esophageal varices, portal hypertension, hepatic encephalopathy, hepatopulmonary syndrome and hepatocellular carcinoma may occur. Cirrhosis is also associated with several abnormalities in kidney function, which most frequently manifests as sodium and water retention. However, hepatorenal syndrome or renal failure can also occur in these patients (Gentilini and Laffi, 1992). To date, two major cardiovascular complications- cirrhotic cardiomyopathy and hyperdynamic circulation- have been shown to exist in cirrhotic patients (Lee et al., 2007). Traditionally, liver damage from cirrhosis cannot be reversed but treatment may stop or delay further progression and reduce complications from the disease.

1.3 The Heart

The heart is a complex, muscular organ responsible for pumping blood throughout the body (Hole Jr., 1984). It is enclosed by a double-layered pericardium and is composed of three distinct layers within the wall- an outer epicardium, a middle myocardium and an inner endocardium. The outer epicardium provides a protective layer that consists of blood capillaries, lymph capillaries and nerve fibres. The middle layer, or myocardium, is responsible for muscle contraction that forces blood from the heart. Lastly, the endocardium, which consists of epithelium and connective tissues including elastic and collagenous fibres, blood vessels and specialized muscle fibres (Purkinje fibres), provides a protective inner lining for the chambers, valves and blood vessels (Hole Jr., 1984).

Internally, the heart is divided in four chambers- the upper chambers called the atria, which have relatively thin walls and receive blood from the veins, and the lower chambers, or the ventricles, which force blood out of the heart and into arteries. Unidirectional flow of blood through the heart is maintained by cardiac valves. The atria and the ventricles are separated by the atrioventricular valves, while blood flow between the ventricles and the pulmonary arteries or aorta is regulated by the semilunar valves. When the right ventricular wall contracts, the tricuspid valve closes as the blood moves into the pulmonary system. From these vessels, the blood enters the capillaries associated with the alveoli of the lungs where gas exchange occurs. The freshly oxygenated blood then returns to the heart through pulmonary veins that lead to the left atrium,

which contracts to allow blood to move into the left ventricle. When the left ventricle contracts, the bicuspid (mitral) valve closes as blood flows into the aorta and to the rest of the body. Regulation of the cardiac cycle occurs via the sympathetic and parasympathetic divisions of the autonomic nervous systems, which regulates heart rate and force of myocardial contraction by innervating the atrial muscles, ventricular muscles, sinoatrial node and atrioventricular node (Hole Jr., 1984).

Cardiac muscle is characterized by the ordered organization of numerous contractile proteins into the sarcomere. The sarcomere, which is referred to as the functioning unit of the muscle, has been shown to consist of thin and thick filaments. The thin filament is composed largely of actin, tropomyosin and the troponin complex, while the thick filaments contain myosin and myosin binding proteins. However, it has become well established that in addition to thin and thick filaments, the sarcomere contains a third protein known as titin. Titin, which spans the Z-line (line separating different sarcomeres) to the M-line (line in the middle of the sarcomere), is responsible for the elasticity of relaxed striated muscle and plays an essential role in myofibrillar assembly (Figure 1.1A) (Berne and Levy, 1996).

In cardiac muscle, the sarcomere length refers to the distance between the Z-lines. In the human heart, this ranges from 1.6 μm during systole to 2.2 μm during diastole (Klabunde, 2005). The slack or resting sarcomere length refers to a transitional stage during the cardiac cycle when the muscle is neither stretched nor compressed, therefore in essence being at rest (Yastrebov et al., 2006).

Under non-physiological conditions, isolated muscles or cells from the heart have been shown to possess a slack length of 1.8 μm on average and a contracted length of 1.6 μm once stimulated. However, unlike in the physiological settings, isolated muscles from the heart can be stretched to sarcomere lengths greater than the 2.2 μm observed in stretching of the heart (Roos et al., 1982; Opitz et al., 2003; Granzier et al., 2005).

Cardiac excitation-contraction coupling is the process by which electrical excitation of the myocyte is converted to contraction of the heart. It is well established that in cardiac cells, action potentials passing over the surface membrane activate voltage-sensitive L-type Ca^{2+} channels that rapidly open, allowing extracellular Ca^{2+} to flow into the cytoplasm (Lamb, 2000). Ca^{2+} entering the cell triggers the release of Ca^{2+} from the sarcoplasmic reticulum (SR) through specialized channels known as ryanodine receptor type 2 (RyR2). The released Ca^{2+} from the SR results in activation of additional RyR2, thereby propagating further Ca^{2+} release in a process known as Ca^{2+}-induced Ca^{2+}-release. The increase in cytoplasmic Ca^{2+} results in the binding of Ca^{2+} to troponin C. This Ca^{2+}-troponin interaction causes conformational changes in the thin filament as tropomyosin shifts to unblock the myosin binding sites found on actin. This leads to the binding of myosin to actin (cross-bridge cycling) and the subsequent contraction of the myofibrils. Cardiac cells can also be activated by sympathetic stimulation of the heart through β-adrenergic receptors, which results in the activation of adenylyl cyclase via a membrane bound G-protein complex. This results in the conversion of ATP to cAMP, which in turn activates

protein kinase A (PKA). PKA then phosphorylates several proteins related to excitation-contraction coupling, including L-type Ca^{2+} channels, ryanodine receptor, phospholamban, troponin I and myosin binding protein C, which ultimately leads to the release of Ca^{2+} from the SR (Bers, 2002). Increase in cytoplasmic Ca^{2+} levels leads to the activation of the contractile apparatus and the subsequent production of force. However, during relaxation, the Ca^{2+} is subsequently removed from the cytosol by Ca^{2+} transporters of the SR and plasma membrane leading to the disassociation of Ca^{2+} from troponin and the realignment of tropomyosin over the myosin binding sites to prevent further binding (Labeit et al., 1997). (Figure 1.2)

1.3.1 Titin and the heart

Over half a century ago, Huxley et al was able to demonstrate the existence of a third sarcomere filament when the extraction of actin and myosin did not result in disintegration of the sarcomere (Huxley and Hanson, 1954). Today, it has been well established that the sarcomere contains, in addition to thin and thick filaments, a filament composed of the giant muscle protein titin. Titin is responsible for the elasticity of relaxed striated muscle and plays an essential role in myofibrillar assembly (Labeit et al., 1997). Evidence to support these claims have been provided by experiments with low doses of ionizing radiation to degrade titin, which resulted in the reduced ability of muscle fibres to generate the elasticity associated with passive force and also resulted in the axial misalignment of thick filaments (Horowits et al., 1986).

Two classes of titin isoforms have been shown to exist in cardiac muscle- N2B isoforms containing the N2B segment; and the N2BA isoforms containing the N2B and N2A segment. The elastic region of cardiac titin is located in the I band (isotropic region surrounding the Z lines) of the sarcomere and has a complex sequence comprised of three extensible segments: (1) tandem immunoglobulin(Ig)-like domains that make up a proximal and a distal segment, (2) a PEVK segment containing proline (P), glutamate (E), valine (V) and lysine (K), and (3) a unique sequence that is part of N2B or N2BA element (Labeit and Kolmerer, 1995). (Figure 1.1B) Passive tension is an important factor in cardiac muscle because it is a part of the diastolic wall tension that determines the extent of filling of the heart and its subsequent stroke volume (Granzier and Irving, 1995). As the heart fills during diastole myofibrils develop a passive force, which is independent of the interaction between thin and thick filaments. This passive force is largely derived from the extensible region of titin in the I-band (Trombitas et al., 1995). As the sarcomere is stretched from its slack length, the serially linked Ig segments are straightened, followed by extension of the PEVK and N2B unique sequence, resulting in an exponential rise in passive force (Fukuda and Granzier, 2004). (Figure 1.3) Due to the longer PEVK segment and additional Ig domains found in N2BA isoforms, it results in a lower extension of titin for a given sarcomere stretch. As a result, cardiac myocytes that express high levels of N2B titin have higher passive stiffness than those that express N2BA titin. Due to the high N2B expression levels that are encountered in small animals with high heart rates, such as mouse and rat, it has been suggested that high N2B allows rapid

early diastolic filling (due to high restoring forces) and rapid setting of end diastolic volume (due to the high stiffness at long sarcomere lengths) when diastolic filling times are short (Granzier et al., 2005). Therefore, N2B and N2BA expression varies between and within species in different locations of the heart, and in some cases with co-expression of these isoforms at different levels to modulate stiffness and thus filling of the heart (Cazorla et al., 2000). Previous studies have provided evidence of the change in co-expression ratio of titin isoforms during different disease states, where there can be an increase or decrease in the N2B to N2BA ratio depending on the condition of the heart (Wu et al., 2002; Makarenko et al., 2004).

1.3.2 Collagen and the heart

The myocardial extracellular matrix is composed of a complex network of structural proteins including fibrillar proteins, such as collagen I (COL I) and III (COL III) and elastin, proteoglycans and basement membrane proteins including collagen IV, laminin and fibronectin (Leite-Moreira, 2006). There are more than 20 types of collagen that participate in the formation of distinct extracellular matrix in various tissues. Although they may differ in certain structural features and tissue distribution, all collagens are trimeric proteins made from three polypeptides called collagen α chains (Lodish et al., 2008). COL I is a long (300 nm), thin (1.5 nm) triple helix consisting of two α1 chains and one α2 chain, while COL III is also 300 nm long but its triple helix is composed of only α1 chains. Collagen α chains are synthesized by ribosomes as longer pro-α chain

precursors, which undergo a series of covalent modifications and fold into triple-helical procollagen molecules. Once secreted from the cell, the procollagen molecules are cleaved and the triple-stranded molecules associate into higher-order polymers called collagen fibrils, which have a diameter of 50-200 nm and repeat every 67 nm. These fibrils can align laterally into larger bundles called collagen fibers (Figure 1.4).

The epimysium, the sheath of connective tissue that surrounds the muscle, contains large fibres of collagen and elastin. In papillary muscles of rat, it has been shown that the large collagen fibres of the epimysium form a weave pattern at slack length (sarcomere length of 1.8 to 2.0 μm), but become well aligned once the muscle is stretched (Robinson et al., 1983). The endomysium, which are connective tissues that surround and interconnect myocytes, consist of intracellular struts (bundles of collagen fibrils acting as tethers or tensile structures between cells), a weave of bundles of collagen fibrils that envelopes the myocytes and a collagen fibril lattice that bridges cells and fills the extracellular matrix (Robinson et al., 1983). The perimysial collagen fibres, which group myocytes by connecting epimysium and endomysium and surrounding myocytes, are arranged parallel to the sarcomeres (Figure 1.5 and 1.6). Both papillary and trabeculae muscle studies have shown that the perimysial collagen fibres are wavy cords that straighten considerably as the sarcomere is stretched (Figure 1.7) (Hanley et al., 1999). Using antibody localization with fluorescent markers in light microscopy, COL I and III have been shown to be colocalized in

the endomysium in intracellular struts and pericellular fibres that lie along the surfaces of myocytes (Robinson et al., 1988; Marijianowski et al., 1995).

COL I forms large, well-structured fibres that resist extension, while COL III forms a fine reticular network that is more compliant (Wu et al., 2000). Several studies have shown that remodelling of collagen occurs in the heart during different diseases. For instance, hearts with dilated cardiomyopathy or congestive heart failure show an increase in the ratio of COL I to COL III, which corresponded to an increase in passive tension due to the rigidity of COL I (Marijianowski et al., 1995; Pauschinger et al., 1999). The changes occur in the endomysium and perimysium, although there are differences in distribution. Therefore, due to collagen's role in providing architectural support for muscle cells and its importance in myocardial functioning, its composition in the normal and diseased heart is of great significance (Pauschinger et al., 1999).

1.3.3 Protein Kinase A and the heart

PKA is a heterotetramer composed of two regulatory and two catalytic subunits. It is a broad-specificity, serine and threonine protein kinase that is activated by the second messenger cAMP (Scott, 1991; Kapiloff, 2002). During sympathetic stimulation, activation of the β-adrenergic receptor leads to activation of adenylyl cyclase via a membrane bound G-protein complex. This results in the conversion of ATP to cAMP, which in turn activates PKA and increases chronotropic (heart rate), inotropic (strength of contraction) and lusitropic (extent of relaxation) conditions of the heart (Bers, 2002). In cardiac

myocytes, phosphorylation by PKA is central to the regulation of many cellular processes, such as contraction, relaxation, metabolism, ion fluxes and gene expression (Kapiloff, 2002). PKA is known to phoshorylate several proteins related to excitation-contraction coupling, including L-type Ca^{2+} channels, ryanodine receptor, phospholamban, troponin I and myosin binding protein C (Bers, 2002). However, not all extracellular agonists that induce cAMP and PKA have the same effects on cardiac function. Therefore, specificity of PKA signalling is conferred in part by the binding of PKA to A-kinase anchoring proteins (AKAPs) that are targeted to specific intracellular locations to allow for activation of various substrates by PKA after it is activated locally by cAMP (Colledge and Scott, 1999; Kapiloff, 2002).

1.3.4 Titin and Protein Kinase A

Many studies have examined the role of post-translational modulators, such as PKA, on titin's actions. β-adrenergic stimulation of intact cardiac myocytes and incubation of skinned cardiac myocytes with PKA have been shown to result in the phosphorylation of both titin's unique cardiac-specific N2B and N2BA segments (Yamasaki et al., 2002; Fukuda et al., 2005; Kruger and Linke, 2006). Mechanical experiments with isolated myocytes revealed that PKA significantly reduced passive tension (Yamasaki et al., 2002). Using skinned cardiac tissues that express different isoforms of titin, Fukuda et al found that the reduction in passive tension, upon PKA phosphorylation, was less in muscles that had a lower N2B to N2BA ratio (Fukuda et al., 2005). This increase in

compliance would allow for more rapid and complete cardiac chamber filling. Many possible explanations have been offered to clarify this shift in passive tension. One suggestion is that this change occurs due to destabilization of native structures within titin, which causes it to extend and increase compliance. The changes have also been suggested to occur as a compensatory mechanism that would promote ventricular filling in the presence of the possible chronotropic effect of β-adrenergic stimulation (Fukuda et al., 2005). Therefore, these experiments provide another possible pathway for modulation of diastolic function through the direct phosphorylation of titin and alteration of titin-based passive tension.

1.4 Cirrhotic Cardiomyopathy

Liver cirrhosis has been shown over the years to be associated with numerous cardiovascular abnormalities. In 1953, Kowalski and Abelmann found that patients with alcoholic cirrhosis showed an increased cardiac output and decreased arterial pressure and total peripheral resistance (Kowalski and Abelmann, 1953). Despite this increased baseline cardiac output, patients with cirrhosis still showed an abnormal ventricular contractile responsiveness. After infusing 10 alcoholic cirrhotic patients with angiotensin, a known vasoconstrictor, Limas et al. found that systemic vascular resistance was increased to normal levels and arterial pressure was doubled without any change in cardiac output, thereby indicating the presence of impaired ventricular function (Limas et al., 1974). Over the years this blunted response was believed to be a manifestation

of alcohol-induced cardiomyopathy until 1986 when Caramelo et al. infused saline to rats with carbon tetrachloride-induced cirrhosis. They observed a 50% reduction in cardiac output, in the presence of a significant increase in total peripheral resistance; thereby indicating that the impaired ventricular responsiveness was due to cirrhosis *per se* rather than the direct effect of alcohol (Caramelo et al., 1986). This phenomenon has since been termed "cirrhotic cardiomyopathy", where in the face of pharmacological, physiological and surgical stresses, as well as cardiac electrical abnormalities such as prolonged QT interval, patients with cirrhosis show an attenuated systolic and diastolic function (Ma and Lee, 1996).

Many possible pathogenic mechanisms have been shown to contribute to cirrhotic cardiomyopathy. These include impairment of the β-adrenergic receptor signalling, altered cardiomyocyte membrane physiology, downregulation of intracellular calcium kinetics and increased activity of inhibitory pathways through the actions of endocannabinoids, nitric oxide and carbon monoxide (Liu et al., 2006). All of these contribute to providing some possible explanation for the blunted ventricular contractile response often observed in cirrhotic patients (Figure 1.8).

1.4.1 Pathogenic Mechanisms of Cirrhotic Cardiomyopathy

1.4.1.1 β-Adrenergic Receptor Signalling

In view of the relationship between the β-adrenergic receptor and cardiac contractility, this system has been subjected to detailed study in cirrhotic

cardiomyopathy. In the bile duct-ligated (BDL) rat heart, a host of abnormalities in the β-adrenergic receptor signalling pathway has been shown (Ma et al., 1996; Ma et al., 1999). The G-protein subunits, G_s and $G_{i2\alpha}$, are significantly decreased, in both content and function, without any change to the G_β subunit. cAMP generation was also shown to be attenuated in BDL. This decrease of cAMP is due to impairment of adenylyl cyclase activity, which is partly secondary to decreased G-protein stimulation of the catalytic subunit of the enzyme, and also due in part to an inhibitory effect of jaundice (Ma et al., 1999). Due to the relationship that is known to exist between the stimulatory effects of the β-adrenergic system and the inhibitory effects of the muscarinic cholinergic system, it was important to determine if the contractile impairment results from overactivity of muscarinic M_2 receptors. Jaue et al demonstrated that M_2 receptor density and binding in cirrhotic rat hearts are unchanged in comparison to controls, but muscarinic responsiveness is blunted in cirrhotic myocardium (Jaue et al., 1997). However, this attenuated response was not caused by receptor down-regulation, suggesting that the changes observed in muscarinic function are likely compensatory in response to the impaired β-adrenergic stimulatory system.

1.4.1.2 Membrane Fluidity

Membrane fluidity represents the freedom with which lipid and protein molecules are able to move in the plasma membrane lipid bilayer. It has been

well established that a normal biochemical and biophysical membrane environment is critical to the proper functioning of many membrane receptors, including the β-adrenergic receptors (Ladbrooke and Chapman, 1969). Several studies have demonstrated that in cirrhosis, the plasma membrane fluidity in cells from the heart (Ma et al., 1994), erythrocytes (Kakimoto et al., 1995), kidneys (Imai et al., 1992) and liver (Reichen et al., 1992) is abnormal, and in some cases have reduced fluidity due to an increase in membrane cholesterol content. Furthermore, studies in the BDL cirrhotic cardiomyocytes have not only demonstrated this decrease in plasma membrane fluidity and its associated lipid composition changes, but also that these changes play an integral role in diminished β-adrenergic receptor functioning through interference with G-protein coupling (Ma et al., 1997) and cAMP production (Ma et al., 1994). When membrane fluidity was increased to normal levels *in vitro* by a fatty acid fluidizing agent, isoproterenol-stimulated adenylate cyclase activity and cAMP production were also restored to normal (Ma et al., 1994; Ma et al., 1997). This suggests that alterations in plasma membrane fluidity play an important role in the β-adrenergic receptor dysfunction and thus in the pathogenesis of cardiac contractility in cirrhosis.

1.4.1.3 Endocannabinoids

By definition, endogenous cannabinoids or endocannabinoids are endogenous ligands capable of binding to and functionally activating cannabinoid receptors- CB_1 and CB_2. Cannabinoid receptors are seven-transmembrane-

domain proteins coupled to inhibitory G-proteins (G_i). The endocannabinoid mediated activation of these receptors results in intracellular signalling events that are coupled to the G_i proteins. The endocannabinoids that are known to bind to these receptors include anandamide, 2-arachidonoylglycerol, and more recent candidates- 2-arachidonyl-glyceryl ether, O-arachidonoyl-ethanolamine (virhodamine) and N-arachidonoyl-dopamine (De Petrocellis et al., 2004).

Since their discovery, anandamide and 2-arachidonoylglycerol have been implicated in a variety of physiological and pathological processes. Batkai et al and Ros et al documented the mediatory effect of increased expression of anandamide and CB_1 on the pathogenesis of arterial hypotension observed in cirrhotic rat models (Batkai et al., 2001; Ros et al., 2002). More recently, Domenicali et al showed anandamide as a selective splanchnic vasodilator in cirrhosis acting predominately through two receptors- one of which is CB_1 (Domenicali et al., 2005). Gaskari et al demonstrated a negative inotropic effect of anandamide in left ventricular papillary muscles of cirrhotic rats. This inhibitory effect on contractility was completely blocked by incubation with AM251- a known CB_1 antagonist, thus confirming that the effect of anandamide is mediated by CB_1 receptors. Force-frequency relationship studies showed that at higher frequencies of contraction, anandamide reuptake blockers (VDM11 and AM404) enhanced cirrhotic papillary muscle relaxation. This effect was blocked by AM251 and pertussis toxin treatment, suggesting that not only are the effects of anandamide CB_1 receptor mediated but more specifically that the effects are

mediated by an inhibitory G_i-protein-dependent CB_1 responsive pathway (Gaskari et al., 2005).

1.4.1.4 Calcium Kinetics

Stimulation of the β-adrenergic pathway or excitation-contraction coupling leads to the activation of numerous calcium related systems that are crucial for cardiac contraction. Therefore, a defect in either the initial entry of Ca^{2+} or the ability to trigger release of Ca^{2+} from its intracellular storage may explain the attenuated contractile responsiveness observed in the cirrhotic myocardium. Studies performed on the cellular calcium dynamic in our BDL cardiomyocytes showed a significant decrease in receptor density and electrophysiological function of voltage-gated L-type Ca^{2+} channel ($I_{Ca,L}$) compared to control myoctes (Ward et al., 2001). $I_{Ca,L}$ protein expression is quantitatively decreased in BDL cardiomyocytes. Furthermore, isoproterenol stimulation of $I_{Ca,L}$ is also decreased in BDL while the proportional response to forskolin- a direct stimulator of adenylyl cyclase is the same for BDL and sham controls. These results point to an alteration in the β-adrenergic signalling pathway upstream of adenylyl cyclase. In terms of the intracellular calcium kinetics, molecular analysis of sarcoplasmic reticulum Ca^{2+} pump adenosine triphosphatase (SERCA2), which is responsible for the reuptake of Ca^{2+} into the SR, and RyR2 showed no difference in either mRNA transcription or expressed protein levels in the BDL compared with the sham controls. RyR2 receptor binding characteristics were also unaltered between the two groups (Ward et al., 2001). These researchers concluded that

the primary defect of the calcium delivery system, and thus impaired contraction, lies in the cardiomyocyte plasma membrane, including $I_{Ca,L,}$ whereas the intracellular calcium systems are intact (Ward et al., 2001).

1.4.1.5 Nitric Oxide

Over the past decade, a large number of studies have provided great insights into the multitude of functions and roles of nitric oxide (NO) in normal physiology and disease states. NO, a known vasodilator, is synthesized from L-arginine via the catalytic action of NO synthase (NOS). There are three known isoforms of NOS: neuronal (nNOS or NOS1), inducible (iNOS or NOS2) and endothelial (eNOS or NOS3).

It had been hypothesized by Vallance and Moncada that cirrhosis resulted in augmented levels of cytokines, which in turn led to the induction of iNOS to overproduce NO (Vallance and Moncada, 1991). The use of NOS inhibitors, such as N omega-monomethyl-L-arginine (L-NMMA), has provided further insight into the pathophysiological role of NO in cirrhosis. Balligand et al found that the inhibition of NOS synthesis by L-NMMA significantly increased the contractile response of rat ventricular myocytes to the β-agonist isoproterenol without affecting baseline contractility (Balligand et al., 1993). In the BDL cirrhotic model, baseline isoproterenol-stimulated papillary muscle contractile force was shown to be lower than in the control groups. However, when the papillary muscles were preincubated with the NOS inhibitor L-NAME, contractile force increased significantly in the cirrhotic rats, whereas control muscles were unaffected (Liu et

al., 2000). This group also showed that cirrhotic cardiomyocytes have an increased iNOS mRNA and protein expression, whereas eNOS shows no significant difference in expression between the BDL and the sham control hearts. Moreover, the NO donor S-nitroso-N-acetyl penicillamine inhibited papillary muscle contractility. Whether the effects of NO are mediated by inhibition of adenylyl cyclase activity or through cGMP remains to be further clarified. However, Liu et al have shown that tumor necrosis factor - alpha (TNF-α) and cGMP content in cardiac homogenates are significantly increased in BDL rats (Liu et al., 2000); suggesting a possible cytokine – iNOS - cGMP mediated pathway of action for NO in the pathogenesis of cirrhotic cardiomyopathy.

1.4.1.6 Carbon Monoxide

Carbon monoxide (CO) is produced in the body mainly through the enzymatic actions of heme oxygenase (HO), which is known to exist as inducible (HO-1, also known as heat shock protein 32) and constitutive (HO-2) isoforms. HO catalyses the oxidation of heme to iron, biliverdin and CO. Over the years, the physiological roles of CO have been elucidated in the cardiovascular, nervous and immune systems (Maines, 1997). Increasing levels of cGMP through activation of guanylyl cyclase has also been linked to the actions of CO (Ewing et al., 1994). In BDL rats, a significant increase was observed for HO-1 mRNA and protein expression, whereas neither HO-2 mRNA nor protein content differed between the BDL and control hearts. The ventricular concentration of cGMP was also shown to be higher in cirrhotic rats. However, treatment with HO

inhibitor zinc protoporphyrin IX restored the cGMP level and increased the contractile force of isoproterenol-stimulated papillary muscles. These findings suggest that activation of the HO-CO pathway in cirrhosis involves the catalytic action of HO-1, with the cardiodepressant effects of increasing levels of CO occurring via stimulation of cGMP (Liu et al., 2001).

1.5 Diastolic Dysfunction

It is generally accepted that the cardiac cycle is composed of systole and diastole. Systole refers to the ability of the ventricle to contract and eject blood, while diastole reflects its ability to relax and fill. Diastolic filling is comprised of two parts: rapid, early diastolic (active) relaxation and late diastolic (passive) filling. The early phase relies on the rate of ventricular relaxation, elastic ventricular recoil, the atrioventricular pressure gradient and the passive elastic characteristics of the left atrium and ventricle. The late phase depends on the strength of left atrial contraction and the stiffness of the left ventricle (Carroll and Hess, 2005). Determinants of diastolic filling include myocardial relaxation and passive properties of the ventricular wall, such as myocardial stiffness, wall thickness and chamber geometry (size or volume), structures surrounding the ventricle, the left atrium, pulmonary veins, mitral valve and heart rate (Leite-Moreira, 2006).

Diastolic dysfunction refers to the disturbance in ventricular relaxation, where the time period during which the myocardium loses its ability to generate force and shorten and return to an unstressed length and force is prolonged,

slowed or incomplete (Zile and Brutsaert, 2002). Diastolic dysfunction can be caused by mechanisms that are intrinsic to the cardiac muscle cells themselves, as well as factors that are extrinsic to the myocardium (Table 1.1). Intrinsic factors are divided into structures and processes within the cardiomyocytes (for example calcium homeostasis, myofilaments, ATP energetics and the cytoskeleton), extracellular matrix that surrounds the cardiomyocytes and neurohormonal activation. Extrinsic factors include hemodynamic load and the pericardium (Zile and Brutsaert, 2002). In a normal heart, myocardial relaxation comprises the major part of ventricular filling, pressure fall and the initial part of rapid filling, and is modulated by load (preload/ afterload), inactivation and non-uniformity (Brutsaert and Sys, 1989). Severe afterload elevation (force against which cardiac muscle contracts), changes in calcium homeostasis, impairment of myocardial relaxation and heart rate can lead to abnormalities in relaxation. Additionally, alterations of passive properties of the ventricular wall, such as myocardial stiffness, wall thickness and chamber geometry can also result in abnormalities in relaxation (Apstein and Morgan, 1994; Leite-Moreira and Correia-Pinto, 2001; Zile and Brutsaert, 2002; Leite-Moreira, 2006). Similarly, changes in cardiomyocyte cytoskeletal proteins, such as titin, have been shown to result in diastolic dysfunction through alterations of passive properties of the ventricular wall (Bell et al., 2000; Cazorla et al., 2000). Furthermore, a shift in titin isoforms or regulation of titin can result in a faster heart rate that may shorten diastole to an extent that prevents relaxation from being complete between

beats, resulting in increased filling pressure and therefore diastolic dysfunction (Leite-Moreira, 2006).

1.5.1 Diastolic Dysfunction and Cirrhotic Cardiomyopathy

Abnormalities of diastolic function are often reported in patients with cardiac disease and its presence is considered an early marker of cardiac impairment. Although systolic function has been extensively investigated, changes in diastolic function in cirrhotic cardiomyopathy remains to be elucidated (Valeriano et al., 2000). Abnormalities of ventricular filling pattern and consequent variation in the ratio of early (E) and late (A) phase of ventricular filling, as recorded by Doppler echocardiography, are used as markers of diastolic dysfunction. Studies evaluating ventricular diastolic filling in patients with cirrhosis have provided supportive evidence of the presence of diastolic dysfunction, which was marked by a reduction in E/A ratio (Pozzi et al., 1997; Valeriano et al., 2000). The decrease in E/A ratio could be due to a reduction in preload (pressure inside left ventricle at the end of diastole i.e. when the heart is the fullest), an increase in afterload (force against which cardiac muscle contracts) or to abnormalities in ventricular relaxation or compliance. However, patients with cirrhosis have hemodynamic changes that are characterized by an expanded blood volume that increases the cardiac preload, decreases peripheral resistance and reduces afterload, thus contributing to the persistent increase in cardiac output, with overloading and impaired contractility as the outcome (Moller and Henriksen, 2002). Therefore, Valeriano et al. speculated that the emergence

of diastolic dysfunction in their experimental model was likely due to impaired ventricular relaxation (Valeriano et al., 2000). However, more studies are needed to examine the mechanisms behind the prevalence of diastolic dysfunction in cirrhotic cardiomyopathy.

1.5.2 Diastolic Dysfunction and Titin

Titin, the giant protein spanning half the sarcomere, is responsible for passive force during sarcomere elongation and restoring force during sarcomere compression of cardiac myofilaments. As the heart fills during diastole, the myocardium stretches and passive force is generated. Over the normal operating range of the sarcomere length (<2.2 μm) a substantial component of this passive force generation arises from the titin isoforms, which are expressed by the N2B and N2BA isoforms (Kass et al., 2004). However, before the onset of diastolic dysfunction, expression of sarcomeric proteins or protein isoform expression can be altered (Neagoe et al., 2002). Titin's adaptive ability during cardiac disease is evident from numerous studies performed to date. Warren et al found that in the spontaneously hypertensive rat model there is an increased expression of N2B titin in response to pressure overload, which ultimately resulted in higher passive tension upon stretching of the sarcomere and thus an adverse effect on cardiac performance (Warren et al., 2003). On the other hand, Nagueh et al reported an isoform switch that resulted in an increase ratio of N2BA to N2B in patients with dilated cardiomyopathy, which they concluded significantly impacted diastolic filling by lowering myocardial stiffness (Nagueh et

al., 2004). Therefore, even though there appears to be consistency among studies regarding the relationship between titin isoforms and muscle stiffness, isoform switching and mechanisms that might lead to one type of shift over another in heart failure remains to be completely clarified.

1.5.3 Diastolic Dysfunction and Collagen

Extrinsic factors such as changes in the extracellular matrix have also been shown to affect diastolic functioning. The myocardial extracellular matrix is composed of fibrillar proteins, such as COL I and III and elastin, proteoglycans and basement membrane proteins including collagen IV, laminin and fibronectin (Leite-Moreira, 2006). However, the most important component that contributes to the development of diastolic dysfunction is fibrillar collagen (Borg and Caulfield, 1981; Covell, 1990). Therefore, the control of collagen biosynthesis and degradation are important aspects in diastolic dysfunction. These regulatory processes include: 1) transcriptional regulation by physical (for example preload and afterload), neurohormonal (renin-angiotensin-aldosterone and sympathetic nervous systems) and growth factors; 2) post-translational regulation, such as collagen cross-linking; and 3) enzymatic degradation by matrix metalloproteinases (MMPs) (Leite-Moreira, 2006). Therefore, changes in either synthesis or degradation of collagen can lead to the development of diastolic dysfunction.

Evidence has shown that diseases that alter diastolic function also alter extracellular fibrillar collagen, in terms of its amount, geometry, distribution,

degree of cross-linking and ratio of COL I versus COL III. Treatment of these disease conditions resulted in correction of diastolic function and normalization of fibrillar collagen (Villari et al., 1993; Kato et al., 1995; Villari et al., 1995; Zile and Brutsaert, 2002). Pauschinger et al examined the role of collagen in the diastolic dysfunction of dilated cardiomyopathy in patients undergoing endomyocardial biopsies obtained from the right ventricular septum (Pauschinger et al., 1999) . They found that the ratio of COL I to COL III was increased in the myocardium, which they concluded would contribute to an increase in tensile strength and stiffness and therefore alter diastolic function by rendering the heart less compliant. An avian model of dilated cardiomyopathy also confirmed that alteration in passive myocardial properties was due to increased collagen-based stiffness (Wu et al., 2004). Therefore, mechanisms both intrinsic and extrinsic to the cardiomyocyte play a critical role in the pathophysiology of this disease.

1.5.4 Diastolic Dysfunction and Protein Kinase A

Regulation of intracellular Ca^{2+} levels during diastole is an important factor in the proper functioning of the heart. The SR is an intracellular membrane system that plays a predominant role in cardiac contractility and relaxation through the regulation of Ca^{2+} levels. In cardiac muscle cells, depolarization of the sarcolemma membrane results in the influx of Ca^{2+} into the cell and the activation of the ryanodine receptor, which leads to the release of Ca^{2+} from the SR and muscle contraction. During relaxation, SERCA2 is responsible for the reuptake of Ca^{2+} back into the lumen of the SR (Tada and Toyofuku, 1996).

SERCA2 activity is modulated by its accessory phosphoprotein phospholamban, which functions as an inhibitory cofactor. PKA-catalyzed phosphorylation of phospholamban results in the dissociation of phospholamban from SERCA2, which leads to activation of SERCA2 and the removal of Ca^{2+} from the intracellular space during diastole (Frank et al., 2003). Another important element in diastole is troponin I, which is phosphorylated by PKA to inhibit the binding of Ca^{2+} to troponin C thereby repositioning tropomyosin and preventing further binding of actin and myosin during diastole (Figure 1.2).

In human heart failure, several lines of evidence suggest that there are alterations in intracellular Ca^{2+}-homeostasis, which may be related to an altered expression, function or regulation of the abovementioned Ca^{2+}-handling proteins (Frank et al., 2003). Several groups have reported diminished peak and prolonged decay of Ca^{2+} transients in cardiomyocytes and papillary muscle strips from patients with end-stage heart failure (Beuckelmann et al., 1992; Brixius et al., 1999; Frank et al., 2003). These alterations have important implications for excitation-contraction coupling as well as the development of increased diastolic wall tension in heart disease. In the BDL rat heart, a host of abnormalities in the β-adrenergic receptor signalling pathway have been shown (Ma et al., 1996; Ma et al., 1999). Although the changes in mRNA and protein levels of PKA have yet to be analyzed in the BDL heart, it seems likely that a decrease in PKA would exist. This decrease in PKA would affect diastolic function through the decreased phosphorylation of a variety of proteins including the SERCA2-phospolamban pump, troponin I as well as titin.

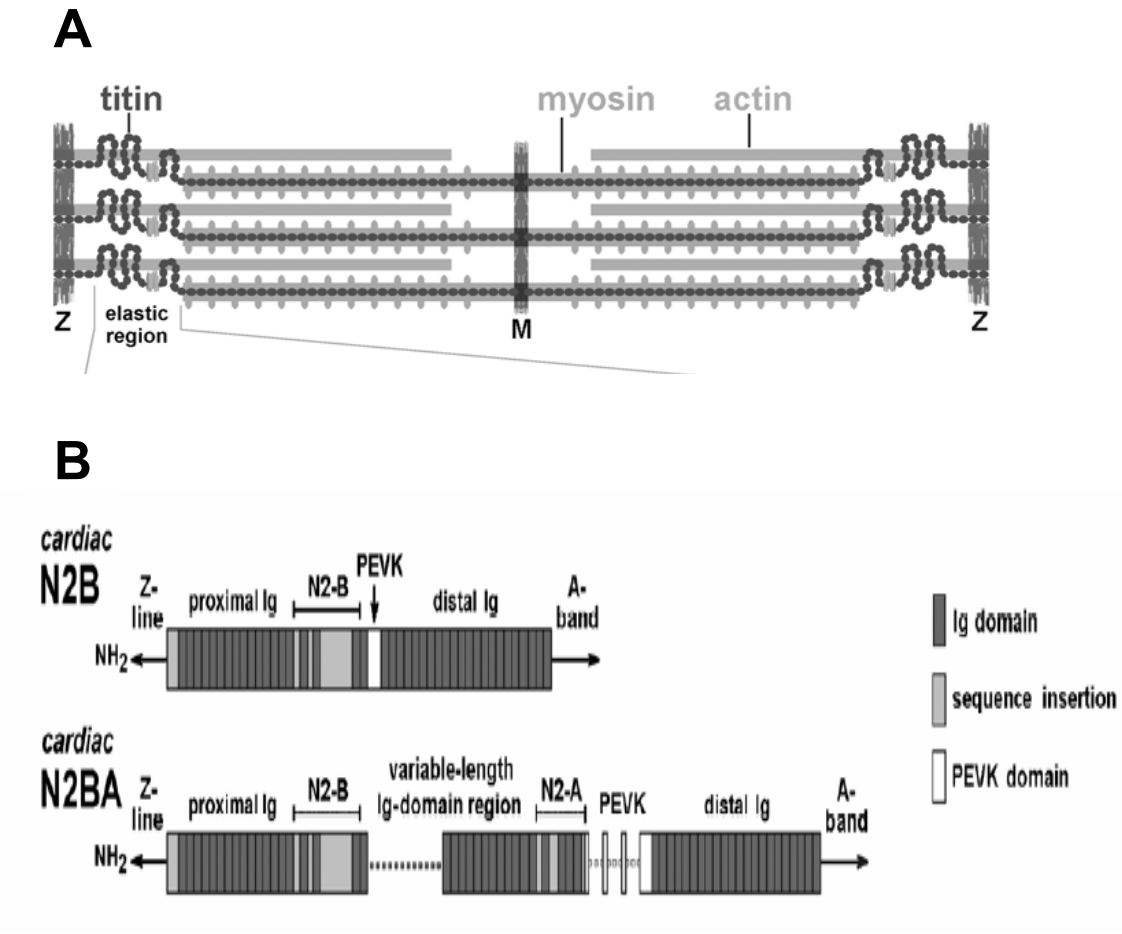

Figure 1.1 (A) Arrangement of filaments in sarcomere and (B) domain structures of the elastic region of titin coexpressing two principal isoforms, N2B and N2BA. (Neagoe et al., 2003)

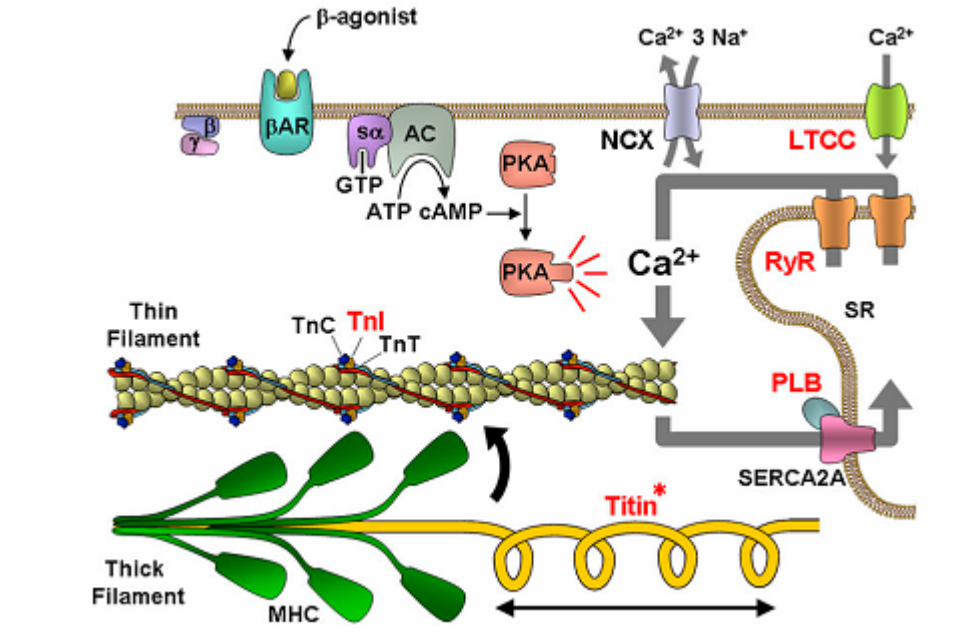

Figure 1.2 Excitation-contraction coupling and the response to β-adrenergic receptor stimulation. (Lim and Sawyer, 2005)

Abbreviations: β-AR, β-adrenergic receptor; AC, adenylyl cyclase; GTP, guanosine triphosphate; sα, β and γ, G-protein subunits; ATP, adenosine triphosphate; cAMP, cyclic adenosine monophosphate; PKA, protein kinase A; LTCC, L-type Ca^{2+} Channel; Ca^{2+}, calcium; Na^{+}, sodium; NCX, sodium-calcium exchanger; RyR, ryanodine receptor; SR, sarcoplasmic reticulum; PLB, phospholamban; SERCA2A, sarcoplasmic/ endoplasmic reticulum calcium ATPase; TnC, troponin C; TnI, troponin I; TnT, troponin T; MHC, myosin heavy chain

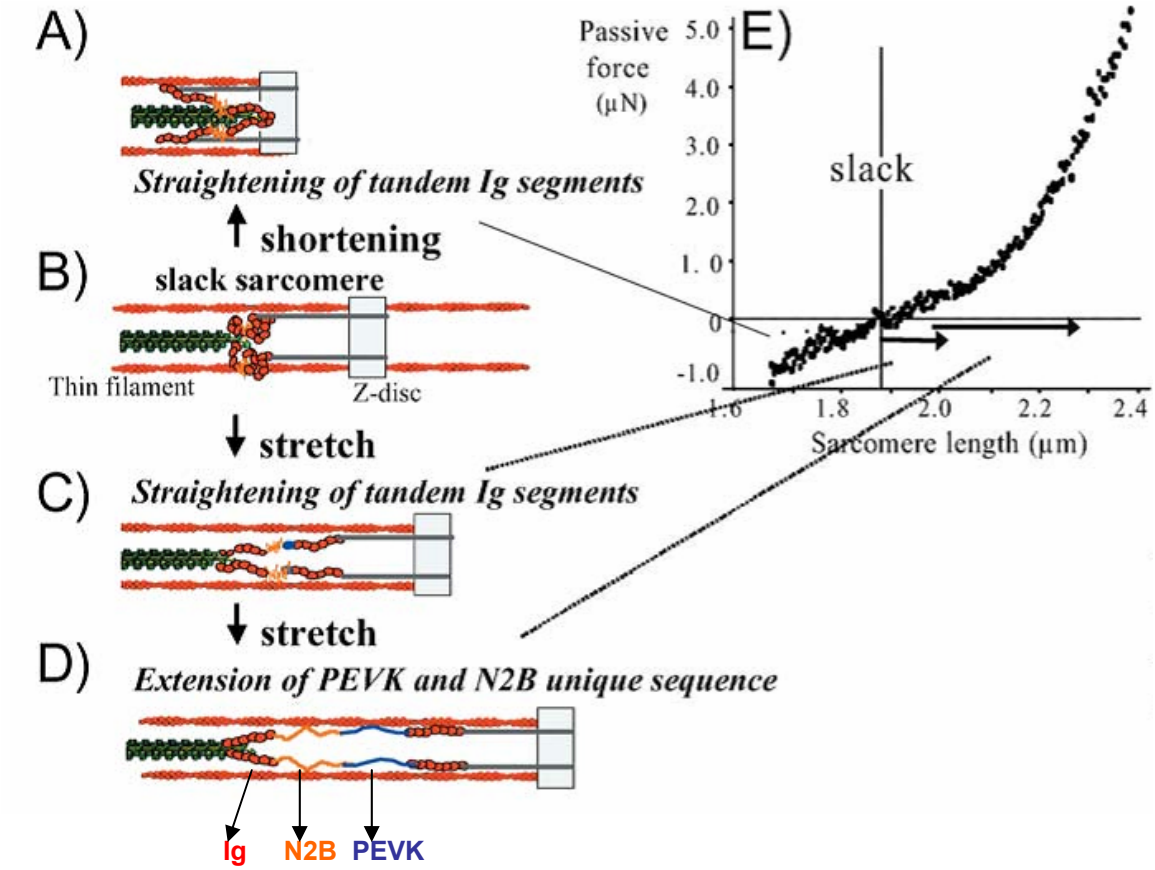

Figure 1.3 (A)–(E) Schematic representation of the extensible I-band region of cardiac titin in sarcomeres of different length and the corresponding force-sarcomere length curve. (Granzier et al., 2005)

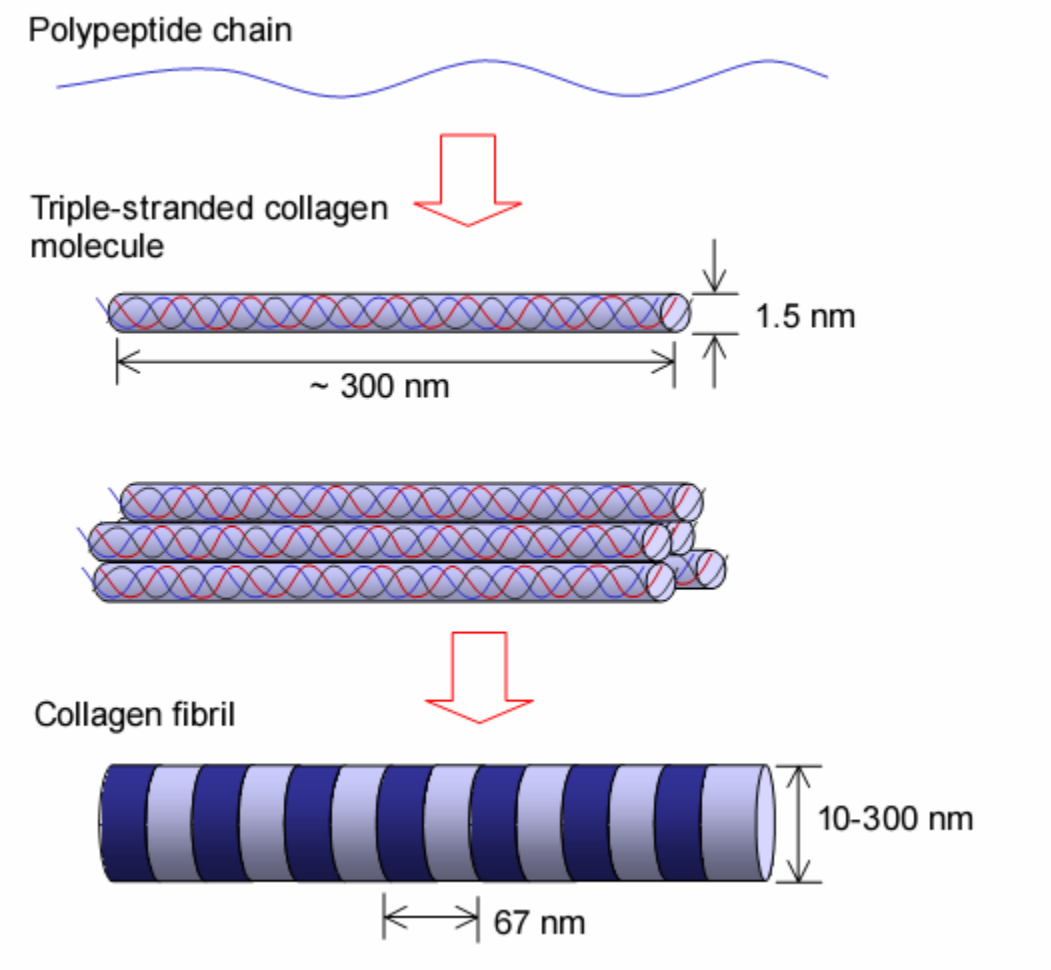

Figure 1.4 Diagram of collagen fibril structure assembly (Owen, 2005)

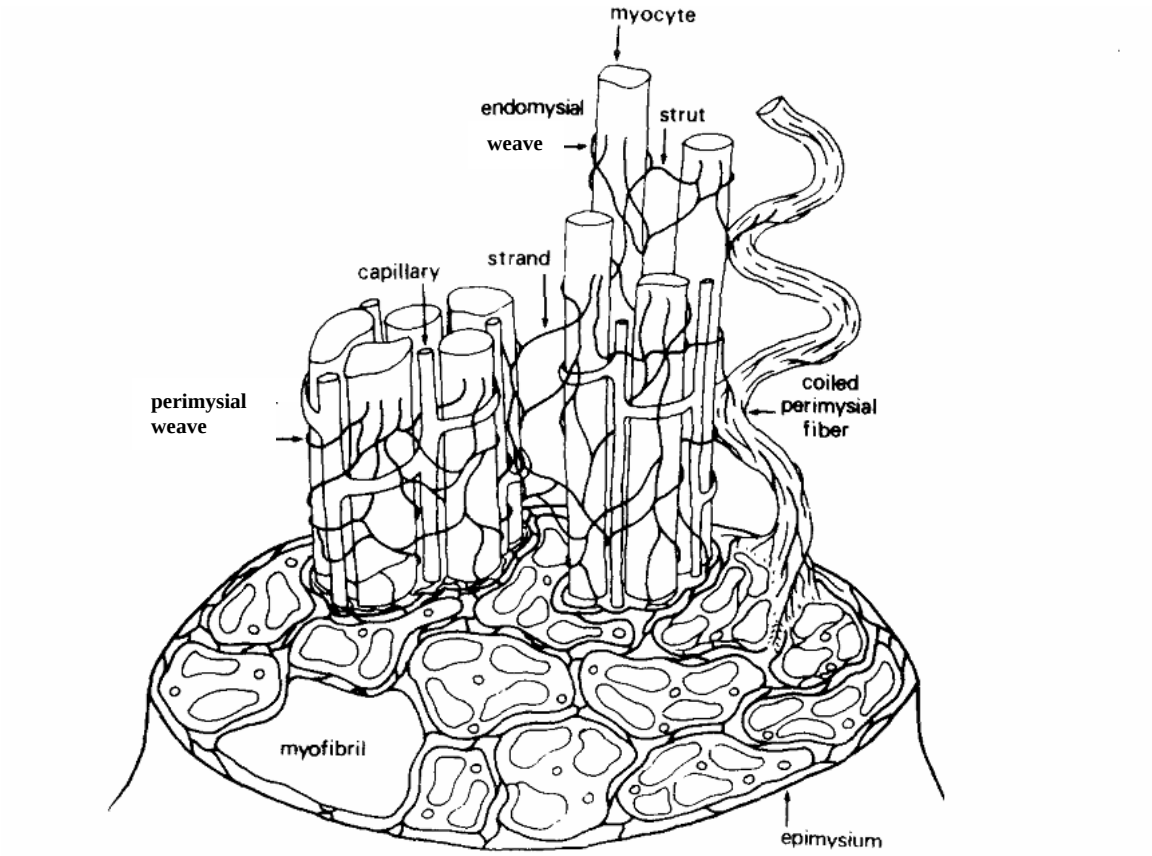

Figure 1.5 Schematic representation of the extracellular matrix showing the endomysium, perimysial and epimysium components (Sanchez-Quintana et al., 1994).

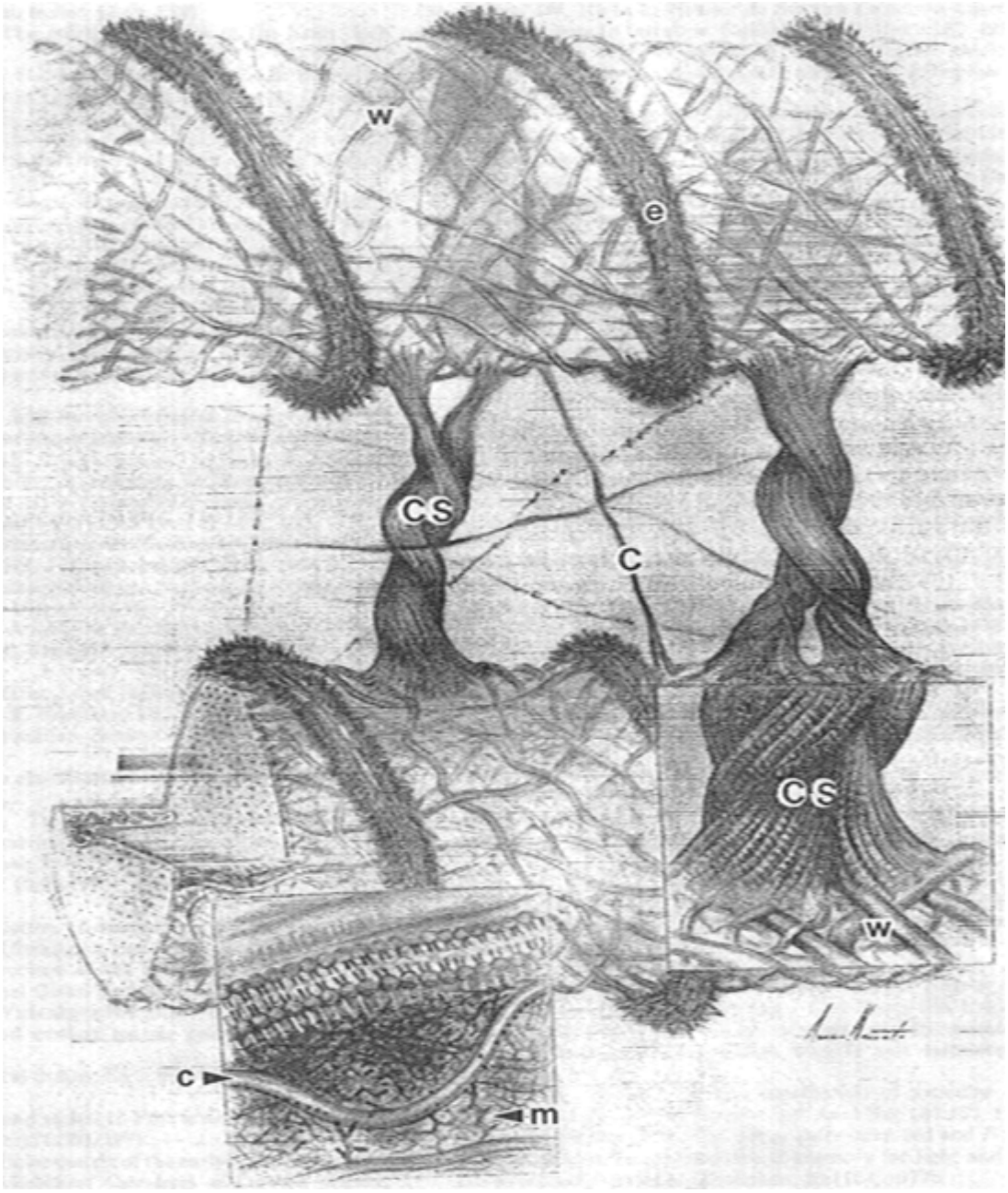

Figure 1.6 Diagrammatic representation of laterally connected myocytes, showing collagen struts (CS), elastic fibres (e), and small collagen bundles (C). Insets show the insertion of struts into the collagen weave (w) of the cell and the relationship between collagen fibril (c)-microthreads (m)-granules and the membrane and cell coat (Robinson et al., 1983).

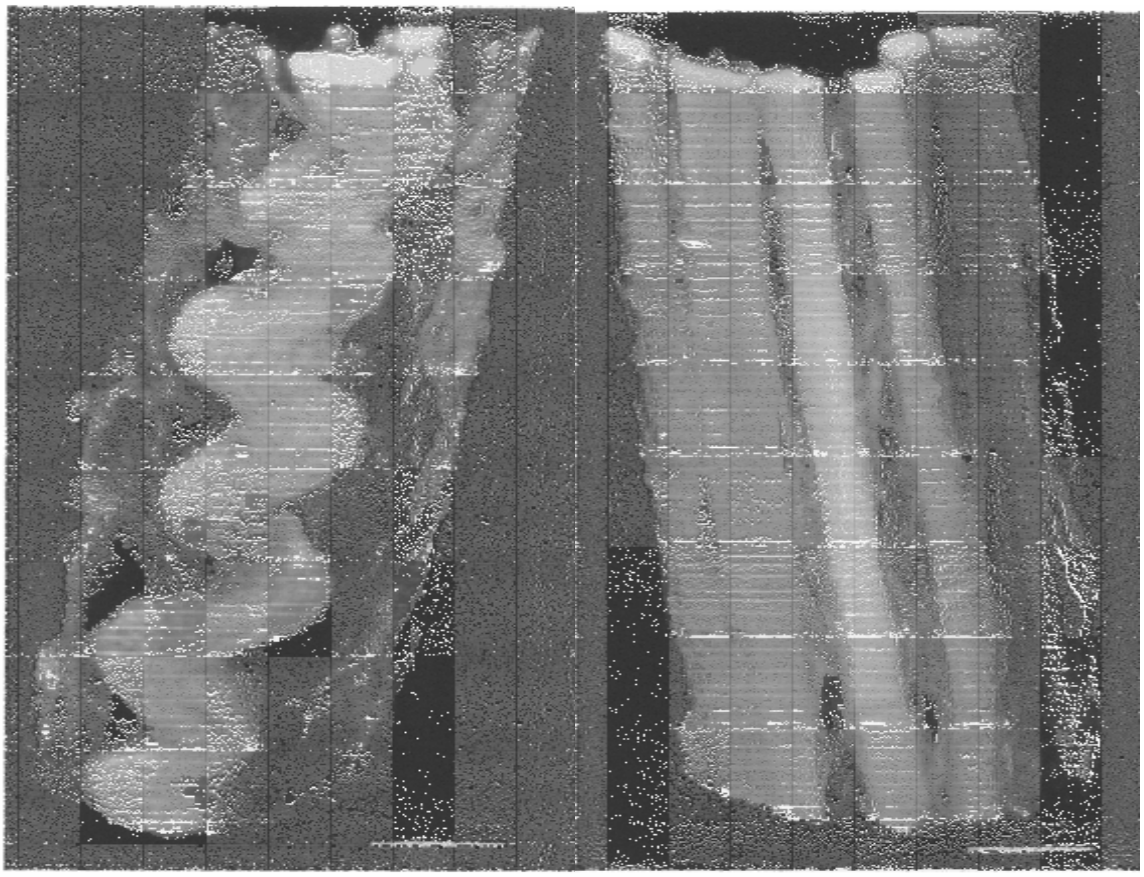

Figure 1.7 3-D reconstruction of a perimysial collagen fibre at near resting sarcomere length (1.81 μm) and at an extended sarcomere length (2.27 μm) in ventricular rat trabeculae (Hanley et al., 1999).

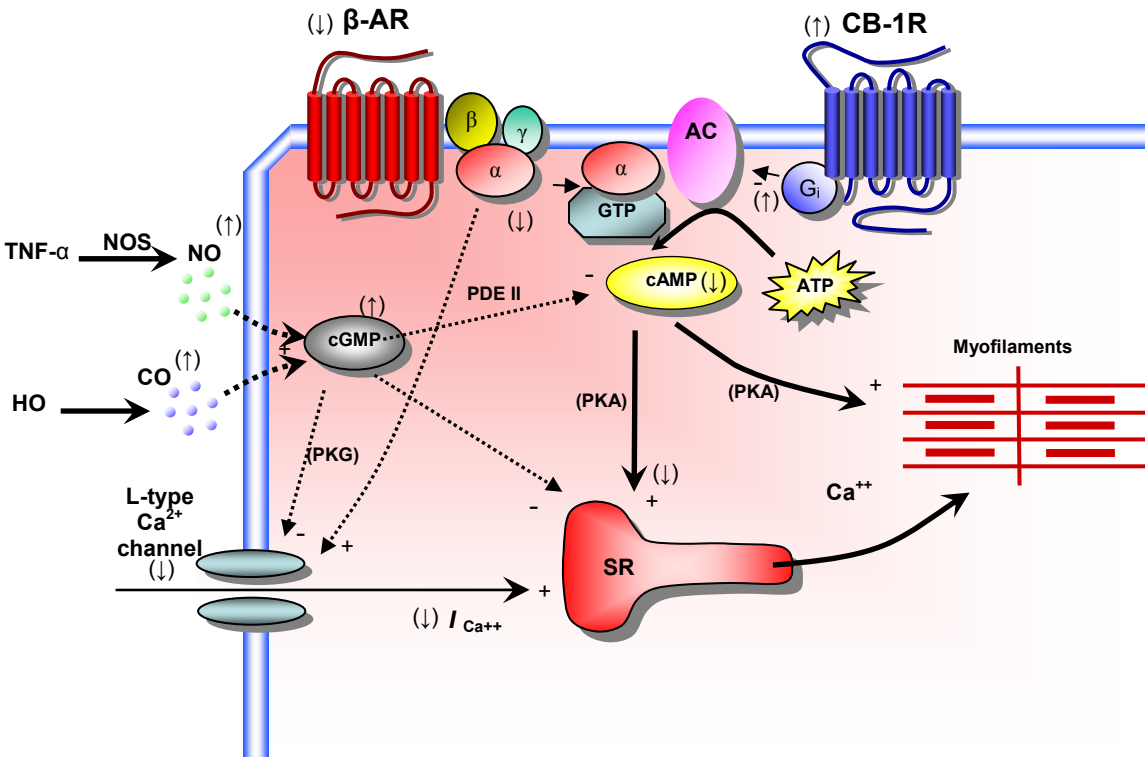

Figure 1.8 Schematic representation of the β-adrenergic signal transduction pathway and the possible pathogenic mechanisms of cirrhotic cardiomyopathy shown to date (Lee et al., 2007).

Abbreviations: β-AR, β-adrenergic receptor; AC, adenylyl cyclase; α, β and γ represent the heterotrimeric components of G-protein; Gi, inhibitory G-protein complex; GTP, guanosine triphosphate; cGMP, cyclic guanosine monophosphate; ATP, adenosine triphosphate; cAMP, cyclic adenosine monophosphate; PKA, protein kinase A; PKG, protein kinase G; PDE II, phosphodiesterase II; CB-1R, cannabinoid receptor 1; NO, nitric oxide; CO, carbon monoxide; HO, heme oxygenase; NOS, nitric oxide synthase; TNF-α, tumor necrosis factor; SR, sarcoplasmic reticulum; + stimulatory influence; – inhibitory influence.

Table 1.1 Some possible intrinsic and extrinsic mechanisms of diastolic dysfunction

Extrinsic
Hemodynamic load: early diastolic load, afterload
Heterogeneity
Pericardium
Intrinsic
Cardiomyocyte
Calcium homeostasis
Calcium concentration
Sarcolemmal and SR calcium transport function
Modifying proteins (phospholamban, calmodulin, calsequestran)
Myofilaments
Tn-C calcium binding
Tn-I phosphorylation
Myofilament calcium sensitivity/ myosin heavy chain ATPase ratio
Energetics
ADP/ATP ratio
ADP and Pi concentration
Cytoskeleton
Microtubules
Intermediate filaments (desmin)
Microfilaments (actin)
Endosarcomeric skeleton (titin, nebulin)
Extracellular matrix
Fibrillar collagen
Basement membrane proteins
Proteoglycans
MMP/TIMP
Neurohormonal activation
Renin-angiotensin-aldosterone
Sympathetic nervous system
Endothelin
Nitric oxide
Natriuretic peptides

Modified from (Zile and Brutsaert, 2002)

CHAPTER TWO: HYPOTHESIS AND AIMS

Cirrhosis of the liver is known to be associated with many cardiovascular disturbances. These disturbances include increased cardiac output, decreased arterial pressure and decreased total peripheral resistance. Despite this increased baseline cardiac output, patients with cirrhosis still show a blunted ventricular contractile response to stimuli, for which many possible pathogenic mechanisms have been suggested (Liu and Lee, 1999; Milani et al., 2007). Cirrhotic cardiomyopathy is defined by this ventricular hyporesponsiveness that is observed under conditions of pharmacological, physiological and surgical stresses (Ma and Lee, 1996). Over the years the story of cirrhotic cardiomyopathy has been extended to include diastolic dysfunction, which has been brought to the forefront by several reports of unexpected heart failure following liver transplantation and transjugular intrahepatic portosystemic stent-shunt (Merli et al., 2002; Moller and Henriksen, 2002; Gaskari et al., 2006). However, the underlying mechanisms behind this observed diastolic dysfunction remains to be completely clarified.

Titin isoforms N2B and N2BA as well as collagen have been shown to be a prime source of passive tension and an important determinant of diastolic stiffness in the heart. Moreover, PKA phosphorylation of titin reduces passive tension allowing rapid diastolic filling. Therefore, the aim of this project was to determine the pathological role of diastolic dysfunction in cirrhotic cardiomyopathy in a rat model, and to clarify the possible roles of titin and

collagen in the pathogenesis of this condition. The following hypotheses were tested:

1. Changes in N2B titin levels will lead to increased passive tension in the cirrhotic rats. Additionally, due to the decrease in β-adrenergic receptor signalling pathway that has been shown to exist in cirrhotic cardiomyopathy (Ma et al., 1999), a decrease in PKA will result in decreased phosphorylation of titin and an increase in passive tension in the BDL rats.
2. Knowing that titin is not the sole determining factor of passive tension and that collagen plays a significant role at large sarcomere lengths, an increase in the ratio of COL I to COL III will also result in slower diastolic filling and an increase in passive tension.

To test the above mentioned hypotheses, the experimental procedures were divided into specific aims.

Aim 1: Determine any cardiac abnormalities that may be observed in the cirrhotic model using cell isolation and trabeculae experiments.

Aim 2: Determine the mRNA and protein expression levels of N2B and N2BA titin isoforms in cirrhotic and control groups.

Aim 3: Determine the mRNA and protein expression levels of PKA in the cirrhotic and control groups.

Aim 4: Determine the role of extracellular factors, such as COL I and COL III, which may be involved in observed cardiac abnormalities.

CHAPTER THREE: MATERIALS AND METHODS

3.1 Animal Model

The study protocols were approved by the Animal Care Committee of the University of Calgary, Faculty of Medicine, under the guidelines of the Canadian Council on Animal Care. Male Sprague-Dawley rats (Charles River, St.Laurent, QC, Canada) and male Lewis Brown Norway rats (Harlan, Chicago, IL) weighing 175-250 g were used in this study. The animals were housed in an environmentally controlled vivarium with a 12:12-h light-dark cycle and allowed access to rat chow and water ad libitum. Common bile duct ligation was performed to induce cirrhosis. The surgical procedures for this cirrhotic model have been previously described in detail (Moezi et al., 2006). In brief, rats were anaesthetized by isoflurane inhalation. Rats were then injected with 0.2cc of buprenorphine (0.03 mg/kg in water) intramuscularly. The common bile duct was then exposed by a midline abdominal excision. The duct was doubly ligated with 4.0 silk thread and sectioned between the ligatures. The sham-operated rats were treated in the same manner as above, except that the bile duct was only visually inspected and not ligated. After surgery, neosporin antibiotic ointment was administered at the incision site to prevent infection. All studies were performed 4 weeks after bile duct ligation or sham operation. Cirrhosis was characterized by massive hepatomegaly, splenomegaly and ascites, and microscopically by widespread bile ductular proliferation, necrosis and moderate to extensive fibrosis.

3.2 Sample Preparation

For mRNA and protein analysis, the heart was dissected from Sprague-Dawley rats, frozen in liquid nitrogen and stored in a –70˚C freezer prior to gel sample preparation. Rabbit soleus muscle, which was used as a molecular marker for titin N2BA isoform, was dissected from female New Zealand white rabbits weighing 4.5 kg (Reimans Fur Ranch, St. Agatha, ON, Canada), flash frozen in liquid nitrogen and stored in a –70˚C freezer. The soleus muscles were kindly provided by Dr. Herzog's lab (University of Calgary, Calgary, AB, Canada). Bovine left ventricle was also used as a molecular marker for cardiac N2B and N2BA. The samples were flash frozen in liquid nitrogen and stored in a –70˚C freezer (kindly provided by Dr. Granzier's lab; Washington State University, Pullman, WA, USA).

3.3 Quantification of mRNA expression by reverse transcriptase-polymerase chain reaction (RT-PCR)

Total RNA from the rat ventricular tissue was extracted using a modified version of the acid guanidinium isothiocyanate method (Chomczynski and Sacchi, 1987; Wong et al., 1994). 0.1 g of frozen heart sample from the right ventricle was minced on ice and homogenized with 1 ml of Trizol. 0.2 ml of chloroform was then added and the mixture was centrifuged at 12,000 g for 15 mins at 2-8°C. Sequentially, 0.5 ml of isopropanol and 1 ml of 75% ethanol was added to the supernatant and centrifuged at 7,500 g for 5 mins. Tubes were then placed in -20°C to allow for precipitation of RNA. Total RNA was quantified

using a GeneQuant spectrophotometer (Pharmacia, Piscataway, NJ, USA). Complimentary DNA was obtained through RT–PCR by the method of Wong et al (Wong et al., 1994). Briefly, the reaction mixture containing 2 µg of the above total RNA, first-strand buffer, 20 nM of each deoxyadenosine triphosphate, deoxyguanosine triphosphate, deoxycytidine triphosphate and deoxyribosylthymidine triphosphate, 160 units of Superscript-RT, 100 pmol of random hexamer oligodeoxynucleotides and RNasin (Invitrogen, Carlsbad, CA, USA) was incubated at 20°C for 10 mins. The reverse-transcription reaction was carried out in a thermal cycler (Barnstead/ Thermolyne, Dubuque, IA, USA) at 42°C for 50 mins and heated to 95°C to stop the reaction.

The primer sequences for each gene are presented in Table 3.1. The primers were synthesized by Invitrogen (Burlington, ON, CA). The reaction mixture contained 2 µl of reverse-transcription product, 10X PCR buffer, 4 nM of each deoxynucleotide and 2 units of Taq DNA polymerase. For each gene amplified, 10 pmol of the upstream and downstream primer was used per reaction and 4 pmol of GAPDH (GibcoBRL, Burlington, ON, CA) was coamplified as an internal control. A set of 36 cycles was chosen to ensure that the amplification of PCR products was in the exponential range according to preliminary cycle test experiments. In each PCR cycle, heat denaturation was set at 94°C for 1 min, primer annealing at 60°C for 30 s and polymerization at 72°C for 1 min. PCR product (10 µl) was electrophoresed in 1.5% agarose gels containing 0.2 µl/ml of ethidium bromide. The gels were visualized by computerized ultraviolet densitometric scanning of the images using Bio-Rad Gel

Doc 2000, and analyzed by Quantity One program (Bio-Rad, Hercules, CA, USA). The results are expressed in arbitrary densitometry units normalized to GAPDH expression.

3.4 Western Blot Analysis

Western blots for PKA, COL I(α1), COL I(α2) and COL III were performed as previously described (Ma, 2006). Approximately 0.1 g of frozen heart sample from the right ventricle was homogenized in phosphate buffered saline solution (PBS: 0.137 M NaCl, 0.0027 M KCl, 0.01 M Na_2HPO_4, 0.01 M KH_2PO_4, pH 7.4). The homogenized sample was then centrifuged at 5000 rpm for 10 mins. Laemmili 2X concentrate sample buffer (Sigma Aldrich, St.Louis, MO, USA) was added to the supernatant and boiled for 5 mins. Equal amounts of the denatured proteins were loaded and separated on 8% sodium dodecyl sulphate (SDS) - 5% polyacrylamide gel by electrophoresis. The 5% polyacrylamide stocking gel contained 0.83 ml 30% acrylamide, 0.63 ml 1.5 M Tris (pH 6.8), 50 µl 10% SDS, 50 µl 10% ammonium persulfate (APS), 5 µl N,N,N',N'-tetramethylethylenediamine (TEMED) and 3.4 ml ddH_2O. While the 8% SDS gel contained 5.3 ml 30% acrylamide, 5 ml 1.5 M Tris (pH 8.8), 0.2 ml 10% SDS, 0.2 ml 10% APS, 12 µl TEMED and 9.3 ml ddH_2O. Gels were run at 100 V for an average of 2 hours in running buffer using Bio-Rad Mini Electrophoresis Unit (Hercules, CA, USA). The running buffer contained 125 mM Tris, 1.25 M glycine and 0.5% SDS. Kaleidoscope prestained standard (Bio-Rad, Hercules, CA, USA) was used as a molecular marker for the various proteins. After

electrophoresis, the proteins were transferred to nitrocellulose membrane at 100 V for 2 hours or at 40 V overnight in 4°C. Transfer buffer contained 39 mM glycine, 48 mM Tris, 0.037% SDS, 20% methanol and ddH_2O.

Once the transfer was completed, membranes were blocked with 10% (w/v) non-fat dry milk or albumin in Tween-Tris-buffered saline buffer (TBS-T: 25 mM Tris-HCl, 137 mM NaCl, 3 mM KCl and 0.1% Tween 20, pH 7.4) for 1 hour at room temperature. The blots were then rinsed with water three times for 10 s each and washed two more times in TBS-T for 5 mins each. Membranes were then incubated at room temperature for 1 hour with rabbit polyclonal anti-PKA antibody (1:1500), goat polyclonal anti-COL I(α1) antibody (1:1000), goat polyclonal anti-COL I(α2) antibody (1:1500) or rabbit polyclonal anti-COL III (1:2000) (Santa Cruz Biotechnology, Santa Cruz, CA, USA). After being washed in TBS-T buffer, the membranes were incubated with secondary antibody. Goat anti-rabbit immunoglobulin (IgG) (H+L) horseradish peroxidase (Pierce, Rockford, IL, USA) was used for PKA and COL III, diluted to 1:10000 with TBS-T and incubated for 1 hour. While donkey anti-goat (IgG) (H+L) horseradish peroxidase (Santa Cruz Biotechnology, Santa Cruz, CA, USA) was used for COL I(α1) and COL I(α2), diluted to 1:10000 with TBS-T and incubated for 1 hour. After washing in TBS-T, the blots were detected with enhanced chemiluminescence method (Pierce Super Signal Western Blot Kit, Rockford, IL, USA), followed by exposure to Kodak X-OMAT film. β-tubulin (Santa Cruz Biotechnology, Santa Cruz, CA, USA) was used as an internal control for all proteins examined. The relative expression of each protein was quantified by

computerized densitometric scanning of the images using Bio-Rad Gel Doc 2000, and analyzed by Quantity One program (Bio-Rad, Hercules, CA, USA). The results are expressed in arbitrary densitometry units normalized to internal control expression (Liu et al., 2000).

3.5 Vertical Sodium Dodecyl Sulfate (SDS)-Agarose Gel Electrophoresis (VAGE)

Protein analysis for N2B and N2BA titin were performed using the well established technique of VAGE (Granzier and Wang, 1993; Warren et al., 2003). Tissue samples ranging in weight from 8-150 mg were first ground into a powder using a mortar and pestle in liquid nitrogen, and stored in -20°C freezer for 20-60 mins. The powder was then added to sample buffer containing 8 M urea, 2 M thiourea, 3% SDS, 75 mM DTT, 0.05 M Tris-HCl, 50% glycerol and 0.03% bromophenol blue. After mixing, it was placed in a 60°C water bath for 15 mins. The solution was transferred to 1.5 ml eppendorf tubes and centrifuged for 5 mins at 13,200 g. The supernatant was placed in 50 µl aliquots, quick frozen in liquid nitrogen and stored at -80°C. Prior to each use, the samples were thawed for 30 sec in a 60°C water bath, vortexed and centrifuged. In some cases, if bands were too strong from a particular sample, it was diluted by increasing the ratio of sample buffer.

A Hoeffer SE 600 gel apparatus system (Amersham Pharmacia Biotech, San Francisco, CA, USA) was used to run the 1% VAGE. A 1-2 cm high 12% acrylamide plug was poured into the bottom of the gel sandwich to prevent the

agarose from sliding out of the glass plates once it was added. The final concentration of the acrylamide plug was 12% acrylamide (30:1 acrylamide to bisacrylamide ratio), 10% APS, 0.152% TEMED, 0.05 M Tris-base, 0.385 M glycine and 0.1% SDS. Isobutanol was overlayed on the acrylamide plug to facilitate formation of a flat acrylamide interface. The plug was left to polymerize for about 20-30 mins, and the isobutanol decanted. The resolving gel, which consisted of 1% Sea Kem Gold agarose (Cambrex Bio Science Rockland, ME, USA), 30% glycerol, 0.05 M Tris-base, 0.385 M glycine and 0.1% SDS, was stored at 4°C overnight before use. The lower chamber buffer contained 0.05 M Tris-base, 0.385 M glycine and 0.1% SDS, while the upper buffer contained the same chemicals with the addition of 10 mM β-mercaptoethanol (BME). After the lanes were cleaned and loaded with samples, the gels were run at 15 mA/gel for 3.5 hours. After running, gels were pre-soaked for 1 hour in a solution containing 20% methanol and 10% ethanol. Gels then underwent coomassie blue staining (2% phosphoric acid, 10% ammonium sulphate and 0.1% coomassie brilliant blue CBB-G250) overnight, and were destained for 1 hour in 20% methanol. This procedure was carried out first with all samples of control and BDL on one gel, followed by gels with varying loading volumes (2-11 µl) of individual sham and BDL (for example one gel would contain varying loads of Sham 1 and BDL 1, while another would contain Sham 2 and BDL 2).

Gels were scanned using a Hewlett Packard 1DScan and software from which integrated optical density (IntOD) values were obtained for each lane corresponding to titin isoforms and the internal control myosin heavy chain

(MHC). Individual linear regression analysis graphs were then created for loading values versus IntOD for N2B and MHC. The slopes were used to determine the ratio of N2B to MHC. The mean ± SD for all the combined shams was compared to the mean ± SD for the combined BDLs.

3.6 Cell Shortening

Male Sprague-Dawley rats were anesthetized with sodium pentobarbital and their hearts rapidly excised (Ward et al., 2001). The hearts were cannulated by the aorta to a Langendorff retrograde perfusion apparatus. It was perfused with 100 ml of calcium-free tyrode solution for 5–10 mins. The tyrode solution consisted of 140 mM NaCl, 5.4 mM KCl, 1 mM $MgCl_2$, 1 mM Na_2HPO_4, 5 mM HEPES and 10 mM glucose, oxygenated with 100% $O_{2;}$ pH 7.4. The heart was then perfused with a low-calcium enzyme solution, containing 250 ml of tyrode solution, 40 μM Ca^{2+} (1 M), 5 mg collagenase, 1 mg protease and 600 mg taurine for 8-10 mins. A small section of the right ventricle was removed, sliced and shaken for 10-30 mins in digestion solution containing 10 ml of tyrode solution, 100 μM Ca^{2+} (1 M), 5 mg collagenase, 1 mg protease, 25 mg taurine and 100 mg of albumin. After shaking, the digested solution was transferred to beakers containing storage solution consisting of 100 ml tyrode solution, 100 μM Ca^{2+} (1M), 250 mg taurine and 1000 mg albumin. After centrifugation, the supernatant was removed and the isolated cells resuspended in fresh storage solution. At this point, 1μl of Ca^{2+} was added at 10 mins intervals for a total of 50 mins. The isolated cells were then mounted in a chamber containing a continuous flow of

tyrode solution, oxygenated with 100% O_2, entering at one end and being removed by a SP100i syringe pump at the other end. In order to obtain a state of equilibrium, care was taken to ensure that the amount of solution being removed from the chamber equalled the amount being added to the chamber. A MyoPacer Field Stimulator (Ion Optix Corporation, MA, USA) was used to generate impulses at a constant voltage of 20 V and frequency interval of 0.3 Hz. Changes to the sarcomeres' velocity and time period of contraction and relaxation were observed through a camera connected to a Nikon Eclipse TE2000-S Microscope. All experiments were performed at room temperature of 22 ± 1 °C and over a period of 3 to 5 hours. All data was recorded and analyzed with Ion Wizard software program (Ion Optix Corporation, MA, USA). From this program, changes in velocity and time period of contraction and relaxation were determined.

3.7 Trabecula Experiments

The methods in the following sections have all been previously described (ter Keurs et al., 1980; Stuyvers et al., 1997; Stuyvers et al., 1998).

3.7.1 Superfusion and dissection solutions

A modified Hepes solution was used for the trabeculae experiments. The solution was composed of 137.2 mM NaCl, 1.2 mM $MgCl_2$, 5 mM KCl, 2.8 mM sodium acetate, 10 mM taurine, 10 mM glucose, 10 mM Hepes and 0.5 mM Ca^{2+}, oxygenated with 100% O_2 at a pH of 7.4 (adjusted with 1M NaOH). For

dissection, the solution contained the modified Hepes solution with 3 M KCl, which was used to arrest the heart after washing.

3.7.2 Trabecula dissection

Male Lewis Brown Norway rats, which possess more ideal trabeculae compared to other species of rats, were anaesthetized with isoflurane and the hearts rapidly excised. The aorta was cannulated and the heart perfused with Hepes buffer solution at room temperature, which allowed for the clearance of blood from the heart. 3 M KCl was then added to the solution to stop the beating of the heart and allow for dissection. An incision was made at the top of the heart below the base of the pulmonary artery, down the edge of the right ventricle along the coronary artery to the base of the heart (Figure 3.1). The right atrium was removed and the ventricular wall lifted outward and secured with a pin to the dissection bath. Right ventricular trabeculae were dissected by first separating the valve end from the residual atrium, and then shaping the ventricular end into a cube. Trabeculae were chosen if they met the following criteria: i) they were uniform virtually along their entire length; ii) they did not possess branches, but if they did then these branches were cut as far as possible from the muscle; iii) the dimensions of the muscle were as close as possible to the ideal measurements of 200 μm wide, 100 μm thick and 2-3 mm long.

3.7.3 Muscle mounting and stimulation

The dissected muscles were mounted in a perfusion chamber embedded in a microscope stage. The valve end was passed through a basket attached to a silicon strain gauge (Sensor One AE801, CA, USA) for measuring force. The ventricular block was made to rest in the basket, while the valve end of the muscle was attached to a stainless steel motor arm hook that was used to stretch the muscle throughout the experiment. Once positioned, the muscle was covered with a glass cover slip to prevent the formation of a meniscus and to allow for uniform flow of the hepes solution. It was important that muscles were mounted in such a way that they showed no evidence of twisting or non-uniform shortening when stimulated. Once properly mounted, oxygenated hepes solution was circulated through the chamber.

The muscles were stimulated at 0.3 Hz with 5 ms pulses 50% above threshold for 30 mins so as to train the muscle. The stimulus was generated by the voltage stimulator Grass S48 Stimulator, Grass Instruments, MA, USA), while the Digitimer Model D4030 (United Kingdom) was used as a timing device to trigger the stimulator. Beginning at slack sarcomere length (the length at which the muscle exerted the least force), the muscles were stretched in increments of 0.05 μm to a maximum sarcomere length of 2.30 μm. During the experiment temperature was regulated at 25.3 ± 0.6°C by a water bath (Haake FK2, Germany), and the perfusion flow was carefully adjusted in order to prevent noise on force and sarcomere length signals.

3.7.4 Force-sarcomere length measurements

Force was measured by a silicon strain gauge (Sensor One AE801, CA, USA) with a resolution of 0.63 μN (Figure 3.2). The force transducer was attached to the ventricular end of the muscle and the sensitivity of the strain gauge was increased by the addition of a stiff carbon fibre rod 8 mm long basket. Linear regression through the values of the maximal force variations (dF) and the corresponding length variation (dL) followed dF = *a*dL, where *a*= 114mN μm^{-1} (r = 0.99) (Stuyvers et al., 1997). Sarcomere length was measured by laser diffraction techniques based on the principle that a diffraction pattern can form once laser is passed through a diffraction grating to provide a resolution. The wavelength of the monochromatic incident light must be the same order of magnitude as that of the grating to allow for a good resolution. The source of the monochromatic light in these experiments was a 5 mW helium-neon (He-Ne) laser with a wavelength of 0.6328 μm (Spectra Physics, USA). The trabeculae muscle act as multiple slits of grating and therefore can diffract the incident light of the laser beam into a zero-order band and multiple symmetrical diffraction band pairs. These diffractions occur at a series of orders predicted by Bragg equation. Sarcomere length was calculated from the median position of the intensity distribution of each of the first-order bands, which was scanned at 2 kHz by a photodiode array (Reticon 256 EC, Sunnyvale, CA, USA). The laser beam was considered to be perpendicular to the long axis of the muscle when the sarcomere length signals from both detectors were identical. Prior to each experiment, the machine was calibrated using calibration gratings. Sarcomere

length and force signals were monitored on a digital oscilloscope (Hitachi Model V680, Japan) and a chart recorder (Gould Model 2800S, Cleveland, OH, USA), and recorded via an analog-digital (A-D) converter with a sampling rate of 9 kHz and attached to a computer. The A-D converter has the ability to convert the output to a voltage proportional sarcomere length. During each experiment, care was taken to ensure that the same area of the muscle was measured as it was stretched. Data was analyzed using Laboratory Virtual Instrumentation Engineering Workbench (LabVIEW) program (National Instruments Corporation, Austin, TX, USA)

3.8 Statistical Analysis

Statistics were performed using a commercially available software program GraphPad InStat (Version 3.05, GraphPad Software Inc., San Diego, CA, USA). The results were expressed as mean ± SD. For all studies, Student's t-test was used to analyze the two groups, except for passive tension studies where Wilcoxon Signed-Rank Test was used. A P-value of < 0.05 was considered significantly different.

Table 3.1 Primers used for RT-PCR

Name	Primer Sequence	Product (base pair, bp)
PKA	Upstream 5'-CCGAGAACCTTCTCATCGAC-3' Downstream 5'-GTAACCAGCAGCCATCTCGT-3'	200
N2B	Upstream 5'-ACCGTCCACCTTACGTCATC-3' Downstream 5'-GACGTCATTGCTTTCCCATT-3'	197
N2BA	Upstream 5'-AATGCCATGTCACAGGAACA-3' Downstream 5'-GGCTGTGCAGGAGTCTTTTC-3'	200
COL 1(α1)	Upstream 5'-GCCAAGAAGACATCCCTGAA-3' Downstream 5'-CTTCTGGGCAGAAAGGACAG-3'	201
COL 1(α2)	Upstream 5'-TTGACCCTAACCAAGGATGC-3' Downstream 5'-CACCCCTTCTGCGTTGTATT-3'	197
COL III	Upstream 5'-TGGTTTCTTCTCACCCTGCT-3' Downstream 5'-GGGCAGTCTAGTGGCTCATC-3'	200
GAPDH	Upstream 5'-CGGAGTCAACGGATTTGGTCGTAT-3' Downstream 5'-AGCCTTCTCCATGGTGGTGAAGAC-3'	306

Figure 3.1 Schematic representation of trabecula dissection from the right ventricle of the rat heart. (Kindly provided by Dr. H.E.D.J ter Keurs)

(i)

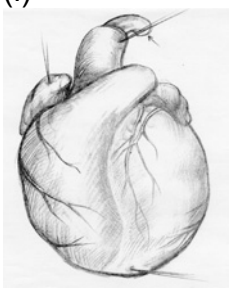

(ii)

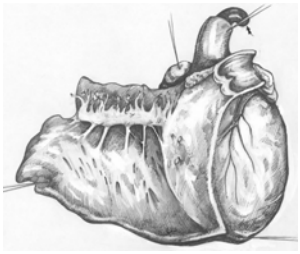

(iii)

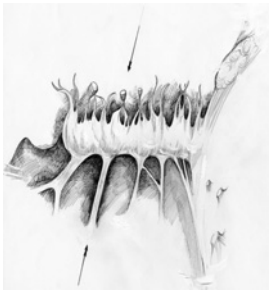

(iv)

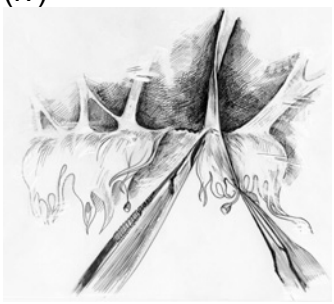

(v)

Figure 3.2 Schematic diagram of experimental setup for recording force-sarcomere length measurements in trabeculae experiments (Kindly provided by Dr. H.E.D.J. ter Keurs)

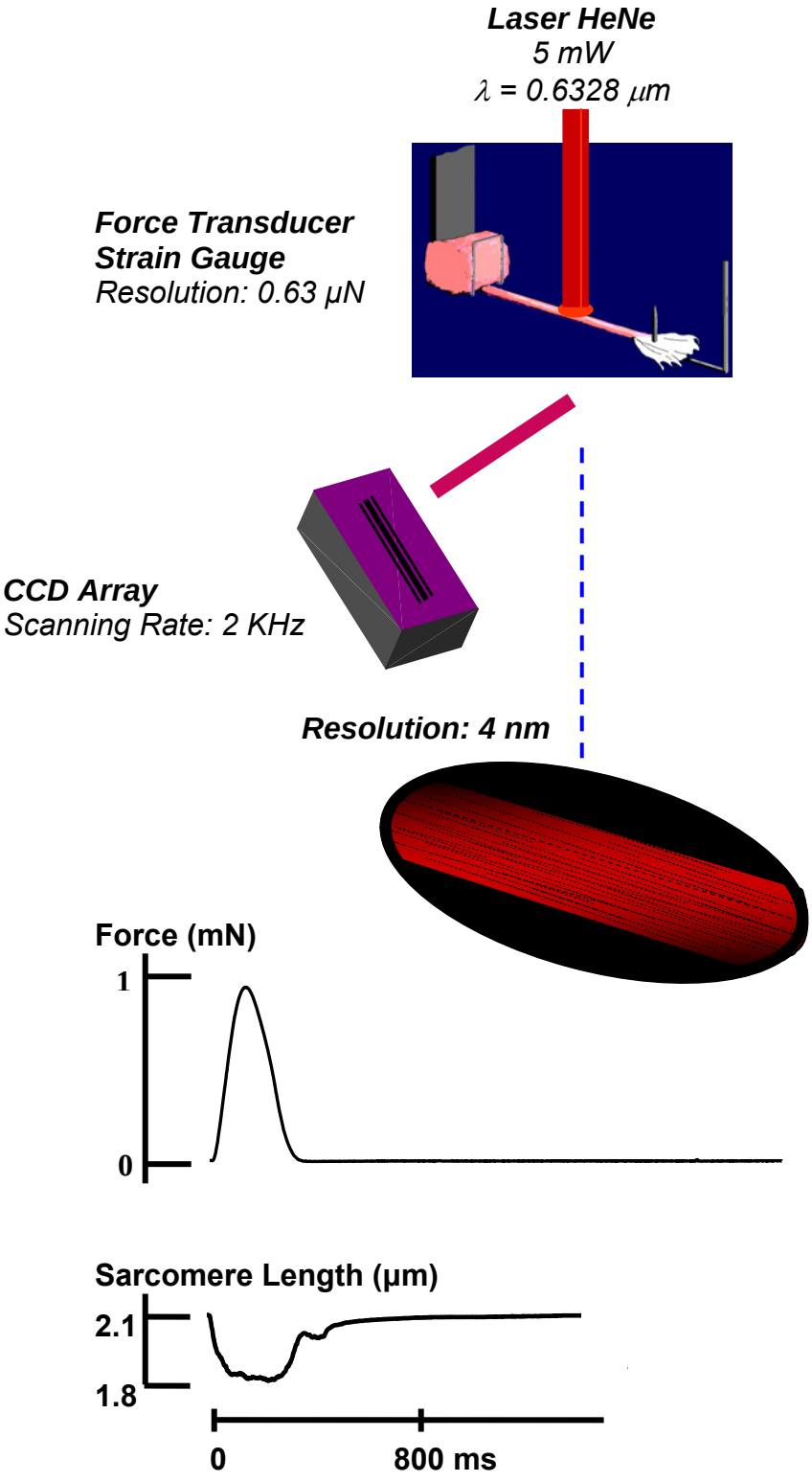

CHAPTER FOUR: RESULTS

4.1 Evidence of impaired cardiac function

Isolated cardiomyocytes from cell shortening techniques as well as trabeculae muscles from the right ventricle wall of the heart were used to analyze cardiac function - both systolic and diastolic function - in the sham and BDL groups.

4.1.1 Isolated cardiomyocyte functioning

Isolated cardiomyocytes showed significant changes in cardiac contractility and relaxation. Maximum systolic velocity, which represents the speed of contraction, was significantly decreased in the BDL cirrhotic group (sham: 2.10 ± 0.48 μm/s vs BDL: 0.80 ± 0.19 μm/s; n = 11; $p < 0.05$) (Figure 4.1). This decrease in systolic functioning corresponded to an increase in the time taken by the cells to complete full contraction (sham: 0.27 ± 0.04 s vs BDL: 0.32 ± 0.06 s; n = 11; $p < 0.05$) (Figure 4.2). In terms of diastolic functioning, diastolic return velocity or the speed of relaxation was significantly decreased in the cirrhotic animals (sham: 1.68 ± 0.19 μm/s vs BDL: 0.42 ± 0.15 μm/s; n = 11; $p < 0.05$) (Figure 4.3). The BDL cardiomyocytes also showed a significant increase in the time taken to complete full relaxation (sham: 0.38 ± 0.05 s vs 0.51 ± 0.13 s; n = 11; $p < 0.05$) (Figure 4.4). In looking at the diastolic interval, it was seen that the time taken to return to 50% and 80% baseline sarcomere length was significantly increased in the BDL animals (0.54 ± 0.13 s and 0.62 ± 0.13 s

respectively; n = 11; $p < 0.05$) compared to the sham-control group (0.39 ± 0.05 s and 0.43 ± 0.06 s respectively; n = 11; $p < 0.05$) (Figure 4.5).

4.1.2 Isolated trabeculae functioning

Trabeculae muscles showed an exponential rise in passive tension as the muscle was stretched. At the initial sarcomere lengths, each muscle consistently showed only a small change in passive tension as the sarcomere was stretched. However, this change in passive tension became much steeper at sarcomere lengths of 2.15 μm and greater. These changes could be observed in both sham and BDL animals. But in comparison to sham animals, the BDL group showed a significant increase in passive tension as the sarcomere was stretched (sham: 0.79 ± 1.34 mN/mm^2 BDL: 3.44 ± 4.50 mN/mm^2; n = 9 sarcomere lengths measured for 5 animals in each group; $p = 0.027$) (Figure 4.6).

4.2 Titin mRNA and protein expression

mRNA expression for N2B and N2BA titin from rat ventricles are shown in Figures 4.7 and 4.8 respectively. RT-PCR experiments showed no significant difference in band intensity between the sham and BDL groups. This was also confirmed using densitometry analysis, which showed no significant difference in either N2B or N2BA expression between the two groups. N2B had an expression level of 1.00 ± 0.02 $uOD*mm^2$ for sham and 0.97 ± 0.05 $uOD*mm^2$ for

BDL ($p = 0.43$), while N2BA levels were 0.9 ± 0.05 uOD*mm^2 and 0.88 ± 0.03 uOD*mm^2 in the sham and BDL groups respectively ($p = 0.26$).

Protein expression of N2B and N2BA from VAGE are shown in Figure 4.9. N2BA protein expression was absent in both the sham and BDL groups, while N2B titin protein levels showed no significant difference between the two groups. Linear regression analysis for N2B and MHC plotted against increasing loading volumes of each sample revealed linear graphs with a squared regression value of 95% or greater for both sham and BDL animals (Figure 4.10 and 4.11 respectively). The ratio of N2B to MHC obtained from the slope of these graphs showed an insignificant difference in the ratio of N2B to MHC in BDL animals (sham: 0.15 ± 0.04 uOD*mm^2 vs BDL: 0.11 ± 0.02 uOD*mm^2; $n = 4$; $p = 0.33$) (Figure 4.12).

4.3 PKA mRNA and protein expression

A representative RT-PCR photograph of PKA mRNA expression in sham and BDL ventricles is shown in Figure 4.13. PKA gene expression was significantly decreased in the BDL rats. Densitometry analysis revealed an approximately 35% decrease in PKA mRNA expression in the cirrhotic animals (0.27 ± 0.03 uOD*mm^2 in sham versus 0.18 ± 0.03 uOD*mm^2 in BDL; $n = 5$; $p = 0.0004$).

Western blot analysis confirmed that this decrease in PKA at the mRNA level corresponded to a significant decrease in PKA at the protein level in the

BDL groups (1.08 ± 0.13 uOD*mm^2; n = 3; p = 0.04) compared to the sham-control animals (0.85 ± 0.10 uOD*mm^2; n = 4) (Figure 4.14).

4.4 COL I and III mRNA and protein expression

COL I is known to consist of two α1 chains and one α2 chain. This configuration was confirmed in this study, which showed that the α1 and α2 expression were present both at the mRNA and protein levels in our animals. RT-PCR showed that both COL I(α1) and COL I(α2) are significantly increased in the BDL group (1.20 ± 0.18 uOD*mm^2 and 1.36 ± 0.04 uOD*mm^2; n = 5 and 6 respectively; p = 0.02) compared to the sham animals (0.98 ± 0.03 uOD*mm^2 and 1.30 ± 0.03 uOD*mm^2; n = 6 and 5 respectively) (Figure 4.15 and Figure 4.16 respectively). This increase was also observed in BDL rats at the protein level (COL I(α1): 0.16 ± 0.02 uOD*mm^2 for sham vs 0.26 ± 0.03 uOD*mm^2 for BDL; n = 4; p = 0.007 and COL I(α2): 0.26 ± 0.04 uOD*mm^2 in sham; n = 4 vs COL I(α1) and 0.36 ± 0.03 uOD*mm^2 in BDL; n = 3; p = 0.018). Figures 4.17 and 4.18 show the protein expression of COL I(α1) and COL I(α2) respectively in sham and BDL animals.

On the other hand, COL III, which is composed of only α1 chains, showed a significant reduction in mRNA expression in the BDL animals compared to the sham group (sham: 1.11 ± 0.03 uOD*mm^2; n = 3 vs BDL: 0.90 ± 0.02 uOD*mm^2; n = 4; p = 0.006) (Figure 4.19). Protein expression of COL III also showed a significant decrease in BDL animals (sham: 1.51 ± 0.15 uOD*mm^2 vs BDL: 1.23 ± 0.09 uOD*mm^2; n = 4; p = 0.016) (Figure 4.20). Therefore, there is a switch in

the cirrhotic heart leading to an increase in the ratio of COL I to COL III through an increased synthesis of COL I both at the mRNA and protein level.

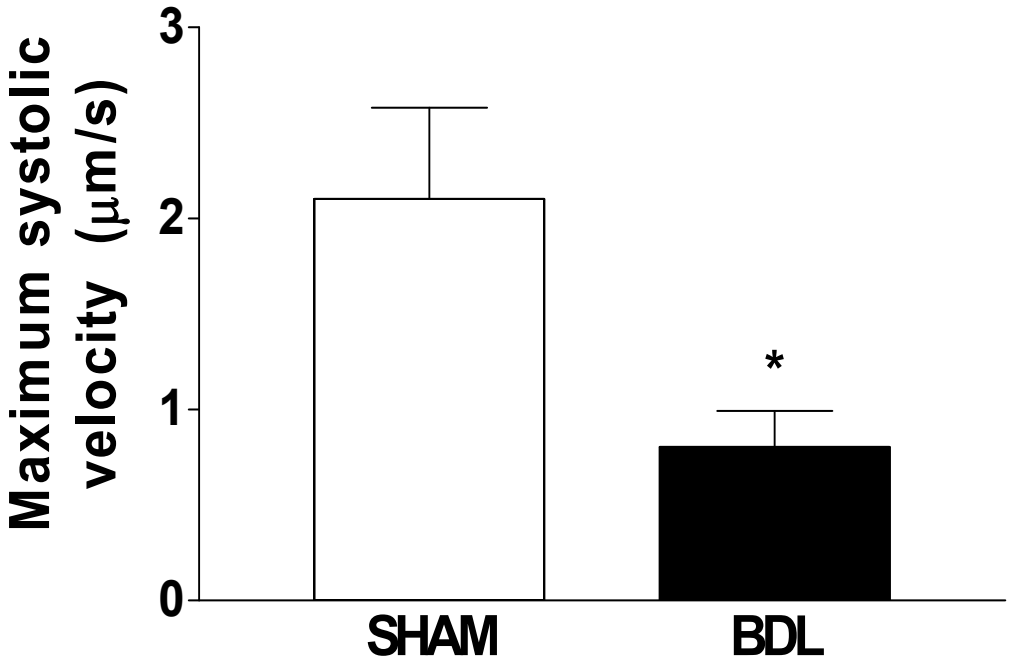

Figure 4.1 Comparison of maximum systolic velocity in isolated cardiomyocytes from sham (n = 11) and BDL (n = 11) groups. Data represented as mean ± SD. *p<0.05, significantly different compared to response in sham group.

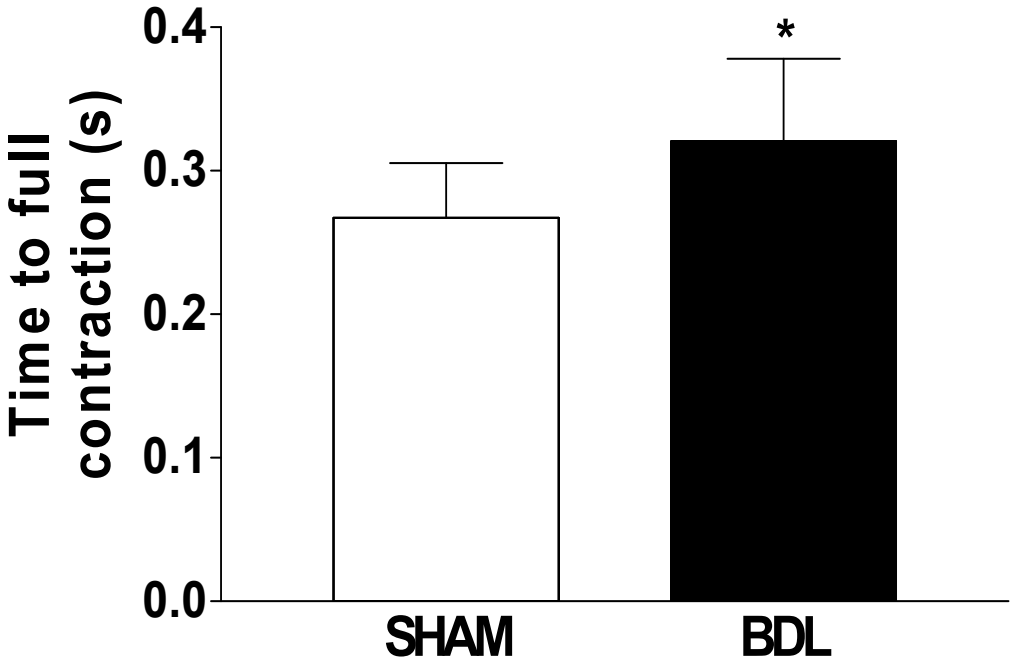

Figure 4.2 Time to complete full contraction in isolated cardiomyocytes from sham (n = 11) and BDL (n = 11) groups. Data represented as mean ± SD. *p<0.05, significantly different compared to response in sham group.

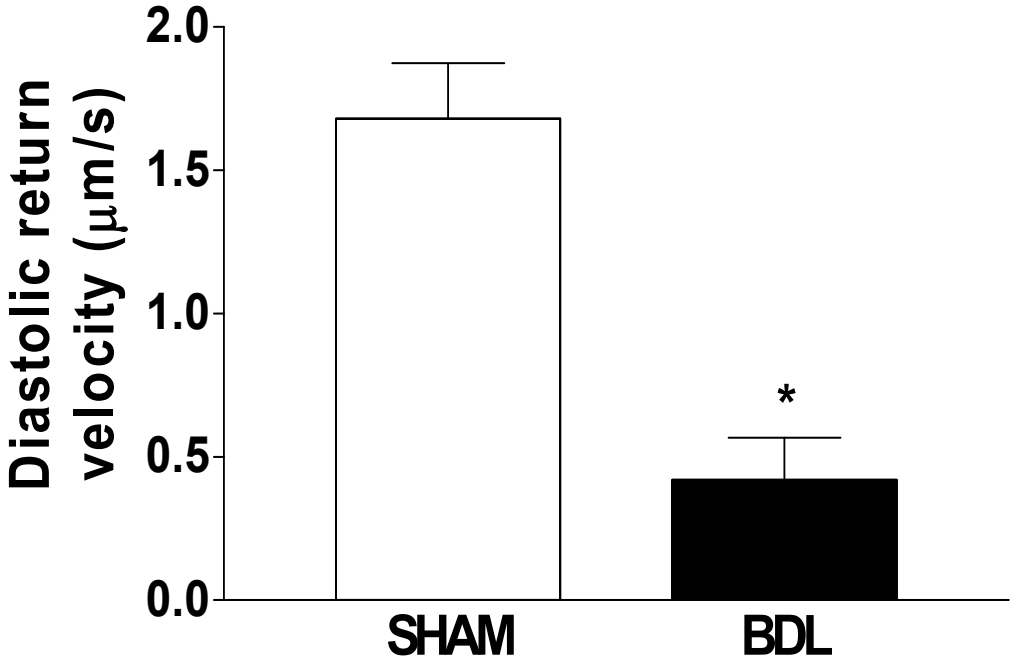

Figure 4.3 Comparison of diastolic return velocity in isolated cardiomyocytes from sham (n = 11) and BDL (n = 11) groups. Data represented as mean ± SD. *p<0.05, significantly different compared to response in sham group.

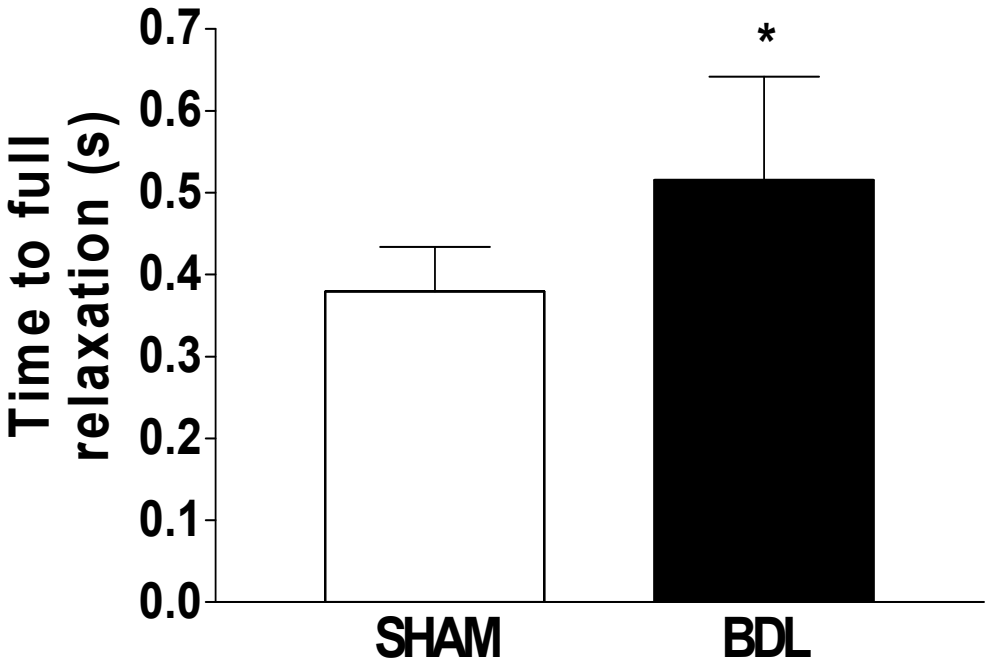

Figure 4.4 Time to complete full relaxation in isolated cardiomyocytes from sham (n = 11) and BDL (n = 11) groups. Data represented as mean ± SD. *p<0.05, significantly different compared to response in sham group.

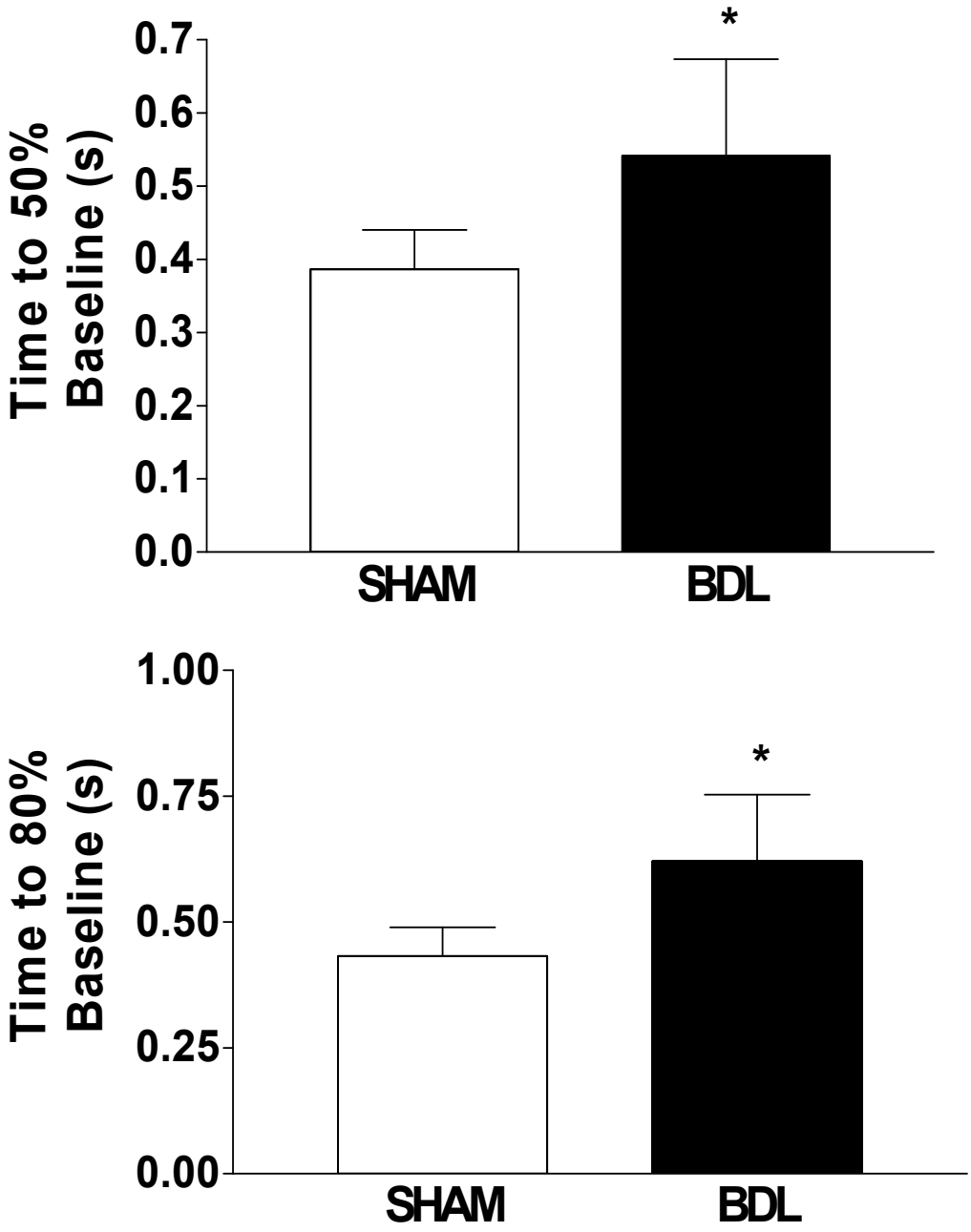

Figure 4.5 Examination of the diastolic interval at 50% and 80% of return to baseline sarcomere length in isolated cardiomyocytes from sham (n = 11) and BDL (n = 11) groups. Data represented as mean ± SD. *p<0.05, significantly different compared to response in sham group.

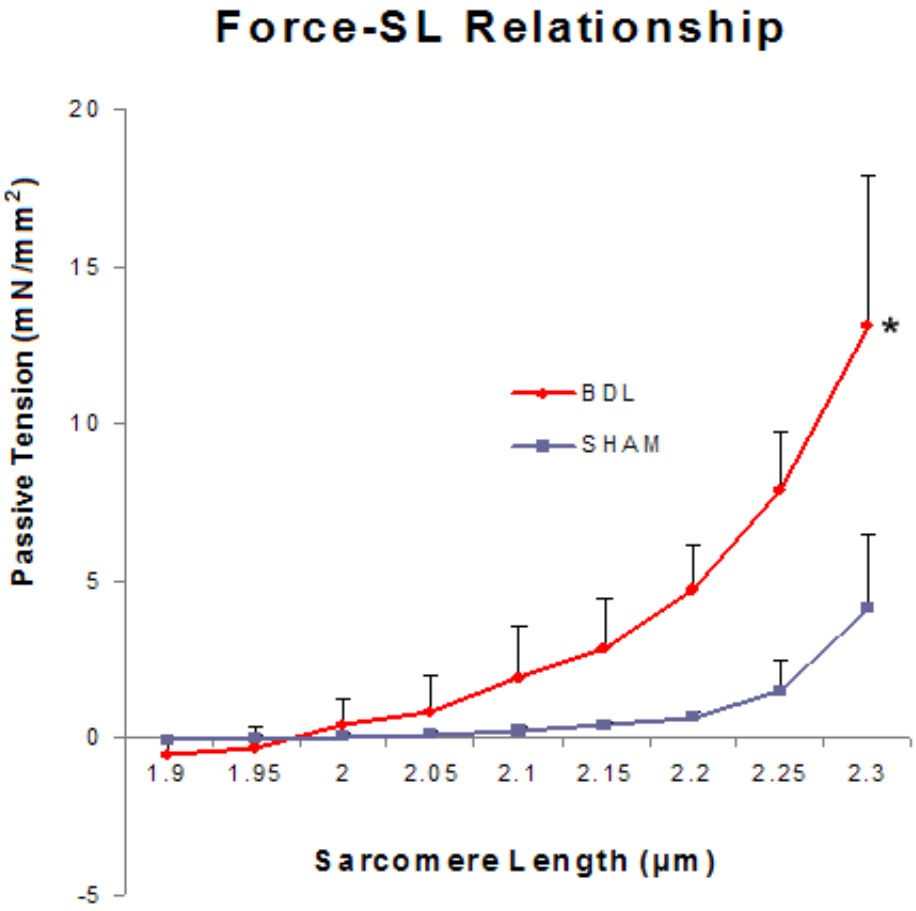

Figure 4.6 Passive tension in trabeculae muscles isolated from the right ventricle of sham (n = 5) and BDL heart (n = 5) as a measurement of force versus sarcomere length. Data represented as mean ± SD. *p = 0.027, significantly different compared to response in sham group.

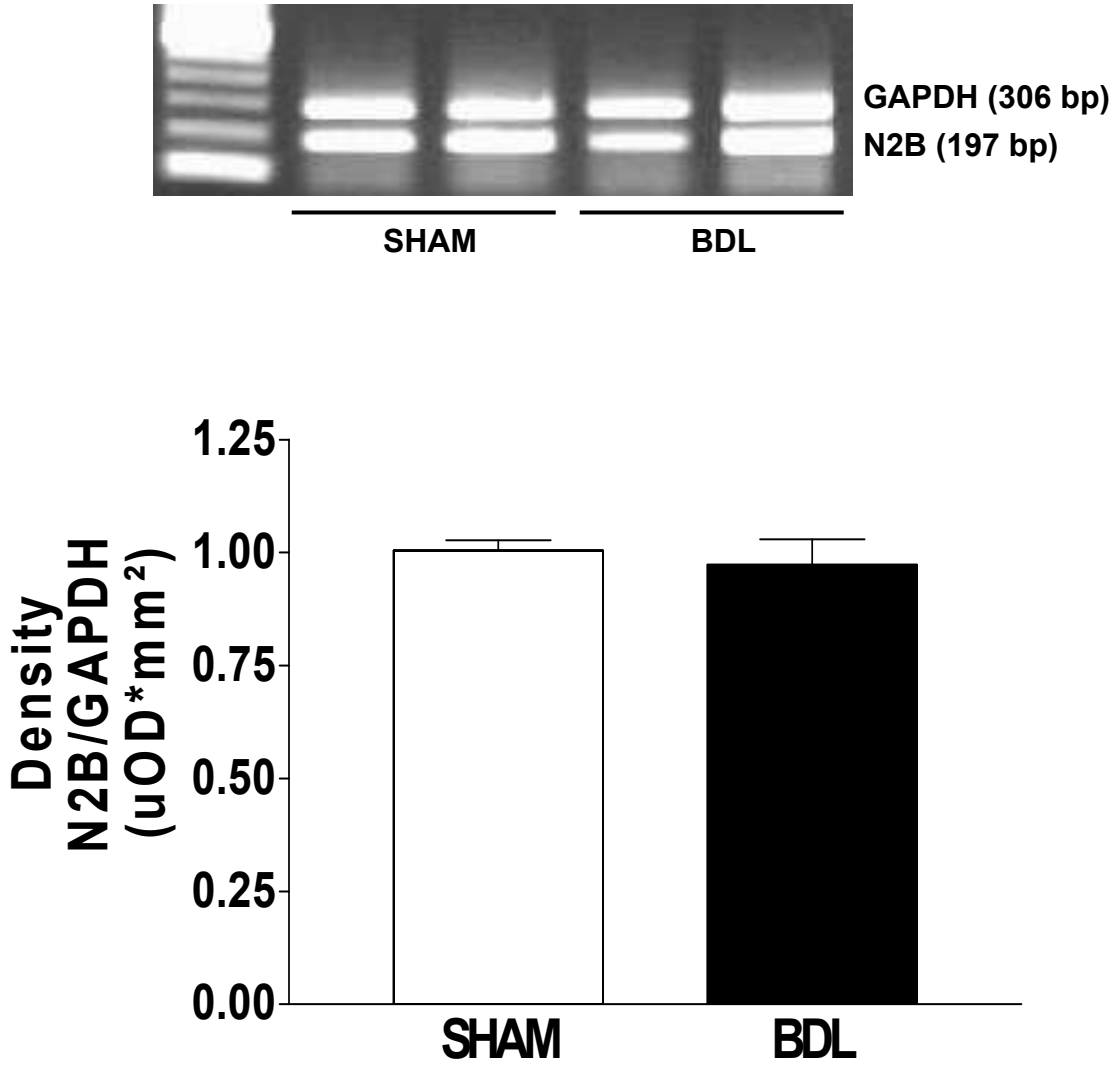

Figure 4.7 mRNA expression of N2B titin in ventricular homogenates using RT-PCR (top) and densitometry analysis (bottom). *Lane 1*, 1 kilobase DNA ladder; *lanes 2* and *3*, sham; *lanes 4* and *5*, BDL. Data represented as mean ± SD. There was no significant difference in band intensity between sham (n = 3) and BDL (n = 3) (p = 0.43).

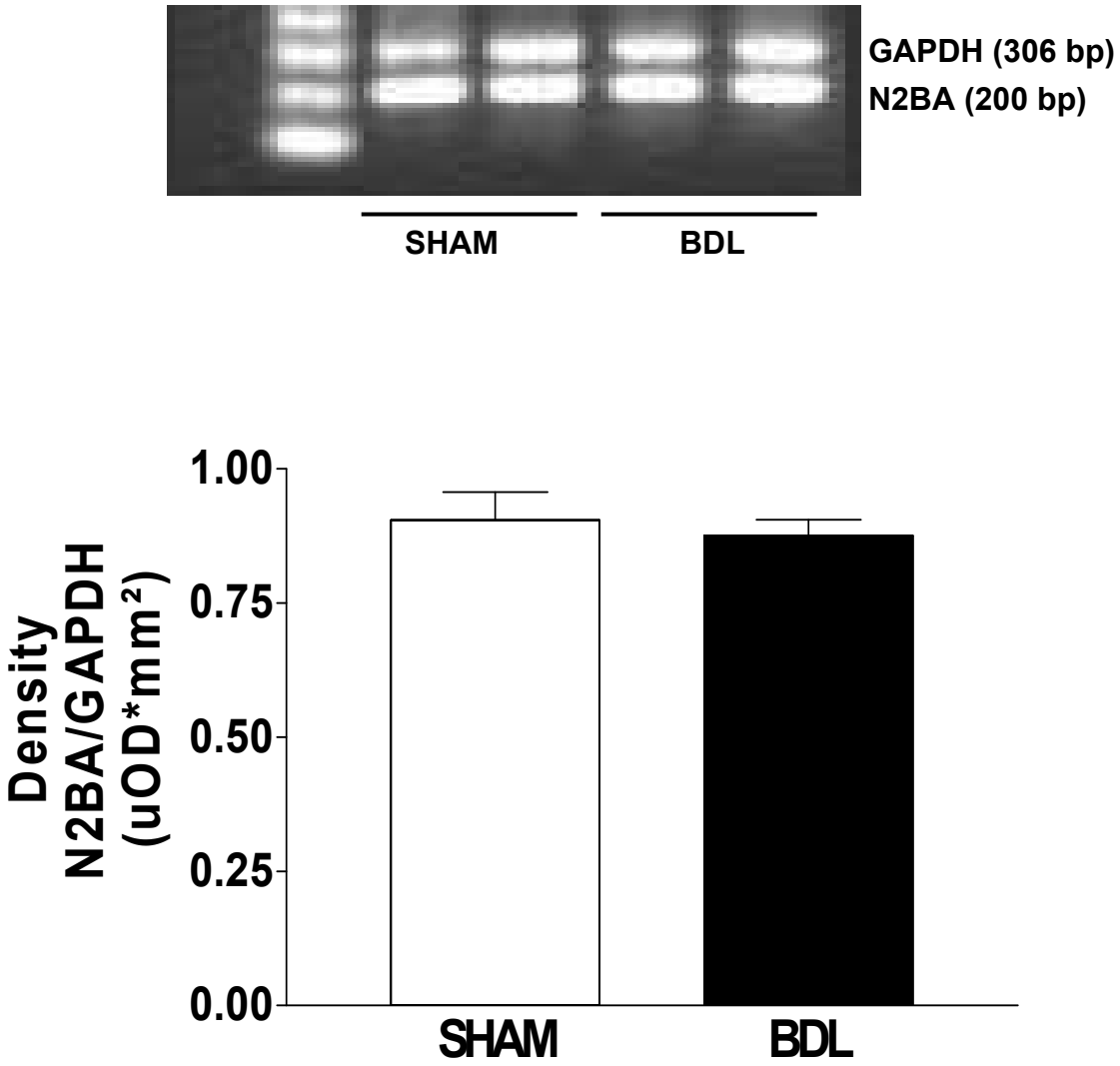

Figure 4.8 mRNA expression of N2BA titin in ventricular homogenates using RT-PCR (top) and densitometry analysis (bottom). *Lane 1*, 1 kilobase DNA ladder; *lanes 2* and *3*, sham; *lanes 4* and *5*, BDL. Data represented as mean ± SD. There was no significant difference in band intensity between sham (n = 6) and BDL (n = 6) (p = 0.26).

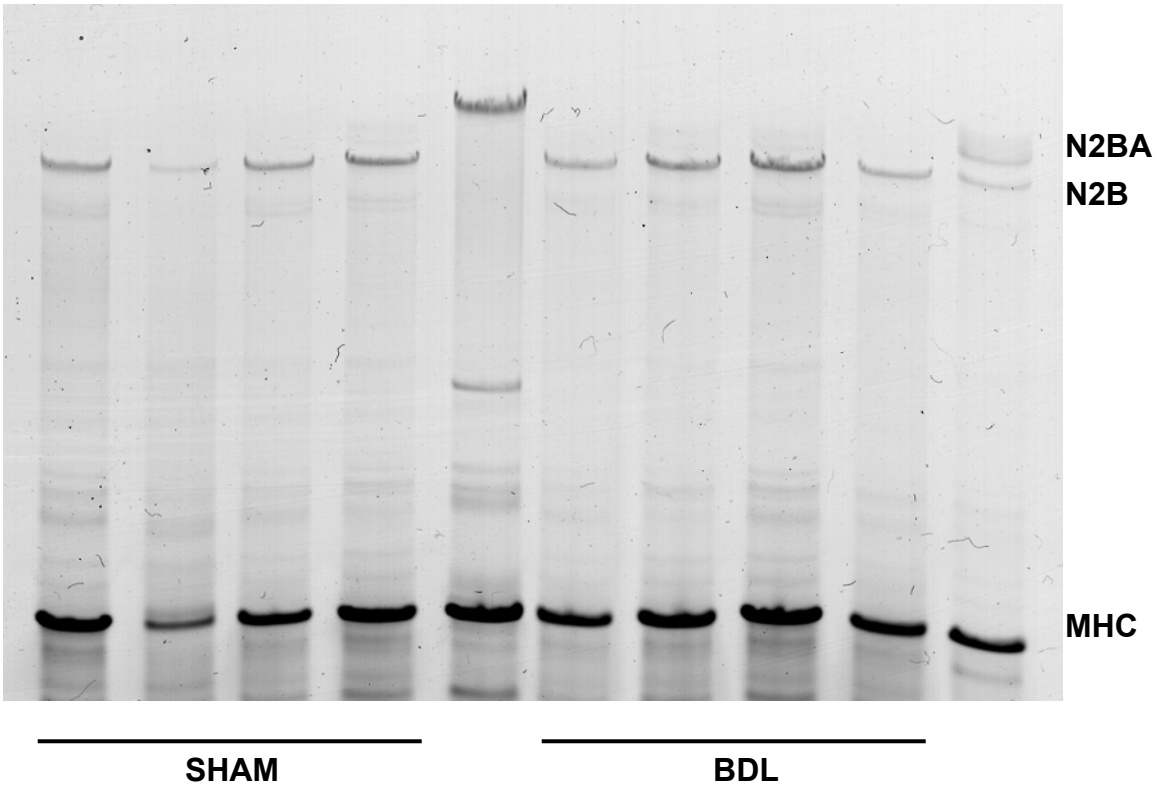

Figure 4.9 VAGE of ventricular homogenates from sham (n = 4) and BDL (n = 4) groups. *Lanes 1-4,* sham; *lane* 5, rabbit soleus N2BA skeletal marker; *lanes 6-9*, BDL.; *lane* 10, bovine left ventricle N2B and N2BA marker. N2BA ~ 3.3 MDa; N2B ~ 3 MDa; MHC ~ 205 kDa.

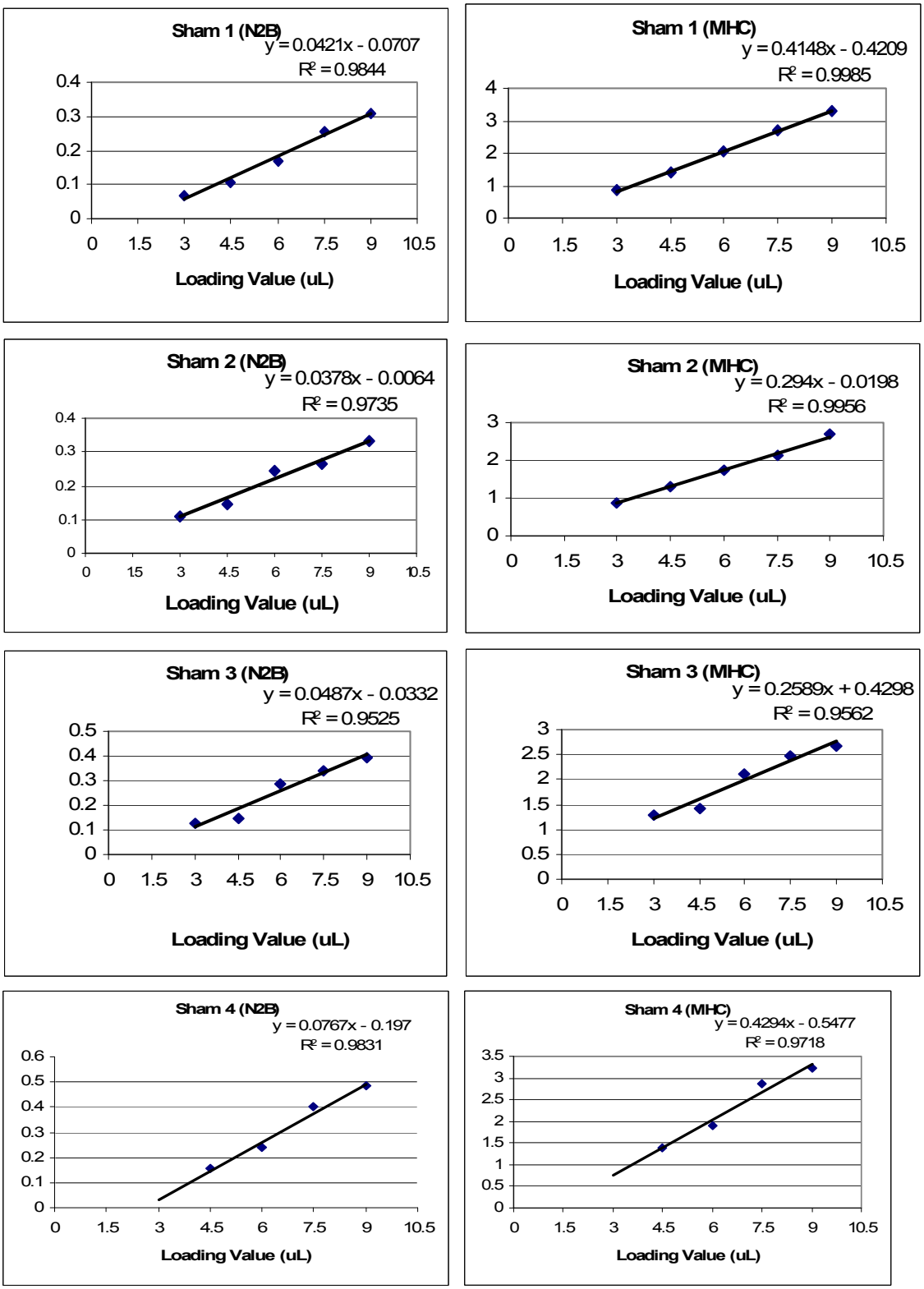

Figure 4.10 Linear regression analysis of N2B and MHC from various loading volumes of each sham ventricular homogenate using VAGE.

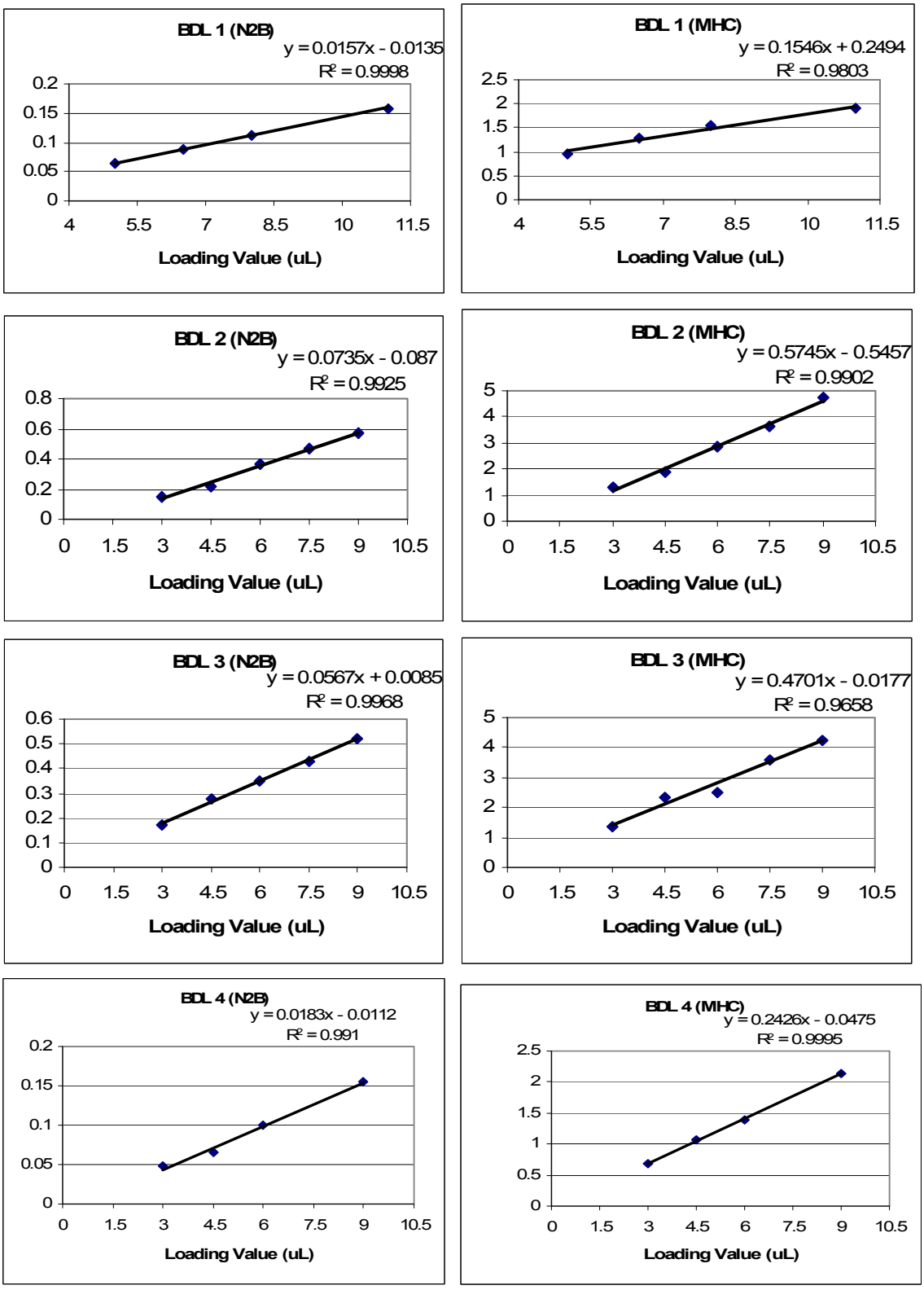

Figure 4.11 Linear regression analysis of N2B and MHC versus various loading volumes of each BDL ventricular homogenate using VAGE.

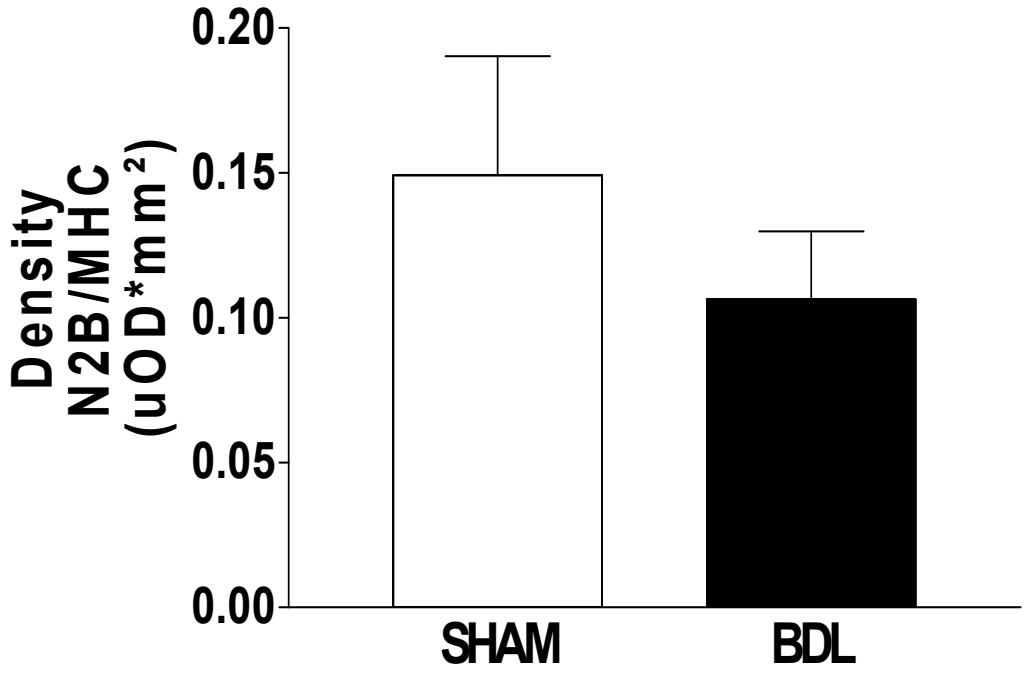

Figure 4.12 Densitometry analysis of protein expression of N2B titin from VAGE. Data represented as mean ± SD. There was no significant difference between sham (n = 4) and BDL (n = 4) (p = 0.33).

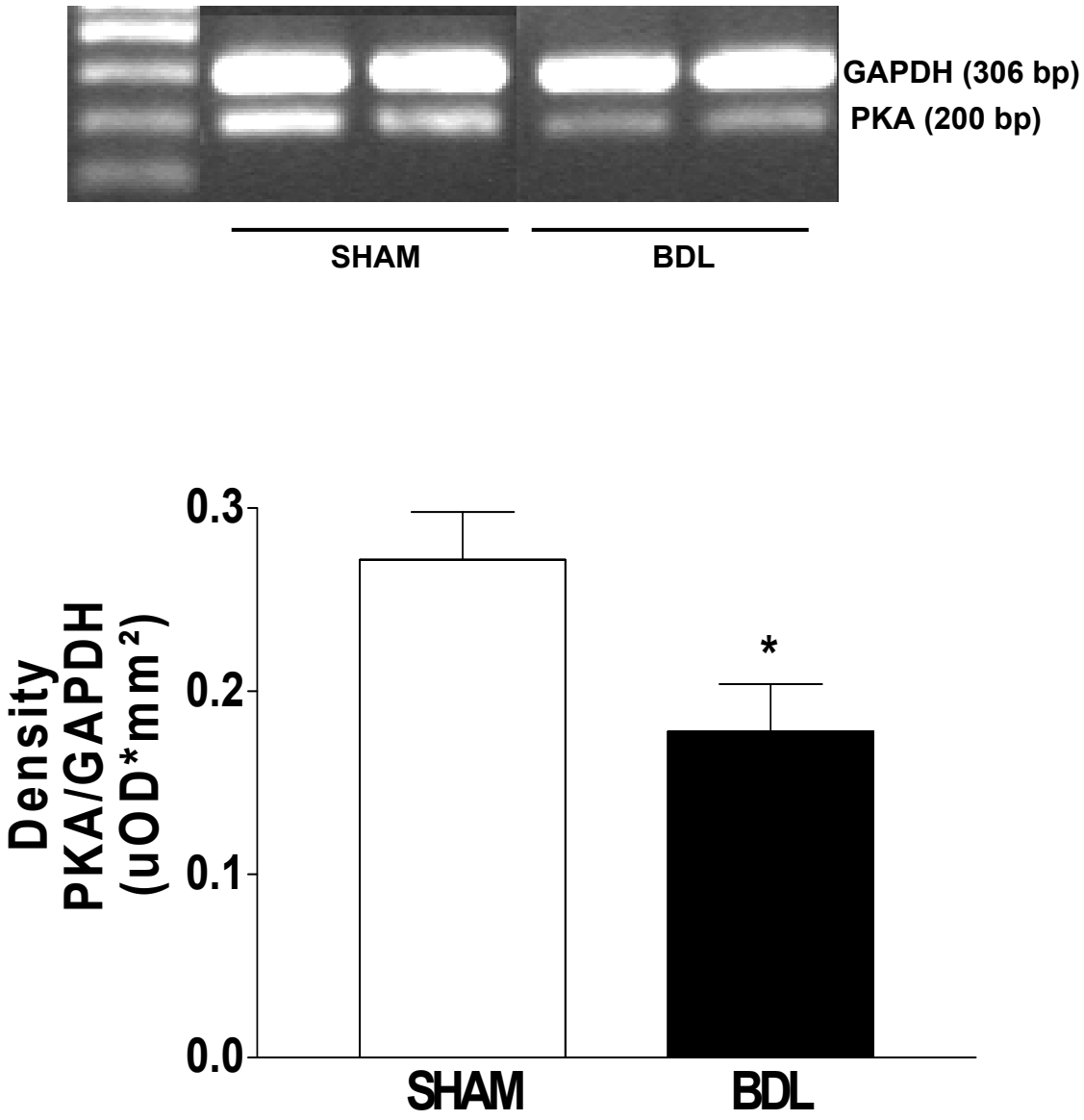

Figure 4.13 mRNA expression of PKA in ventricular homogenates using RT-PCR (top) and densitometry analysis (bottom) from sham (n = 5) and BDL (n = 5). *Lane 1*, 1 kilobase DNA ladder; *lanes 2* and *3*, sham; *lanes 4* and *5*, BDL. Data represented as mean ± SD. *p = 0.0004, significantly different compared to levels in sham group.

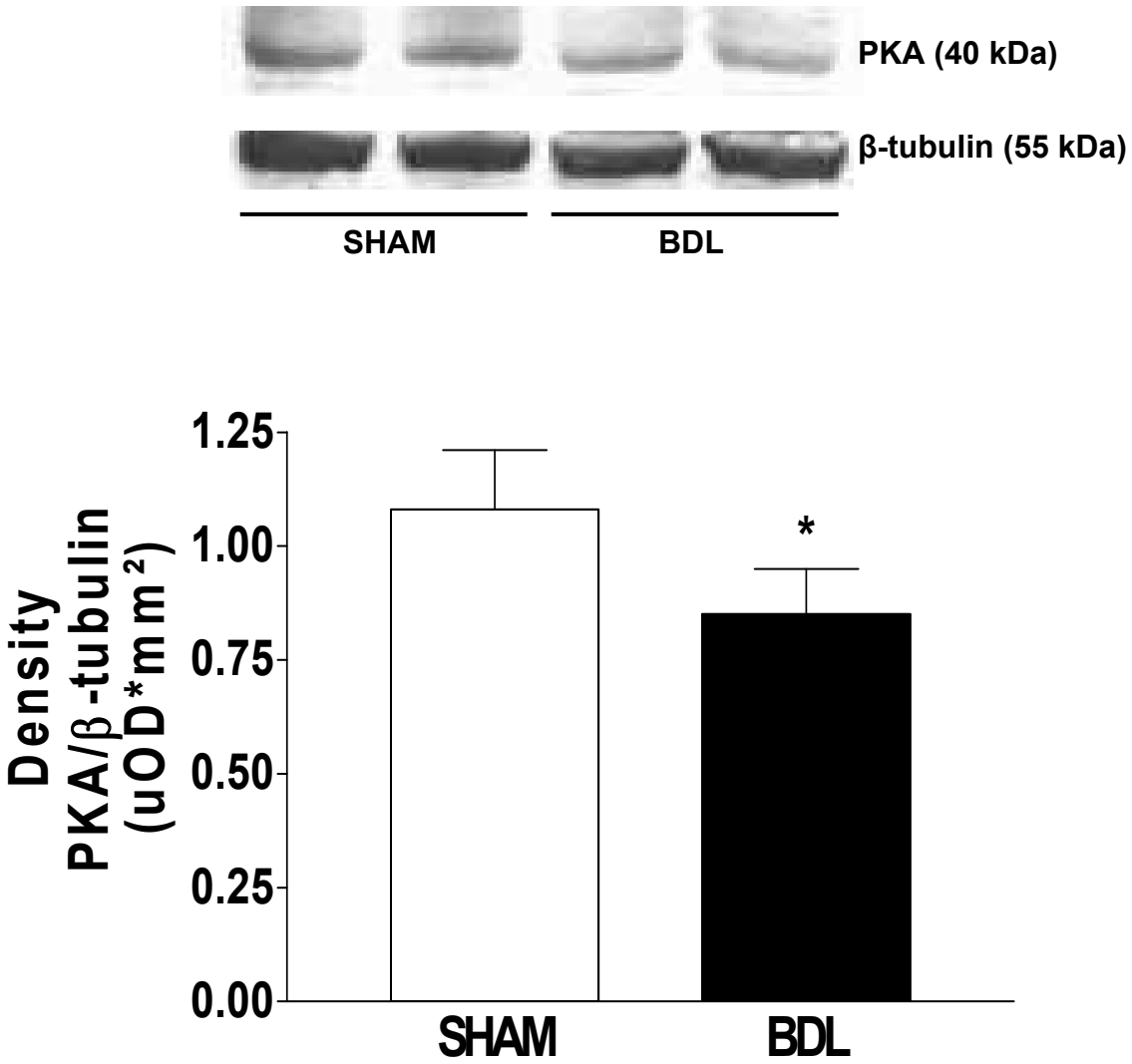

Figure 4.14 Western blot protein expression of PKA in ventricular homogenates (top) and densitometry analysis (bottom) from sham (n = 4) and BDL (n = 3). *Lanes 1* and *2*, sham; *lanes 3* and *4*, BDL. Data represented as mean ± SD. *p = 0.04, significantly different compared to levels in sham group.

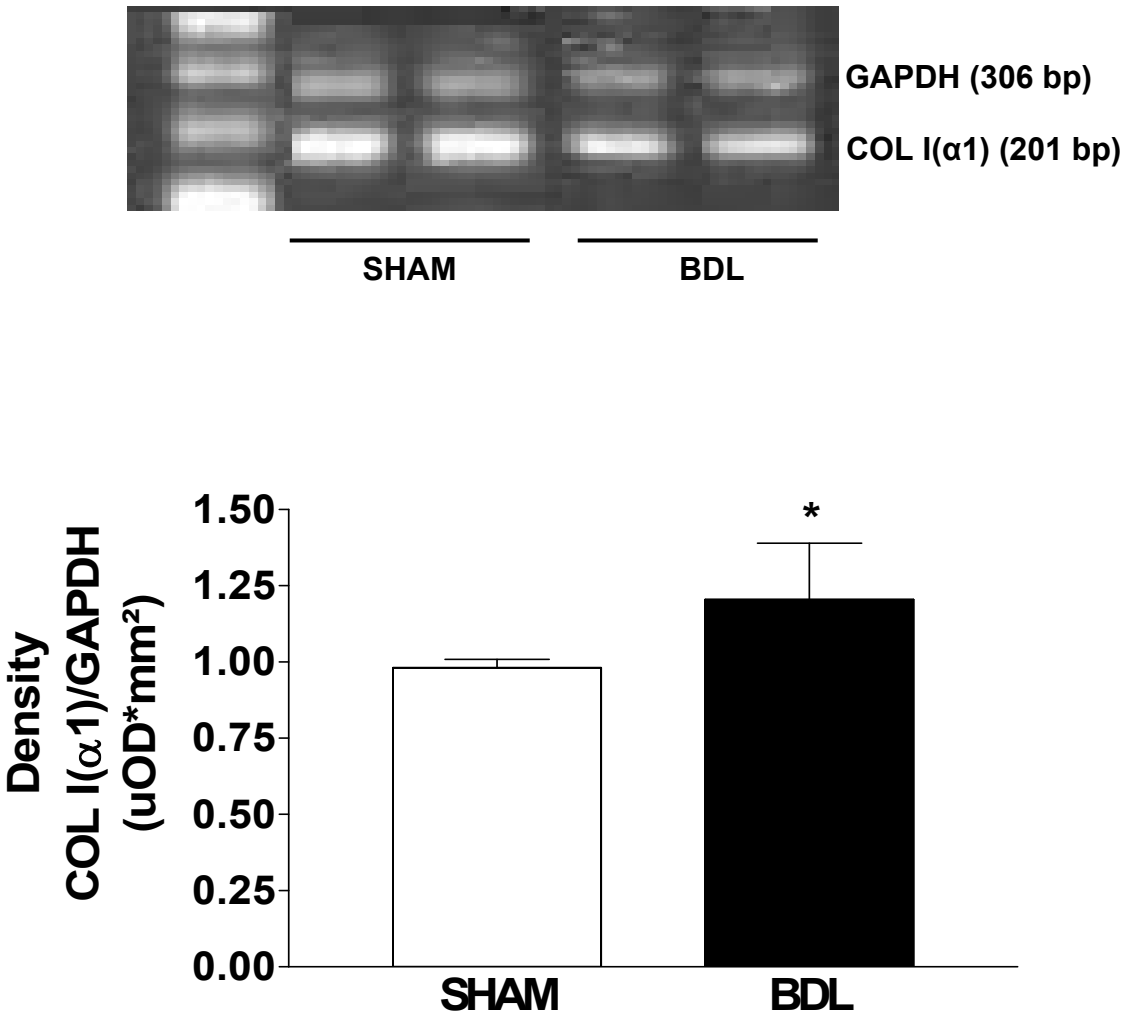

Figure 4.15 mRNA expression of COL I(α1) in ventricular homogenates using RT-PCR (top) and densitometry analysis (bottom) from sham (n = 6) and BDL (n = 5). *Lane 1*, 1 kilobase DNA ladder; *lanes 2* and *3*, sham; *lanes 4* and *5*, BDL. Data represented as mean ± SD. *p = 0.016, significantly different compared to levels in sham group.

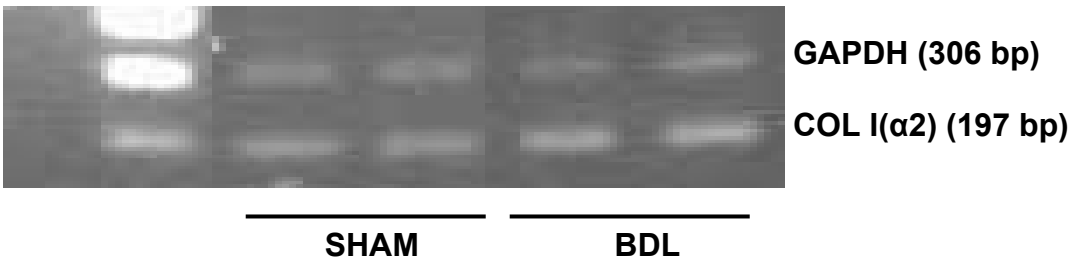

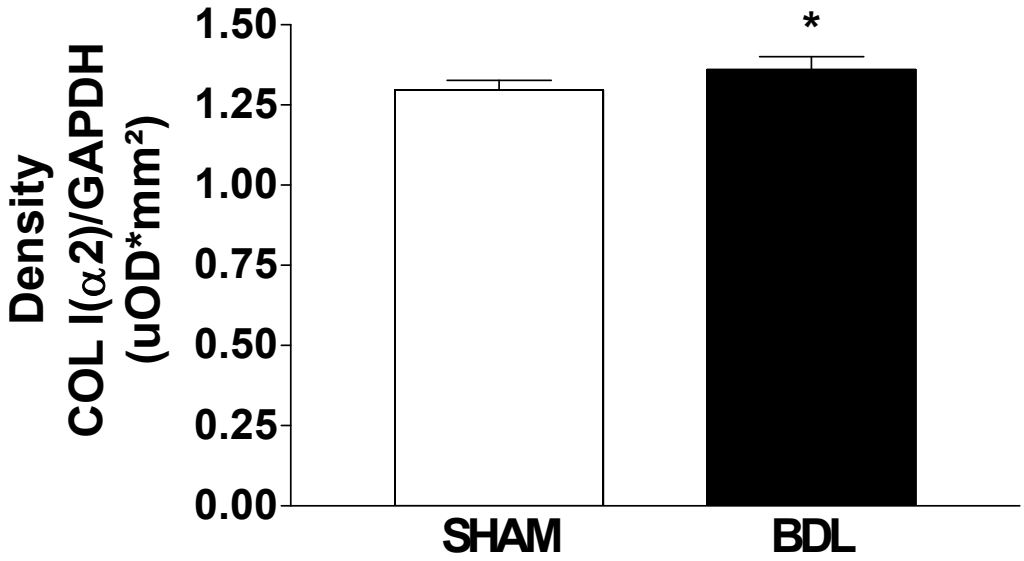

Figure 4.16 mRNA expression of COL I(α2) in ventricular homogenates using RT-PCR (top) and densitometry analysis (bottom) from sham (n = 5) and BDL (n = 6). *Lane 1*, 1 kilobase DNA ladder; *lanes 2* and *3*, sham; *lanes 4* and *5*, BDL. Data represented as mean ± SD. *p = 0.018, significantly different compared to levels in sham group.

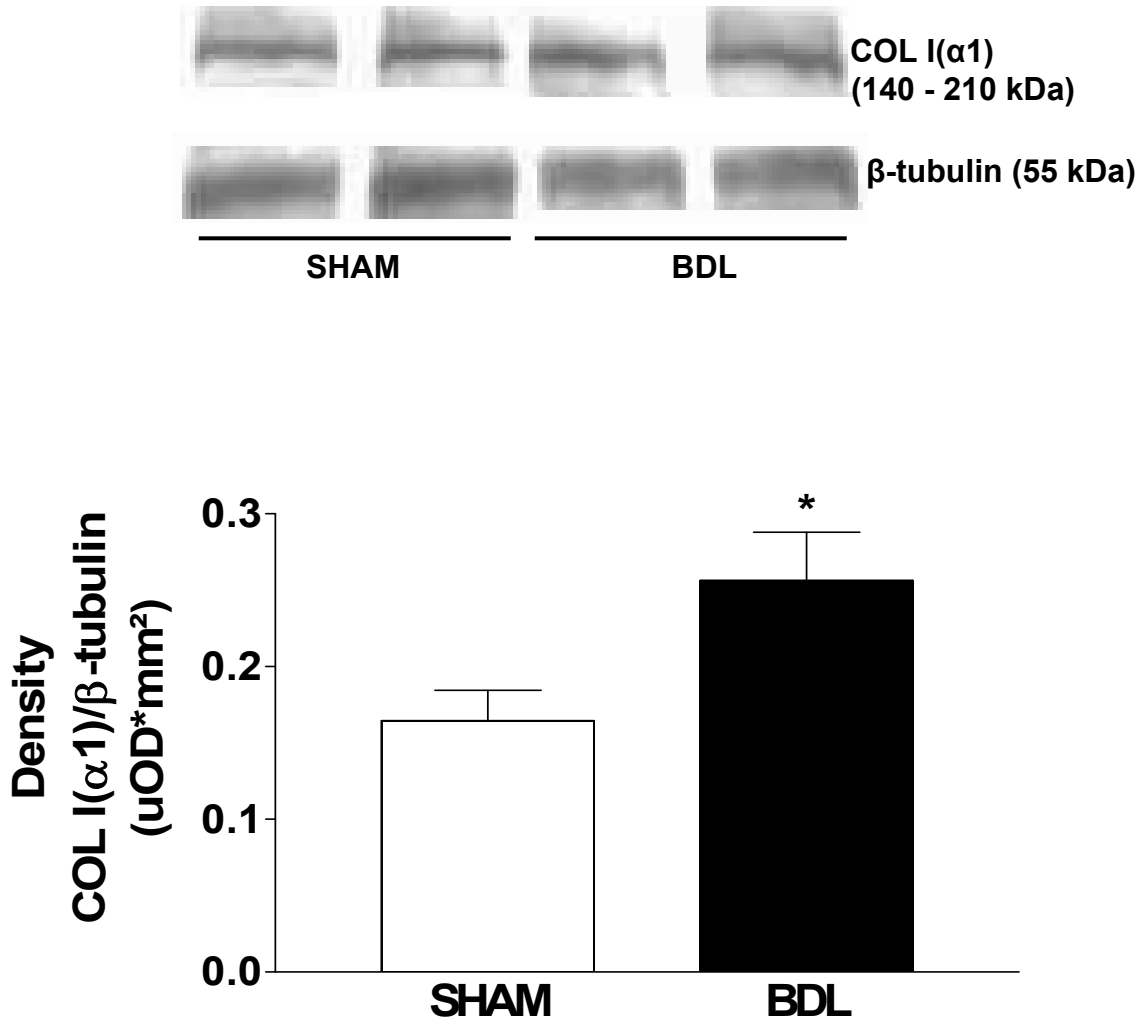

Figure 4.17 Western blot protein expression of COL I(α1) in ventricular homogenates (top) and densitometry analysis (bottom) from sham (n = 4) and BDL (n = 4). *Lanes 1* and *2*, sham; *lanes 3* and *4*, BDL. Data represented as mean ± SD. *p = 0.007, significantly different compared to levels in sham group.

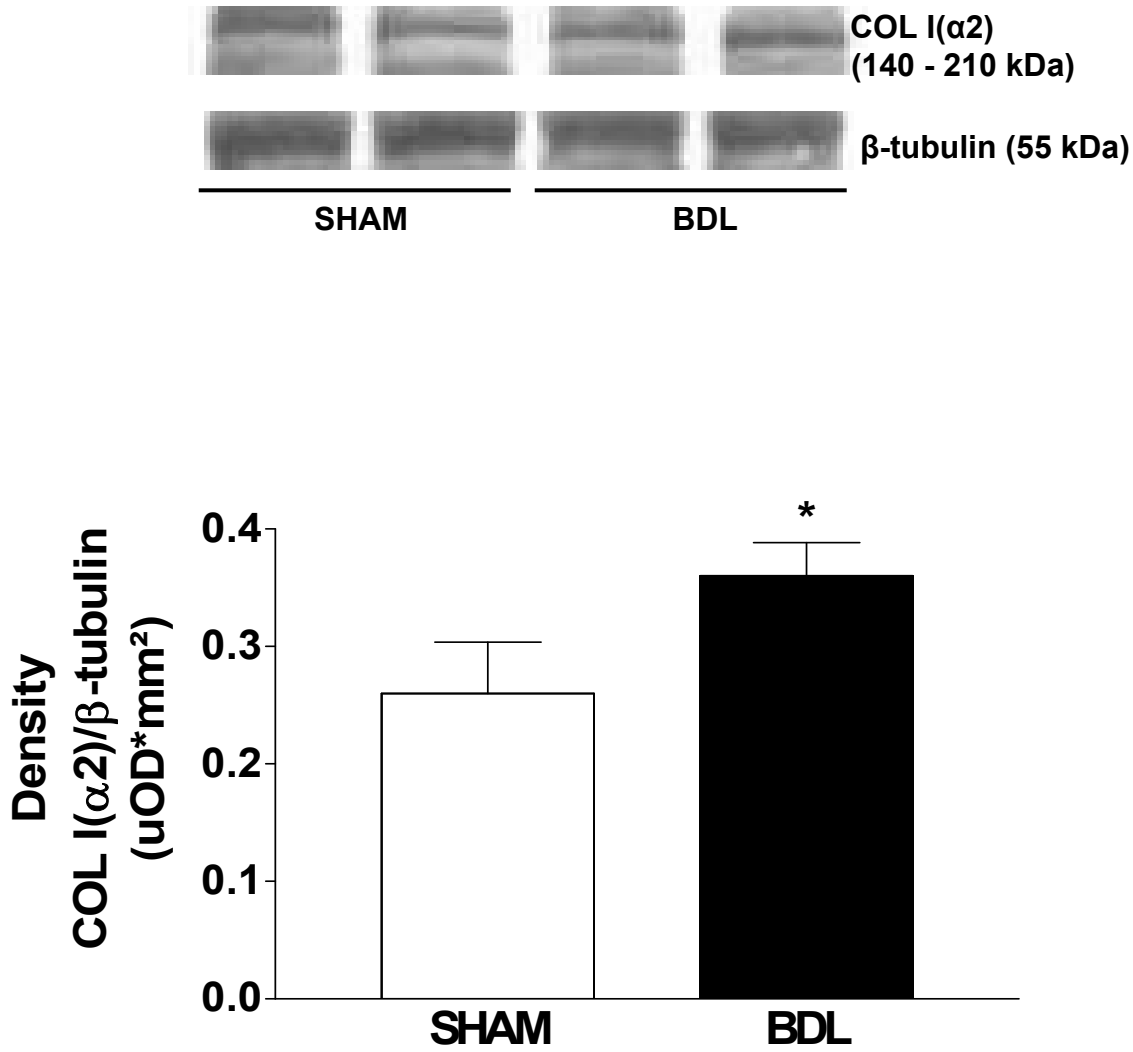

Figure 4.18 Western blot protein expression of COL I(α2) in ventricular homogenates (top) and densitometry analysis (bottom) from sham (n = 4) and BDL (n = 3). *Lanes 1* and *2*, sham; *lanes 3* and *4*, BDL. Data represented as mean ± SD. *p = 0.018, significantly different compared to levels in sham group.

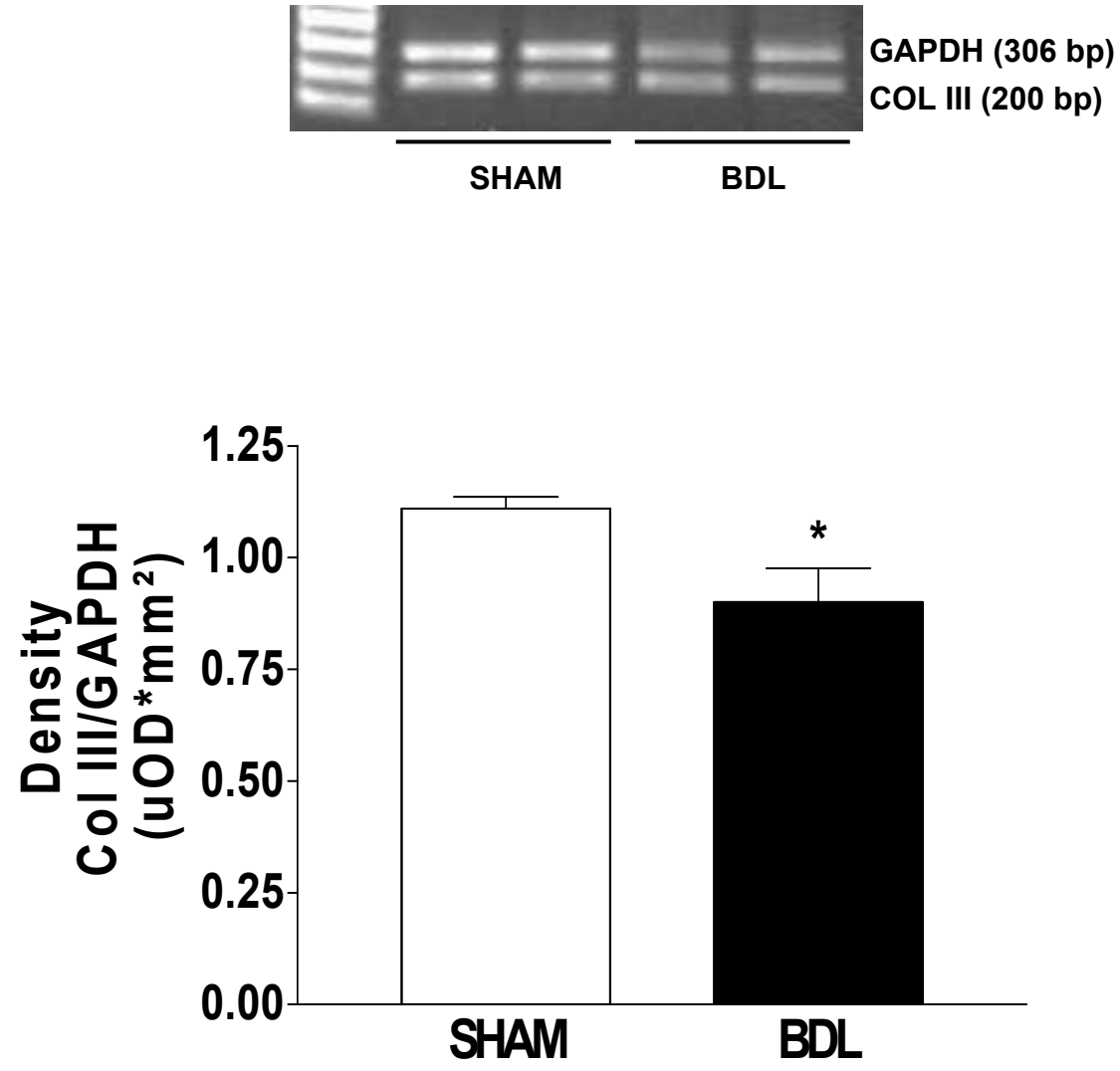

Figure 4.19 mRNA expression of COL III in ventricular homogenates using RT-PCR and (top) densitometry analysis (bottom) from sham (n = 3) and BDL (n = 4). *Lane 1*, 1 kilobase DNA ladder; *lanes 2* and *3*, sham; *lanes 4* and *5*, BDL. Data represented as mean ± SD. *p = 0.006, significantly different compared to levels in sham group.

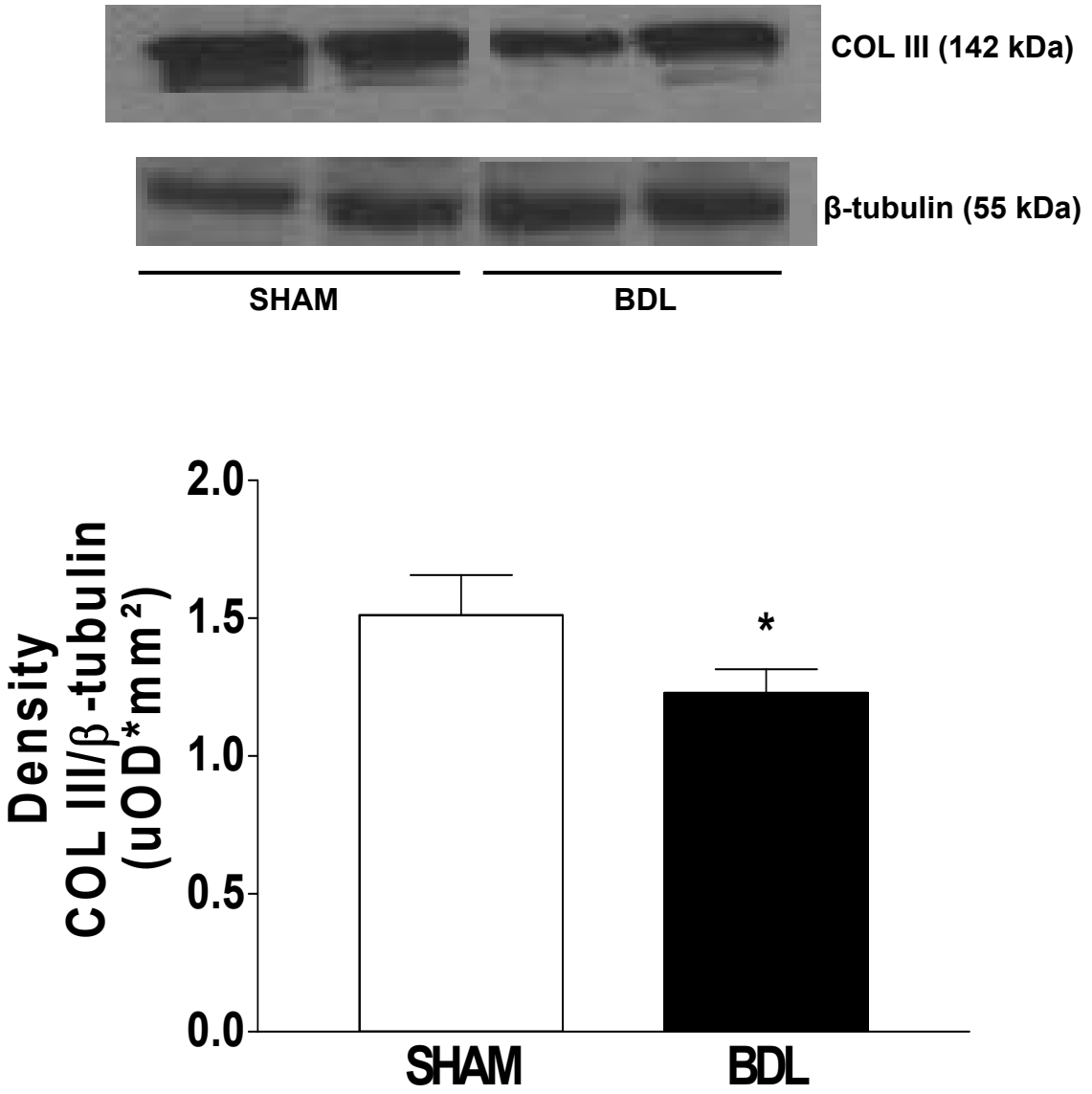

Figure 4.20 Western blot protein expression of COL III in ventricular homogenates (top) and densitometry analysis (bottom) from sham (n = 4) and BDL (n = 4). *Lanes 1* and *2*, sham; *lanes 3* and *4*, BDL. Data represented as mean ± SD. *p = 0.016, significantly different compared to levels in sham group.

CHAPTER FIVE: DISCUSSION

Significance of diastolic dysfunction in cirrhotic cardiomyopathy has been brought to the forefront with several reports of unexpected heart failure following liver transplantation and transjugular intrahepatic portosystemic stent-shunt (TIPS) (Huonker et al., 1999; Liu and Lee, 2005; Al Hamoudi and Lee, 2006). Cardiac failure accounts for 7-15% of postoperative mortality following liver transplantation (Myers and Lee, 2000). Many possible mechanisms have been shown to underlie cirrhotic cardiomyopathy (Baik et al., 2007; Moller and Henriksen, 2008). However, these studies have been focussed on explaining the systolic dysfunction that exists in the cirrhotic heart. Within the last decade, studies evaluating ventricular diastolic filling in patients with cirrhosis have provided supportive evidence of the presence of diastolic dysfunction, which is marked by a reduction in the E/A ratio (Pozzi et al., 1997; Valeriano et al., 2000; Cazzaniga et al., 2007). Researchers have also found that even though most patients with cirrhosis may not all show a clear depression in systolic functioning, most of these patients do show some depression in diastolic functioning as marked by a stiff, noncompliant ventricle (Finucci et al., 1996). This is consistent with the fact that in many myocardial diseases that result in heart failure, there is evidence of diastolic dysfunction before the occurrence of overt systolic contractile failure (Lee, 2003). However, the mechanisms behind the development of diastolic dysfunction in cirrhotic cardiomyopathy remain to be elucidated.

Therefore, we decided to investigate the possible mechanisms that may be involved in the diastolic dysfunction of the cirrhotic heart. The sarcomeric protein titin is the prime source of passive tension and thus an important determinant of diastolic stiffness in cardiomyocytes. Titin's adaptive ability during cardiac disease is evident from numerous studies performed to date (Warren et al., 2003; Nagueh et al., 2004). Warren et al. found that in the spontaneously hypertensive rat model there is an increased expression of N2B titin in response to pressure overload, which ultimately resulted in higher passive tension upon stretching of the sarcomere and thus an adverse effect on cardiac performance (Warren et al., 2003). Also, our lab has previously shown that the β-adrenergic receptor signalling pathway is significantly reduced in the BDL groups (Ma et al., 1999). This would suggest that altered PKA levels, as a possible result of the decrease in the β-adrenergic signalling, could play a role in the cirrhotic heart. PKA is important in the heart as phosphorylation by PKA is central to the regulation of many cellular processes, including relaxation. It is known to phoshorylate several proteins related to excitation-contraction coupling, including L-type Ca^{2+} channels, ryanodine receptor, phospholamban, troponin I and myosin binding protein C (Bers, 2002). Moreover, the role of PKA on titin's action cannot be ignored. Mechanical experiments with isolated myocytes have revealed that PKA can significantly reduce passive tension through the phosphorylation of titin's N2B segment, and thus allow more rapid diastolic filling (Yamasaki et al., 2002). Finally, extrinsic factors such as changes in the extracellular matrix have also been shown to contribute to passive tension.

Diseases that alter diastolic function have been shown to also alter extracellular fibrillar collagen, in terms of content, geometry, distribution, degree of cross-linking and ratio of COL I versus COL III. For example, researchers have found that patients suffering from dilated cardiomyopathy show an increase in the ratio of COL I to COL III. They concluded that this would contribute to an increase in tensile strength and stiffness, and therefore alter diastolic function by rendering the heart less compliant (Pauschinger et al., 1999).

To the best of our knowledge, no research group has specifically looked at the possible implication of titin, COL I and COL III in the diastolic dysfunction of cirrhotic cardiomyopathy. It was important to first confirm the existence of altered diastolic functioning in our BDL groups. Our experiments on isolated cardiomyocytes revealed that not only was systolic function altered, as was evident by the decrease in systolic return velocity, but the speed of relaxation as well as the time to complete full relaxation was also significantly affected. Diastolic return velocity was decreased in the BDL groups, which corresponded to an increase in the time taken to complete full relaxation of the heart. These findings are consistent with previous studies on cirrhotic patients (Finucci et al., 1996). However, despite the fact that isolated cardiomyocytes are widely used in research, they do possess certain limitations in that they do not fully represent the loaded environment of the heart where cells are packed together. Also, collagen, which is an important determinant of diastolic functioning, is not present in isolated cardiomyocytes due to its degradation by the use of collagenase in the isolating procedures (see Materials and Methods).

Therefore, in order to overcome these limitations, trabeculae were also used in the evaluation of diastolic function. Trabeculae are considered to be structurally homologous to the ventricular wall muscle configuration of the heart. As well as having collagen fibres remaining intact; myocytes, fibroblasts and blood vessels are also present in this loaded environment (Hanley et al., 1999). The findings from trabecula experiments showed an increase in passive tension in the BDL groups, which further supports the involvement of titin (at lower sarcomere length) and collagen (at higher sarcomere length) in the diastolic dysfunction of cirrhotic cardiomyopathy. During the experiments, it was observed that BDL trabeculae lacked the ability to be exposed to light or laser for as long a period as sham trabeculae could tolerate before spontaneous activity would begin. It is a reasonable assumption that this photosensitivity in the BDL groups may be related to the effects of cholestasis and/ or cirrhosis on the heart. However, this was not tested in the current studies.

Upon examination of the levels of titin, it was seen that there was no significant difference in the mRNA levels of N2B and N2BA between the sham and BDL animals. At the protein levels, N2B titin was also not significantly changed in the BDL animals and N2BA isoform was absent in both groups. This decreased translation of N2BA is consistent with previous studies that have shown that during the developmental stages of the rat heart, N2BA becomes less prevalent with age and is replaced by the stiffer N2B isoform (Opitz et al., 2004). In contrast to previous studies (Wu et al., 2002; Makarenko et al., 2004), which show either an increase, decrease or a switch in titin isoform expression, our

results failed to show any change in the level of N2B. However, this does not negate the importance of titin, as the differences between studies may have simply been due to differences in animal models or titin composition. This idea is supported by numerous studies on heart conditions that showed differences between humans and animal models or even in some cases differences between animals. For example, human patients suffering from dilated cardiomyopathy showed an increase in the N2BA/N2B ratio (Nagueh et al., 2004), while in the animal models there was a decrease in the N2BA/N2B ratio (Wu et al., 2002; Warren et al., 2003) over time. The severity of heart failure may also be a determinant of the switching in titin isoforms, and the possibility of the existence of an end-stage phenomenon that does not play a role during the earlier progression state of the disease has to also be considered (LeWinter, 2004).

On the other hand, collagen levels were shown to be different between the two groups. The stiffer COL I was significantly increased in the cirrhotic rats, while the more compliant COL III was decreased both at the mRNA and protein levels. This switch in collagen expression can help to explain the increase in passive tension that is seen in BDL animals, with a possible implication for collagen being more pivotal at the working sarcomere lengths of the functioning heart. Although this was not examined in the current study, it is something that can be looked at in the future by directly degrading titin using trypsin (0.20-0.25 μg/ml), and then measuring the passive tension due solely to collagen. Several studies have also examined the direct role of collagen using the abovementioned procedure (Granzier and Irving, 1995; Wu et al., 2000). Knowing whether

collagen or titin is the main contributor to the observed changes in passive tension will become relevant in planning possible therapeutic options and thus knowing what to target. Also, knowing the levels and locations of collagen distribution throughout the heart might be useful in translating these results to the functioning level of the whole heart.

Since N2B levels were not changing in the cirrhotic animals, the next step was to determine the possible role of modulators on titin's action. One such post-translational modulator is PKA, which was shown to be significantly decreased in the cirrhotic animals both at the mRNA and protein levels. These results are consistent with previous studies that have shown a decrease in the β-adrenergic receptor signalling pathway in cirrhotic cardiomyopathy (Lee et al., 2007). During sympathetic stimulation, activation of the β-adrenergic receptor leads to activation of adenylyl cyclase, the conversion of ATP to cAMP and the subsequent activation of PKA and phosphorylation of many substrates. As a result, a decrease in the β-adrenergic receptor signalling pathway leads to a decrease in PKA levels, which in turn can lead to the decreased phosphorylation of titin and increase passive tension that was observed in the BDL animals. However, PKA has numerous substrates and thus the involvement of other diastolic-related proteins is a strong possibility. For instance, a decrease in PKA can also result in a decrease phosphorylation of troponin I, which would lead to a decreased dissociation of Ca^{2+} from troponin C, an increase in Ca^{2+} sensitivity and thus an increase in diastolic time as seen in cirrhosis (Saucerman and McCulloch, 2006). It would also be interesting to look at *in vitro* as well as *in vivo*

studies involving the administration of β-adrenergic agonists to study the effects on passive tension in BDL. Previous studies have examined the direct effect of adding PKA to myocytes (Yamasaki et al., 2002). They found that PKA decreased passive tension and made the muscle more compliant with increasing sarcomere length. Therefore, the role of PKA and its effect on other substrates cannot be ignored.

It is also important to note that as in all studies using animal models there are limitations in translating that to human models. For instance, humans tend to coexpress both N2BA and N2B titin at an approximate ratio of 30:70 (Opitz et al., 2003), while in the adult rat heart, N2BA is absent. Due to the high heart rate that is encountered in these small animals, the high N2B expression levels has been suggested to occur in order to allow rapid early diastolic filling (due to high restoring forces) and rapid setting of end diastolic volume (due to the high stiffness at long sarcomere lengths) when diastolic filling times are short (Granzier et al., 2005). However, despite the lack of change in titin expression in the rat heart, the possibility exists that in the human heart, in addition to the changes occurring due to decreased PKA, there could also be contributions from changing levels of N2B and N2BA, as was hypothesized but not seen in the rat heart.

Also, in examining diastolic function it is important to discuss the means of Ca^{2+} removal from the cytosol. Ca^{2+} removal during relaxation is different in rats than humans. Under normal conditions in humans (and other mammals larger than rodents), Ca^{2+} removal is mainly due to reuptake by the SR SERCA2 pump

and extrusion by the membrane bound sodium-calcium exchanger (NCX). SR removes approximately 70% of the Ca^{2+} involved in the Ca^{2+} transient while NCX extrudes another 28%, leaving only 2% to be taken up by the plasma membrane Ca^{2+}-ATPases (PMCA) or the mitochondria. In rats, SR reuptake accounts for 92% and NCX for 7% of Ca^{2+} removal from the cytosol (Bers, 2002). Studies published from our lab have shown that SR reuptake pump expression is not changed in the BDL heart (Ward et al., 2001). However, preliminary studies have showed a decrease expression in NCX, which could also account for the increase in relaxation time observed in the cirrhotic group. But additional studies in the lab showed that the reuptake of Ca^{2+} by the SR is the same both in sham and BDL animals. These results are interesting because with the increased relaxation time as well as the decrease in PKA that is observed in the cirrhotic rat, it would have been expected for us to see a decreased SR activity in the BDL groups. However, it is known that many other protein kinases exist that can alter the function of key regulator proteins in cardiac function. Ca^{2+}/calmodulin-dependent protein kinase (Ca^{2+}/CaMK) plays a role in the phosphorylation of various proteins, including phospholamban and the SERCA2 SR pump directly (Maier and Bers, 2007). Preliminary studies have shown an increase in CaMK in the BDL groups both at the mRNA and protein levels. This change in CaMK could cause an increase phospholamban activity independent of PKA levels, and thus cause SR activity to remain at a level similar to the control group despite decreased PKA. In addition, the increase in relaxation time could be due to an increase in the amount of $[Ca^{2+}]_i$ inside the cytosol during relaxation.

Researchers have shown that spontaneous SR Ca^{2+} release during the diastolic interval does occur minimally without inducing visible contractile activity in the normal rat trabeculae (Obayashi et al., 2006). In contrast, rats with congestive heart failure tend to show propagating contractile waves or spontaneous activity due to propagating Ca^{2+} release in the cells of the trabeculae during diastole (Obayashi et al., 2006). Therefore, eventually looking at the $[Ca^{2+}]_i$ during relaxation will be very useful in fully elucidating what is occurring at the cellular level. This can be accomplished by examining the extent of Ca^{2+} sparks within the cell using fluorescence and laser scanning confocal microscopic imaging. Ca^{2+} sparks were discovered to be discrete, localized Ca^{2+} release events that reflect the activation of a cluster of RyR2 and subsequent Ca^{2+} release from the SR (Cheng et al., 1993). If there is an increase in $[Ca^{2+}]_i$ during diastole, these experiments will also help in determining whether or not the changes could be due to a possible Ca^{2+} leak occurring in the SR of the BDL rats.

The possibility of additional contributors in the diastolic dysfunction of cirrhotic cardiomyopathy cannot be ignored. Due to the changes that are observed with collagen, the role of MMPs activity and fibrosis are prime candidates in the observed dysfunction in cirrhotic patients. MMPs are zinc-dependent proteases that are essential to the normal turnover of extracellular matrix proteins, such as the fibrillar and basement membrane collagens, proteoglycans and fibronectin (Malemud, 2006). By degrading collagen, MMPs are able to reduce the degree of fibrosis that can occur in an organ. The role of MMPs in liver fibrosis and the heart is well established (Hemmann et al., 2007;

Spinale, 2007). Many MMPs, including MMP-1-3, 7-9, 13 and 14, have been identified in the failing and non-failing myocardium (Spinale, 2007). A decrease in MMP levels and an increase in fibrosis would be expected in our BDL heart due to the increase in collagen that is observed. Changes in MMP activity can be regulated by its endogenous inhibitor- tissue inhibitor of metalloproteinases (TIMPs). As a result the determination of the expression level of TIMPs would also be beneficial. By establishing the possible role of MMPs and TIMPs in cirrhotic cardiomyopathy, we will be able to better understand the means by which COL I and III are being upregulated and downregulated respectively, and therefore how they can be targeted in possible therapeutic treatments.

The involvement of another myofilament protein, such as MHC, is also a strong possibility. MHC, which is composed of two isoforms - α and β-MHC, is the site of actin and ATP binding, and as such plays an essential role in relaxation through regulation of ATPase activity and cross-bridge detachment (Palmer, 2005). Expression of these isoforms have been shown to change in different cardiac diseases (Lowes et al., 1997; Harada et al., 1999). Preliminary studies in the lab showed a shift from α-MHC to β-MHC in our cirrhotic rats. The increase in β-MHC would result in lower ATPase activity, decreased filament sliding velocity, and the ability to generate cross-bridge force with less energy consumption in the BDL heart. This decrease in ATPase activity can affect diastolic return velocity and relaxation time by decreasing ATP binding and dissociation of actin from myosin.

In addition, the role of endotoxin in the liver and in the heart is well documented (Isayama et al., 2006; Nielsen et al., 2007; Risoe et al., 2007) and could also be playing a role in the diastolic dysfunction of cirrhotic cardiomyopathy. Patients show an increase in bacterial endotoxin lipopolysaccharide (LPS), which is a major structural component of gram-negative bacteria and a key modulator of the bodies immune system. It has been implicated in the stimulation of proinflammatory cytokines, such as TNF-α and NO (Geoghegan-Morphet et al., 2007). Research in cirrhotic cardiomyopathy has also shown an increase in TNF-α and NO in the BDL rats (Liu et al., 2000). In addition, Risoe et al showed a possible role of LPS in reducing cAMP mRNA levels (Risoe et al., 2007). Therefore, in light of these studies it is possible that an increase in endotoxin in the BDL heart can lead to an increase in TNF-α and NO, which can in turn decrease cAMP activity through cGMP, or the endotoxin can directly decrease cAMP production. In either case, both pathways could result in the decreased expression of PKA that was observed in this study. However, the idea that a few or all of the mentioned possibilities throughout this thesis are working together to cause the observed condition is a strong possibility, and also an indication of the multifaceted nature of the heart.

In the past, the absence of accepted parameters to define cirrhotic cardiomyopathy and the lack of a universally accepted definition had led to some skeptics concluding that the syndrome did not exist due to the rareness of heart failure that is usually seen with other cardiomyopathies (Lee, 2003). In these

patients, heart failure may have been rare due to the vasodilation of the peripheral circulation unloading the ventricle and in effect "autotreating" the failure by masking the ventricular insufficiency. This is supported by evidence from transjugular intrahepatic portosystemic stent-shunt and liver transplantation, which both normalize peripheral vascular tone and thus result in overt heart failure (Lee, 2003). However, in the last few years, specific diagnostic criteria for cirrhotic cardiomyopathy have been formulated. The consensus definition of cirrhotic cardiomyopathy is: chronic cardiac dysfunction in patients with cirrhosis, characterised by blunted contractile responsiveness to stress, and/or altered diastolic relaxation with electrophysiological abnormalities, in the absence of known cardiac disease. Therefore, with a consensus definition of cirrhotic cardiomyopathy, the numerous amounts of data supporting its existence and the increase in heart failure in patients with no previous history of heart problem, highlights the need to better understand the mechanisms behind this condition.

As knowledge on the etiology of diastolic dysfunction in cirrhotic cardiomyopathy will undoubtedly grow, there is an interesting challenge of creating therapeutic strategies to target these underlying mechanisms. Currently, non-pharmacological and pharmacological treatment exists for patients with diastolic dysfunction (Zile and Brutsaert, 2002; Borlaug and Kass, 2006). In terms of non-pharmacological treatment, the restriction of sodium and fluid to prevent volume overload, increasing exercise tolerance in order to improve cardiovascular conditioning and to decrease heart rate are among a few options. The use of pharmacological agents such as diuretics, nitrates, renin-angiotensin-

aldosterone antagonists including angiotensin converting enzymes (ACE) inhibitors, angiotensin II receptor blocker and aldosterone antagonists to modulate neurohumoral systems for decrease blood volume and extracellular matrix collagen synthesis, as well as Ca^{2+} channel blockers are currently recommended to patients.

With the advances in gene therapy it seems reasonable that new therapeutic strategies targeting passive tension, collagen configuration, fibrosis and calcium homeostasis will be beneficial in treating this condition. Studies using different genetic manipulations have been able to create rat models with reduced expression or knockout of NCX. These studies have been very promising as the rats showed an enormous capacity to adapt to the changing conditions by decreasing the inward Ca^{2+} current through the L-type Ca^{2+} channels and thereby reducing Ca^{2+} influx, while still maintaining proper systolic and diastolic functioning when compared to controls (Henderson et al., 2004; Pott et al., 2007). In addition a study involving a 16 week treatment with alagebrium chloride (ALT-711), a glucose crosslink breaker, was used to target myocardial stiffness caused by general collagen cross-linking (Little et al., 2005). This resulted in a decrease in left ventricular mass and improvements in diastolic filling in elderly patients suffering from diastolic heart failure. Another group, using β-aminopropionitrile (BAPN) to inhibit collagen cross-linking, showed a reduction in chamber and myocardial stiffness; thereby, showing the importance of the collagen matrix in determining diastolic stiffness (Kato et al., 1995). Therefore, studies possibly targeting an upregulation (ex. PKA, MMPs) or a

downregulation (ex. COL I, TIMPs) of specific genes would be beneficial in understanding this condition and finding possible treatment options targeting the mechanisms affected in cirrhotic patients.

In conclusion, the present study shows that diastolic dysfunction exists in cirrhosis, and is marked by a decrease in diastolic return velocity, increase in relaxation time and increase in passive tension. The mechanisms behind these changes are both intrinsic and extrinsic to the myocytes. Alterations in titin modulation, PKA levels and collagen configuration may all contribute to the pathogenesis of diastolic dysfunction in cirrhotic cardiomyopathy.

REFERENCES

Al Hamoudi W. and Lee S. S. Cirrhotic cardiomyopathy. Ann Hepatol 2006; 5(3): 132-9.

Apstein C. and Morgan J. Cellular mechanisms underlying left ventricular diastolic dysfunction. In Left Ventricular Diastolic Dysfunction and Heart Failure. W. H. Gaasch and M. M. LeWinter (eds.). Philadelphia, PA: Lea and Febuger, 1994. p.3-24.

Baik S. K., Fouad T. R. and Lee S. S. Cirrhotic cardiomyopathy. Orphanet J Rare Dis 2007; 2: 15.

Balligand J. L., Kelly R. A., Marsden P. A., Smith T. W. and Michel T. Control of cardiac muscle cell function by an endogenous nitric oxide signaling system. Proc Natl Acad Sci U S A 1993; 90(1): 347-51.

Batkai S., Jarai Z., Wagner J. A., Goparaju S. K., Varga K., Liu J., Wang L., Mirshahi F., Khanolkar A. D., Makriyannis A., Urbaschek R., Garcia N., Jr., Sanyal A. J. and Kunos G. Endocannabinoids acting at vascular CB1 receptors mediate the vasodilated state in advanced liver cirrhosis. Nat Med 2001; 7(7): 827-32.

Bell S. P., Nyland L., Tischler M. D., McNabb M., Granzier H. and LeWinter M. M. Alterations in the determinants of diastolic suction during pacing tachycardia. Circ Res 2000; 87(3): 235-40.

Berne R. and Levy M. Molecular Basis of Contraction. In Principles of Physiology. R. Berne and M. Levy (eds.). St. Loius: Mosby, 1996. pp.148-153.

Bers D. M. Cardiac excitation-contraction coupling. Nature 2002; 415(6868): 198-205.

Beuckelmann D. J., Nabauer M. and Erdmann E. Intracellular calcium handling in isolated ventricular myocytes from patients with terminal heart failure. Circulation 1992; 85(3): 1046-55.

Borg T. K. and Caulfield J. B. The collagen matrix of the heart. Fed Proc 1981; 40(7): 2037-41.

Borlaug B. A. and Kass D. A. Mechanisms of diastolic dysfunction in heart failure. Trends Cardiovasc Med 2006; 16(8): 273-9.

Brixius K., Pietsch M. and Schwinger R. H. The intracellular Ca(2+)-homeostasis influences the frequency-dependent force-generation in man. Basic Res Cardiol 1999; 94(3): 152-8.

Brutsaert D. L. and Sys S. U. Relaxation and diastole of the heart. Physiol Rev 1989; 69(4): 1228-315.

Caramelo C., Fernandez-Munoz D., Santos J. C., Blanchart A., Rodriguez-Puyol D., Lopez-Novoa J. M. and Hernando L. Effect of volume expansion on hemodynamics, capillary permeability and renal function in conscious, cirrhotic rats. Hepatology 1986; 6(1): 129-34.

Carroll J. and Hess O. Assessment of normal and abnormal cardiac function. In Braunwald's Heart Disease: A Textbook of Cardiovascular Medicine. L. P. Zipes D.P., Bonow R.O. and Braunwald E. (eds.). Philadelphia: Elsevier Saunders, 2005. Vol 2. p.498.

Cazorla O., Freiburg A., Helmes M., Centner T., McNabb M., Wu Y., Trombitas K., Labeit S. and Granzier H. Differential expression of cardiac titin isoforms and modulation of cellular stiffness. Circ Res 2000; 86(1): 59-67.

Cazzaniga M., Salerno F., Pagnozzi G., Dionigi E., Visentin S., Cirello I., Meregaglia D. and Nicolini A. Diastolic dysfunction is associated with poor survival in patients with cirrhosis with transjugular intrahepatic portosystemic shunt. Gut 2007; 56(6): 869-75.

Cheng H., Lederer W. J. and Cannell M. B. Calcium sparks: elementary events underlying excitation-contraction coupling in heart muscle. Science 1993; 262(5134): 740-4.

Chomczynski P. and Sacchi N. Single-step method of RNA isolation by acid guanidinium thiocyanate-phenol-chloroform extraction. Anal Biochem 1987; 162(1): 156-9.

Colledge M. and Scott J. D. AKAPs: from structure to function. Trends Cell Biol 1999; 9(6): 216-21.

Covell J. W. Factors influencing diastolic function. Possible role of the extracellular matrix. Circulation 1990; 81(2 Suppl): III155-8.

De Petrocellis L., Cascio M. G. and Di Marzo V. The endocannabinoid system: a general view and latest additions. Br J Pharmacol 2004; 141(5): 765-74.

Desmet V. Organizational Principles. In The Liver: Biology and Pathobiology. 4th edition. I. Arias, J. Boyer, F. Chisari et al (eds.). Philadelphia, PA: Lippincott Williams & Wilkins, 2001. p.3-15.

Domenicali M., Ros J., Fernandez-Varo G., Cejudo-Martin P., Crespo M., Morales-Ruiz M., Briones A. M., Campistol J. M., Arroyo V., Vila E., Rodes J. and Jimenez W. Increased anandamide induced relaxation in mesenteric arteries of cirrhotic rats: role of cannabinoid and vanilloid receptors. Gut 2005; 54(4): 522-7.

Ewing J. F., Raju V. S. and Maines M. D. Induction of heart heme oxygenase-1 (HSP32) by hyperthermia: possible role in stress-mediated elevation of cyclic 3':5'-guanosine monophosphate. J Pharmacol Exp Ther 1994; 271(1): 408-14.

Finucci G., Desideri A., Sacerdoti D., Bolognesi M., Merkel C., Angeli P. and Gatta A. Left ventricular diastolic function in liver cirrhosis. Scand J Gastroenterol 1996; 31(3): 279-84.

Frank K. F., Bolck B., Erdmann E. and Schwinger R. H. Sarcoplasmic reticulum Ca2+-ATPase modulates cardiac contraction and relaxation. Cardiovasc Res 2003; 57(1): 20-7.

Fukuda N. and Granzier H. Role of the giant elastic protein titin in the Frank-Starling mechanism of the heart. Curr Vasc Pharmacol 2004; 2(2): 135-9.

Fukuda N., Wu Y., Nair P. and Granzier H. L. Phosphorylation of titin modulates passive stiffness of cardiac muscle in a titin isoform-dependent manner. J Gen Physiol 2005; 125(3): 257-71.

Gaskari S. A., Honar H. and Lee S. S. Therapy insight: Cirrhotic cardiomyopathy. Nat Clin Pract Gastroenterol Hepatol 2006; 3(6): 329-37.

Gaskari S. A., Liu H., Moezi L., Li Y., Baik S. K. and Lee S. S. Role of endocannabinoids in the pathogenesis of cirrhotic cardiomyopathy in bile duct-ligated rats. Br J Pharmacol 2005; 146(3): 315-23.

Gentilini P. and Laffi G. Pathophysiology and treatment of ascites and the hepatorenal syndrome. Baillieres Clin Gastroenterol 1992; 6(3): 581-607.

Geoghegan-Morphet N., Burger D., Lu X., Sathish V., Peng T., Sims S. M. and Feng Q. Role of neuronal nitric oxide synthase in lipopolysaccharide-induced tumor necrosis factor-alpha expression in neonatal mouse cardiomyocytes. Cardiovasc Res 2007; 75(2): 408-16.

Granzier H., Wu Y., Siegfried L. and LeWinter M. Titin: physiological function and role in cardiomyopathy and failure. Heart Fail Rev 2005; 10(3): 211-23.

Granzier H. L. and Irving T. C. Passive tension in cardiac muscle: contribution of collagen, titin, microtubules, and intermediate filaments. Biophys J 1995; 68(3): 1027-44.

Granzier H. L. and Wang K. Gel electrophoresis of giant proteins: solubilization and silver-staining of titin and nebulin from single muscle fiber segments. Electrophoresis 1993; 14(1-2): 56-64.

Guyot C., Lepreux S., Combe C., Doudnikoff E., Bioulac-Sage P., Balabaud C. and Desmouliere A. Hepatic fibrosis and cirrhosis: the (myo)fibroblastic cell subpopulations involved. Int J Biochem Cell Biol 2006; 38(2): 135-51.

Hanley P. J., Young A. A., LeGrice I. J., Edgar S. G. and Loiselle D. S. 3-Dimensional configuration of perimysial collagen fibres in rat cardiac muscle at resting and extended sarcomere lengths. J Physiol 1999; 517 (Pt 3): 831-7.

Harada K., Sugaya T., Murakami K., Yazaki Y. and Komuro I. Angiotensin II type 1A receptor knockout mice display less left ventricular remodeling and improved survival after myocardial infarction. Circulation 1999; 100(20): 2093-9.

Harrison D. J. and Burt A. D. Pathology of alcoholic liver disease. Baillieres Clin Gastroenterol 1993; 7(3): 641-62.

Hemmann S., Graf J., Roderfeld M. and Roeb E. Expression of MMPs and TIMPs in liver fibrosis - a systematic review with special emphasis on anti-fibrotic strategies. J Hepatol 2007; 46(5): 955-75.

Henderson S. A., Goldhaber J. I., So J. M., Han T., Motter C., Ngo A., Chantawansri C., Ritter M. R., Friedlander M., Nicoll D. A., Frank J. S., Jordan M. C., Roos K. P., Ross R. S. and Philipson K. D. Functional adult myocardium in the absence of Na+-Ca2+ exchange: cardiac-specific knockout of NCX1. Circ Res 2004; 95(6): 604-11.

Hole Jr. J. The Cardiovascular System. In Human Anatomy and Physiology. J. Hole Jr. (eds.). Dubuque, Iowa: Wm. C. Brown Publishers, 1984. p.647-713.

Horowits R., Kempner E. S., Bisher M. E. and Podolsky R. J. A physiological role for titin and nebulin in skeletal muscle. Nature 1986; 323(6084): 160-4.

Huonker M., Schumacher Y. O., Ochs A., Sorichter S., Keul J. and Rossle M. Cardiac function and haemodynamics in alcoholic cirrhosis and effects of the transjugular intrahepatic portosystemic stent shunt. Gut 1999; 44(5): 743-8.

Huxley H. and Hanson J. Changes in the cross-striations of muscle during contraction and stretch and their structural interpretation. Nature 1954; 173(4412): 973-6.

Imai Y., Scoble J. E., McIntyre N. and Owen J. S. Increased Na(+)-dependent D-glucose transport and altered lipid composition in renal cortical brush-border membrane vesicles from bile duct-ligated rats. J Lipid Res 1992; 33(4): 473-83.

Isayama F., Hines I. N., Kremer M., Milton R. J., Byrd C. L., Perry A. W., McKim S. E., Parsons C., Rippe R. A. and Wheeler M. D. LPS signaling enhances

hepatic fibrogenesis caused by experimental cholestasis in mice. Am J Physiol Gastrointest Liver Physiol 2006; 290(6): G1318-28.

Jaue D. N., Ma Z. and Lee S. S. Cardiac muscarinic receptor function in rats with cirrhotic cardiomyopathy. Hepatology 1997; 25(6): 1361-5.

Kakimoto H., Imai Y., Kawata S., Inada M., Ito T. and Matsuzawa Y. Altered lipid composition and differential changes in activities of membrane-bound enzymes of erythrocytes in hepatic cirrhosis. Metabolism 1995; 44(7): 825-32.

Kapiloff M. S. Contributions of protein kinase A anchoring proteins to compartmentation of cAMP signaling in the heart. Mol Pharmacol 2002; 62(2): 193-9.

Kass D. A., Bronzwaer J. G. and Paulus W. J. What mechanisms underlie diastolic dysfunction in heart failure? Circ Res 2004; 94(12): 1533-42.

Kato S., Spinale F. G., Tanaka R., Johnson W., Cooper G. t. and Zile M. R. Inhibition of collagen cross-linking: effects on fibrillar collagen and ventricular diastolic function. Am J Physiol 1995; 269(3 Pt 2): H863-8.

Klabunde R. Introduction to the Cardiovascular System. In Cardiovascular Physiology Concepts(eds.). Philadelphia: Lippincott Williams amd Wilkins, 2005.

Kowalski H. J. and Abelmann W. H. The cardiac output at rest in Laennec's cirrhosis. J Clin Invest 1953; 32(10): 1025-33.

Kruger M. and Linke W. A. Protein kinase-A phosphorylates titin in human heart muscle and reduces myofibrillar passive tension. J Muscle Res Cell Motil 2006; 27(5-7): 435-44.

Kutchai H. Gastrointestinal System. In Principles of Physiology. 3rd edition. R. Berne and M. Levy (eds.). St. Louis, MO: Mosby, Inc., 2000. p.383-7.

Labeit S. and Kolmerer B. Titins: giant proteins in charge of muscle ultrastructure and elasticity. Science 1995; 270(5234): 293-6.

Labeit S., Kolmerer B. and Linke W. A. The giant protein titin. Emerging roles in physiology and pathophysiology. Circ Res 1997; 80(2): 290-4.

Ladbrooke B. D. and Chapman D. Thermal analysis of lipids, proteins and biological membranes. A review and summary of some recent studies. Chem Phys Lipids 1969; 3(4): 304-56.

Lamb G. D. Excitation-contraction coupling in skeletal muscle: comparisons with cardiac muscle. Clin Exp Pharmacol Physiol 2000; 27(3): 216-24.

Lee R. F., Glenn T. K. and Lee S. S. Cardiac dysfunction in cirrhosis. Best Pract Res Clin Gastroenterol 2007; 21(1): 125-40.

Lee S. S. Cardiac dysfunction in spontaneous bacterial peritonitis: a manifestation of cirrhotic cardiomyopathy? Hepatology 2003; 38(5): 1089-91.

Leite-Moreira A. F. Current perspectives in diastolic dysfunction and diastolic heart failure. Heart 2006; 92(5): 712-8.

Leite-Moreira A. F. and Correia-Pinto J. Load as an acute determinant of end-diastolic pressure-volume relation. Am J Physiol Heart Circ Physiol 2001; 280(1): H51-9.

LeWinter M. M. Titin isoforms in heart failure: are there benefits to supersizing? Circulation 2004; 110(2): 109-11.

Lim C. C. and Sawyer D. B. Modulation of cardiac function: titin springs into action. J Gen Physiol 2005; 125(3): 249-52.

Limas C. J., Guiha N. H., Lekagul O. and Cohn J. N. Impaired left ventricular function in alcoholic cirrhosis with ascites. Ineffectiveness of ouabain. Circulation 1974; 49(4): 754-60.

Little W. C., Zile M. R., Kitzman D. W., Hundley W. G., O'Brien T. X. and Degroof R. C. The effect of alagebrium chloride (ALT-711), a novel glucose cross-link breaker, in the treatment of elderly patients with diastolic heart failure. J Card Fail 2005; 11(3): 191-5.

Liu H., Gaskari S. A. and Lee S. S. Cardiac and vascular changes in cirrhosis: pathogenic mechanisms. World J Gastroenterol 2006; 12(6): 837-42.

Liu H. and Lee S. S. Cardiopulmonary dysfunction in cirrhosis. J Gastroenterol Hepatol 1999; 14(6): 600-8.

Liu H. and Lee S. S. What happens to cirrhotic cardiomyopathy after liver transplantation? Hepatology 2005; 42(5): 1203-5.

Liu H., Ma Z. and Lee S. S. Contribution of nitric oxide to the pathogenesis of cirrhotic cardiomyopathy in bile duct-ligated rats. Gastroenterology 2000; 118(5): 937-44.

Liu H., Song D. and Lee S. S. Role of heme oxygenase-carbon monoxide pathway in pathogenesis of cirrhotic cardiomyopathy in the rat. Am J Physiol Gastrointest Liver Physiol 2001; 280(1): G68-74.

Lodish H., Berk A., Kaiser C., Krieger M., Scott M., Bretscher A., Ploegh H. and Matsudaira P. Integrating Cells into Tissues. In Molecular Cell Biology. 6th edition. K. Ahr, M. Tontonoz, E. Frost, E. Rice and N. Tymoczko (eds.). New York: W.H. Freeman and Company, 2008. p.801-46.

Lowes B. D., Minobe W., Abraham W. T., Rizeq M. N., Bohlmeyer T. J., Quaife R. A., Roden R. L., Dutcher D. L., Robertson A. D., Voelkel N. F., Badesch D. B., Groves B. M., Gilbert E. M. and Bristow M. R. Changes in gene expression in the intact human heart. Downregulation of alpha-myosin heavy chain in hypertrophied, failing ventricular myocardium. J Clin Invest 1997; 100(9): 2315-24.

Ma H. Western Blotting Method. The Journal of American Science 2006; 2(2): 23-27.

Ma Z. and Lee S. S. Cirrhotic cardiomyopathy: getting to the heart of the matter. Hepatology 1996; 24(2): 451-9.

Ma Z., Lee S. S. and Meddings J. B. Effects of altered cardiac membrane fluidity on beta-adrenergic receptor signalling in rats with cirrhotic cardiomyopathy. J Hepatol 1997; 26(4): 904-12.

Ma Z., Meddings J. B. and Lee S. S. Membrane physical properties determine cardiac beta-adrenergic receptor function in cirrhotic rats. Am J Physiol 1994; 267(1 Pt 1): G87-93.

Ma Z., Miyamoto A. and Lee S. S. Role of altered beta-adrenoceptor signal transduction in the pathogenesis of cirrhotic cardiomyopathy in rats. Gastroenterology 1996; 110(4): 1191-8.

Ma Z., Zhang Y., Huet P. M. and Lee S. S. Differential effects of jaundice and cirrhosis on beta-adrenoceptor signaling in three rat models of cirrhotic cardiomyopathy. J Hepatol 1999; 30(3): 485-91.

Maier L. S. and Bers D. M. Role of Ca2+/calmodulin-dependent protein kinase (CaMK) in excitation-contraction coupling in the heart. Cardiovasc Res 2007; 73(4): 631-40.

Maines M. D. The heme oxygenase system: a regulator of second messenger gases. Annu Rev Pharmacol Toxicol 1997; 37: 517-54.

Makarenko I., Opitz C. A., Leake M. C., Neagoe C., Kulke M., Gwathmey J. K., del Monte F., Hajjar R. J. and Linke W. A. Passive stiffness changes caused by upregulation of compliant titin isoforms in human dilated cardiomyopathy hearts. Circ Res 2004; 95(7): 708-16.

Malemud C. J. Matrix metalloproteinases (MMPs) in health and disease: an overview. Front Biosci 2006; 11: 1696-701.

Marijianowski M. M., Teeling P., Mann J. and Becker A. E. Dilated cardiomyopathy is associated with an increase in the type I/type III collagen ratio: a quantitative assessment. J Am Coll Cardiol 1995; 25(6): 1263-72.

Merli M., Valeriano V., Funaro S., Attili A. F., Masini A., Efrati C., De C. S. and Riggio O. Modifications of cardiac function in cirrhotic patients treated with transjugular intrahepatic portosystemic shunt (TIPS). Am J Gastroenterol 2002; 97(1): 142-8.

Milani A., Zaccaria R., Bombardieri G., Gasbarrini A. and Pola P. Cirrhotic cardiomyopathy. Dig Liver Dis 2007; 39(6): 507-15.

Moezi L., Gaskari S. A., Liu H., Baik S. K., Dehpour A. R. and Lee S. S. Anandamide mediates hyperdynamic circulation in cirrhotic rats via CB(1) and VR(1) receptors. Br J Pharmacol 2006; 149(7): 898-908.

Moller S. and Henriksen J. H. Cirrhotic cardiomyopathy: a pathophysiological review of circulatory dysfunction in liver disease. Heart 2002; 87(1): 9-15.

Moller S. and Henriksen J. H. Cardiovascular complications of cirrhosis. Gut 2008; 57(2): 268-78.

Myers R. P. and Lee S. S. Cirrhotic cardiomyopathy and liver transplantation. Liver Transpl 2000; 6(4 Suppl 1): S44-52.

Nagueh S. F., Shah G., Wu Y., Torre-Amione G., King N. M., Lahmers S., Witt C. C., Becker K., Labeit S. and Granzier H. L. Altered titin expression, myocardial stiffness, and left ventricular function in patients with dilated cardiomyopathy. Circulation 2004; 110(2): 155-62.

Neagoe C., Kulke M., del Monte F., Gwathmey J. K., de Tombe P. P., Hajjar R. J. and Linke W. A. Titin isoform switch in ischemic human heart disease. Circulation 2002; 106(11): 1333-41.

Neagoe C., Opitz C. A., Makarenko I. and Linke W. A. Gigantic variety: expression patterns of titin isoforms in striated muscles and consequences for myofibrillar passive stiffness. J Muscle Res Cell Motil 2003; 24(2-3): 175-89.

Nielsen S. S., Grofte T., Tygstrup N. and Vilstrup H. Cirrhosis and endotoxin decrease urea synthesis in rats. Hepatol Res 2007; 37(7): 540-7.

Obayashi M., Xiao B., Stuyvers B. D., Davidoff A. W., Mei J., Chen S. R. and ter Keurs H. E. Spontaneous diastolic contractions and phosphorylation of the cardiac ryanodine receptor at serine-2808 in congestive heart failure in rat. Cardiovasc Res 2006; 69(1): 140-51.

Opitz C. A., Kulke M., Leake M. C., Neagoe C., Hinssen H., Hajjar R. J. and Linke W. A. Damped elastic recoil of the titin spring in myofibrils of human myocardium. Proc Natl Acad Sci U S A 2003; 100(22): 12688-93.

Opitz C. A., Leake M. C., Makarenko I., Benes V. and Linke W. A. Developmentally regulated switching of titin size alters myofibrillar stiffness in the perinatal heart. Circ Res 2004; 94(7): 967-75.

Owen R. Collagen: levels of structure and alignment. JPK Instruments: App/Tech Reports 2005: 1-6.

Palmer B. M. Thick filament proteins and performance in human heart failure. Heart Fail Rev 2005; 10(3): 187-97.

Pauschinger M., Knopf D., Petschauer S., Doerner A., Poller W., Schwimmbeck P. L., Kuhl U. and Schultheiss H. P. Dilated cardiomyopathy is associated with significant changes in collagen type I/III ratio. Circulation 1999; 99(21): 2750-6.

Pott C., Yip M., Goldhaber J. I. and Philipson K. D. Regulation of cardiac L-type Ca2+ current in Na+-Ca2+ exchanger knockout mice: functional coupling of the Ca2+ channel and the Na+-Ca2+ exchanger. Biophys J 2007; 92(4): 1431-7.

Pozzi M., Carugo S., Boari G., Pecci V., de Ceglia S., Maggiolini S., Bolla G. B., Roffi L., Failla M., Grassi G., Giannattasio C. and Mancia G. Evidence of functional and structural cardiac abnormalities in cirrhotic patients with and without ascites. Hepatology 1997; 26(5): 1131-7.

Reichen J., Buters J. T., Sojcic Z. and Roos F. J. Abnormal lipid composition of microsomes from cirrhotic rat liver--does it contribute to decreased microsomal function? Experientia 1992; 48(5): 482-6.

Risoe P. K., Wang Y., Stuestol J. F., Aasen A. O., Wang J. E. and Dahle M. K. Lipopolysaccharide attenuates mRNA levels of several adenylyl cyclase isoforms in vivo. Biochim Biophys Acta 2007; 1772(1): 32-9.

Robinson T. F., Cohen-Gould L. and Factor S. M. Skeletal framework of mammalian heart muscle. Arrangement of inter- and pericellular connective tissue structures. Lab Invest 1983; 49(4): 482-98.

Robinson T. F., Cohen-Gould L., Factor S. M., Eghbali M. and Blumenfeld O. O. Structure and function of connective tissue in cardiac muscle: collagen types I

and III in endomysial struts and pericellular fibers. Scanning Microsc 1988; 2(2): 1005-15.

Roos K. P., Brady A. J. and Tan S. T. Direct measurement of sarcomere length from isolated cardiac cells. Am J Physiol 1982; 242(1): H68-78.

Ros J., Claria J., To-Figueras J., Planaguma A., Cejudo-Martin P., Fernandez-Varo G., Martin-Ruiz R., Arroyo V., Rivera F., Rodes J. and Jimenez W. Endogenous cannabinoids: a new system involved in the homeostasis of arterial pressure in experimental cirrhosis in the rat. Gastroenterology 2002; 122(1): 85-93.

Sanchez-Quintana D., Climent V., Garcia-Martinez V., Macias D. and Hurle J. M. Extracellular matrix arrangement in the papillary muscles of the adult rat heart. Alterations after doxorubicin administration and experimental hypertension. Basic Res Cardiol 1994; 89(4): 279-92.

Saucerman J. J. and McCulloch A. D. Cardiac beta-adrenergic signaling: from subcellular microdomains to heart failure. Ann N Y Acad Sci 2006; 1080: 348-61.

Scott J. D. Cyclic nucleotide-dependent protein kinases. Pharmacol Ther 1991; 50(1): 123-45.

Spinale F. G. Myocardial matrix remodeling and the matrix metalloproteinases: influence on cardiac form and function. Physiol Rev 2007; 87(4): 1285-342.

Stuyvers B. D., Miura M., Jin J. P. and ter Keurs H. E. Ca(2+)-dependence of diastolic properties of cardiac sarcomeres: involvement of titin. Prog Biophys Mol Biol 1998; 69(2-3): 425-43.

Stuyvers B. D., Miura M. and ter Keurs H. E. Dynamics of viscoelastic properties of rat cardiac sarcomeres during the diastolic interval: involvement of Ca2+. J Physiol 1997; 502 (Pt 3): 661-77.

Tada M. and Toyofuku T. SR Ca(2+)-ATPase/phospholamban in cardiomyocyte function. J Card Fail 1996; 2(4 Suppl): S77-85.

ter Keurs H. E., Rijnsburger W. H., van Heuningen R. and Nagelsmit M. J. Tension development and sarcomere length in rat cardiac trabeculae. Evidence of length-dependent activation. Circ Res 1980; 46(5): 703-14.

Trombitas K., Jin J. P. and Granzier H. The mechanically active domain of titin in cardiac muscle. Circ Res 1995; 77(4): 856-61.

Valeriano V., Funaro S., Lionetti R., Riggio O., Pulcinelli G., Fiore P., Masini A., De Castro S. and Merli M. Modification of cardiac function in cirrhotic patients with and without ascites. Am J Gastroenterol 2000; 95(11): 3200-5.

Vallance P. and Moncada S. Hyperdynamic circulation in cirrhosis: a role for nitric oxide? Lancet 1991; 337(8744): 776-8.

Villari B., Campbell S. E., Hess O. M., Mall G., Vassalli G., Weber K. T. and Krayenbuehl H. P. Influence of collagen network on left ventricular systolic and diastolic function in aortic valve disease. J Am Coll Cardiol 1993; 22(5): 1477-84.

Villari B., Vassalli G., Monrad E. S., Chiariello M., Turina M. and Hess O. M. Normalization of diastolic dysfunction in aortic stenosis late after valve replacement. Circulation 1995; 91(9): 2353-8.

Wallace K., Burt A. D. and Wright M. C. Liver fibrosis. Biochem J 2008; 411(1): 1-18.

Ward C. A., Liu H. and Lee S. S. Altered cellular calcium regulatory systems in a rat model of cirrhotic cardiomyopathy. Gastroenterology 2001; 121(5): 1209-18.

Warren C. M., Jordan M. C., Roos K. P., Krzesinski P. R. and Greaser M. L. Titin isoform expression in normal and hypertensive myocardium. Cardiovasc Res 2003; 59(1): 86-94.

Warren C. M., Krzesinski P. R. and Greaser M. L. Vertical agarose gel electrophoresis and electroblotting of high-molecular-weight proteins. Electrophoresis 2003; 24(11): 1695-702.

Wong H., Anderson W. D., Cheng T. and Riabowol K. T. Monitoring mRNA expression by polymerase chain reaction: the "primer-dropping" method. Anal Biochem 1994; 223(2): 251-8.

Wu Y., Bell S. P., Trombitas K., Witt C. C., Labeit S., LeWinter M. M. and Granzier H. Changes in titin isoform expression in pacing-induced cardiac failure give rise to increased passive muscle stiffness. Circulation 2002; 106(11): 1384-9.

Wu Y., Cazorla O., Labeit D., Labeit S. and Granzier H. Changes in titin and collagen underlie diastolic stiffness diversity of cardiac muscle. J Mol Cell Cardiol 2000; 32(12): 2151-62.

Wu Y., Tobias A. H., Bell K., Barry W., Helmes M., Trombitas K., Tucker R., Campbell K. B. and Granzier H. L. Cellular and molecular mechanisms of systolic and diastolic dysfunction in an avian model of dilated cardiomyopathy. J Mol Cell Cardiol 2004; 37(1): 111-9.

Yamasaki R., Wu Y., McNabb M., Greaser M., Labeit S. and Granzier H. Protein kinase A phosphorylates titin's cardiac-specific N2B domain and reduces passive tension in rat cardiac myocytes. Circ Res 2002; 90(11): 1181-8.

Yastrebov K., Ketzler J. T. and Coursin D. Slack Myocardium: A New Concept of Myocardial Function. J Clin Basic Cardiol 2006; 9 (online): 15-18.

Zile M. R. and Brutsaert D. L. New concepts in diastolic dysfunction and diastolic heart failure: Part I: diagnosis, prognosis, and measurements of diastolic function. Circulation 2002; 105(11): 1387-93.

Zile M. R. and Brutsaert D. L. New concepts in diastolic dysfunction and diastolic heart failure: Part II: causal mechanisms and treatment. Circulation 2002; 105(12): 1503-8.